CITY UNIVERSITY LONDON

School of Engineering and Mathematical Sciences

Fibre optic sensing techniques for the detection of lead (II) ions

By

Henri Guillemain

A thesis submitted to City University for the Degree of Doctor of Philosophy in Electrical and Electronic Engineering

August 2009

Centre for Measurement and Instrumentation
School of Engineering and Mathematical Sciences
Northampton Square, London EC1V 0HB

Table of contents

List of figures

List of Tables

Acknowledgement

I would like to acknowledge the help and support of Prof K.T.V Grattan and Dr M. Rajarajan throughout this work, in particular for their invaluable experience and guidance in helping me publish part of this work.

Also special thanks to Prof C.-T. Chen from the Chemistry Department at the National Taiwan University who collaborated with us by providing the fluorescent reagent as well as helpful advice and suggestions. I am vastly in her debt for the work done in Chapters 4 and 5.

I am most grateful to my colleagues in the research group for long fruitful discussions and suggestions, especially at the start of this work. The sharing of ideas, successes and problems in a friendly atmosphere contributed to the completion of this research.

Finally, I would like to especially thank my parents and many relatives for their commitment to and belief in me over all these years. Their implicit trust in sending me to a faraway country to study does not go unnoticed.

Declaration

I grant powers of discretion to the University Librarian to allow this thesis to be copied in part or in whole without further reference to the author. This permission covers only single copies made for study purposes, subject to normal conditions of acknowledgements.

Abstract

Lead is an element with harmful effects to man and whose uses are being increasingly subject to legislations. This thesis describes the incorporation of two lead-sensitive reagents in different fibre optic sensing configurations. The reagents were carefully selected for their response towards lead. A probe was built for each reagent and a sensor system designed, constructed and tested with each probe followed by analysis of the experimental data obtained from them.

The first reagent is a chromogenic dye whose absorption spectrum changes in the presence of lead ions. In this work, a reflectance-based probe is built and tested to exploit this feature. A robust referencing technique based on the performance of the probe is developed that allows the sensor to operate amid unstable conditions.

The second reagent is a fluorophore whose fluorescence mechanism and affinity to lead ions are explained in detail. Based on its binding properties with lead, the sol-gel matrix is selected to encapsulate this reagent and a probe is thus constructed but in subsequent tests, no response to lead ion is detected. A hypothesis is put forward to explain the lack of reaction between lead and the fluorophore in its entrapped environment.

As a result, the fluorophore is then utilised in solution where its characteristics have already been established and a capillary probe which exploits the capillary effect for its operation is constructed and evaluated. Existing analytical techniques are reviewed in this work and compared to fibre optic sensors whose various sensing configurations are then described. The instrumentation and measurement techniques used throughout this work are also discussed.

Chapter 1

Introduction

1.1. Motivation for this research

Heavy metals are well-known for their toxicity, even in trace amounts. Lead, in particular, is highly toxic. In view of its toxicity, the World Health Organisation (WHO) recommends a limit of 10 ppb in drinking water while that of copper is as high as 2 ppm [1]. Copper is beneficial to human biological systems in trace amounts while lead has no known biological importance.

The toxicity of lead is well documented [2-6]. Lead affects humans more severely at the infantile stage or even earlier during gestation. The nervous system is impaired, resulting in the lowering of IQ [4]; the reproductive system, haemoglobin synthesis and kidneys are also severely affected [2]. Lead is also a suspected carcinogen and has been classified as a possible carcinogen (category 2B) by WHO [6].

The high toxicity of lead lies in its chronic exposure at low levels as the body cannot get rid of this heavy metal. Once in the body, lead will be stored in the bones and be slowly released even after exposure has ceased. In women, it can cross the placenta during pregnancy and affect the development of unborn babies [4].

Apart from its toxicity, it also has adverse effects on new technology, for example, being a poison for car catalysts [7].

The health/green issue is not always a priority incentive for monitoring. Precision farming requires environmental monitoring to use exact amounts of fertilizers and pesticides for economical reasons. Reducing runoffs of these chemicals for the protection of the ecosystem comes second. Industrial monitoring may be required to show compliance with regulations for e.g. emissions from coal-powered stations but may also be for process efficiency e.g. waste waters from textile factories. Safety monitoring ensures first and foremost the safety of workers in areas of hazardous conditions, for e.g. the storage of combustible or radioactive materials [8].

The main source of exposure to lead in the developed world used to be airborne particles arising from the combustion of leaded fuels. The concentration of lead in the air has dropped by nearly 100% in the US since combustion of leaded fuels has ceased [3]. From 1976 to 1980, before the use of unleaded gasoline, US children 1 to 5 years of age had a median blood lead concentration of 15μg/dL [4]. In 1988–1991, the median was 3.6 μg/dL; in 1999, the median was 1.9 μg/dL, as illustrated in Fig. 1.1. Leaded fuels are, however, still widely in use in developing countries [2].

Other main sources of exposure are from old paint, lead-acid batteries, smelters, solders, lead pipes and agricultural wastes. Fertilizers are a much neglected source of heavy metals which can easily enter the food chain and also expose farm workers. The concentration of heavy metals in fertilizers ranges from 1-10 parts per million (ppm) [9]. Lead, once extracted, cannot degrade and stays in the environment forever. As landfill sites keep accumulating such heavy metals, they become a potentially major source of leaching.

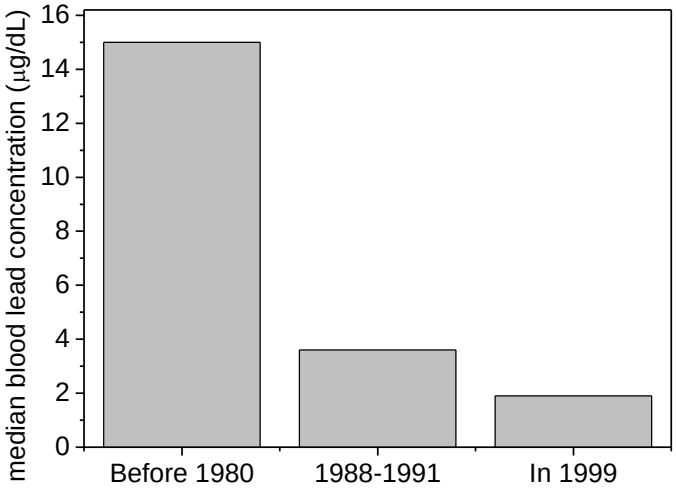

Fig. 1.1 Median lead concentration in blood in children [2].

Uses of lead and its compounds are increasing despite the phasing-out of leaded petrol, greater environmental awareness and tighter regulations. The biggest increase has been in lead batteries. Other applications are wide and varied and have been found in polyvinylchloride (PVC) stabilisers, alloys, ammunition, glass pigments, cable sheathing, cosmetics and foil wine wrappers [2]. An article entitled “Discussions reveal deep division on safety of synthetic ingredients” published by the respectable trade magazine Cosmetics Design Europe mentions that lead was found in lipstick and a full investigation called for in the US [10]. The trend is now to use substitutes for lead where possible, for e.g. lead-free solder, copper or PVC water pipes, steel ammunitions and iron weights on fishing lines [2].

As a result, the use of lead and its compounds are heavily regulated and limits are imposed in various applications. These limits differ depending on countries, agreements and area of application. Examples include the Waste of Electrical and Electronic Equipment (WEEE) [11] and the Restriction of Hazardous

Substances (RoHS) Directives [11]. WEEE regulates heavy metals and toxic substances that can be used in the manufacture of electrical equipment and introduces a recycling scheme for waste electrical equipment. RoHS requires substitution of heavy metals with less hazardous materials where possible.

In addition, an aspect of the EU Directive on toys safety regulates the level of lead and other toxic metals in children's toys [12]; The Registration, Evaluation, Authorisation and restriction of Chemical substances regulation (REACH) [13] restricts the use of a large number of chemicals in industries while there are already limits imposed on lead in *unleaded* petrol in the EU [14]. The Landfill Directive limits the amount of heavy metal wastes that enter these sites; in particular, it defines hazardous wastes and states concentration limits that may be disposed of in landfill sites [15]. In fact, the EU is becoming the world's chief regulator, according to the Economist [16]. From this point of view, any regulations adopted by the EU within its borders are likely to be picked up by other countries, including the US.

It follows that there is an increasing need for monitoring heavy metals to show compliance with the growing number of such regulations. Monitoring or measurement is becoming rapidly an active area. In fact, sensors are ubiquitous and essential to an information-dependent society.

Sensors are used in all types and in a wide range of situations. From simple ones such as outdoor weather stations for home users, carbon monoxide and fire alarm detectors to more sophisticated ones in demanding environments found in car engines and airplanes, there are other systems that may also be viewed as sensors. Traffic-monitoring software gathers all kinds of data on traffic that flows through a website and may be used in e-commerce to build a profile of the clientele. Fingerprint and face recognition systems for ID and security purposes make multiple measurements on the face or fingerprint and are processed against a database for correlation. The scanner may be viewed

as the sensor transducer, the measurements make up the sensor signal and, after data processing and analysis, the output may be a stop or go.

1.2. Existing analytical techniques

1.2.1. Instrumentation type methods

Various techniques exist for the determination of heavy metals. The well-established conventional ones include Atomic Absorption Spectrometry (AAS), Flame Atomic Absorption Spectrometry (FAAS) and Graphite Furnace Atomic Absorption Spectrometry (GF-AAS).

In AAS compounds are broken apart into atoms at sufficiently high temperatures. These gaseous atoms, present in their ground state, can absorb energy of their own specific wavelength. When light of the resonance wavelength is passed through these atoms, it will be absorbed and the extent of absorption will be proportional to the number of atoms in the ground state. Atomization generally requires energy and may use different sources of energy, for example, a flame, an electrically heated furnace or an inductive-coupled plasma [17, 18]. Rapsomanikis reported a detection limit of 0.18pg/mL or 0.18 parts per trillion (ppt) using AAS [19].

In FAAS, the sample and air are mixed before being ignited at 2400 - 2700K with an acetylene-air mixture. The sample solution is drawn into the nebulizer and the liquid is broken down into a fine mist as it leaves the tip of the nebulizer. Only about 5% of the initial sample reaches the flame where it is evaporated and dissociated into its constituent atoms [17, 20]. GF-AAS has a greater sensitivity compared to FAAS. The whole sample injected is atomized and the graphite furnace confines the atomized sample in the optical path for a residence time of several seconds resulting in high sensitivity. Additionally a smaller volume of sample is required [20].

X-ray fluorescence spectrometry is a non-destructive spectrochemical method and can be used to analyse from 100% to a few parts per million. It involves fluorescence measurements of samples after excitation with X-ray radiation. The emission of each element is unique due to its atomic structure [21].

These techniques are well developed and provide excellent results in terms of sensitivity and selectivity but often require extensive sample preparation [22-24]. They are mostly designed as laboratory instrumentation and are therefore bulky and expensive to purchase. As a result, other simpler analytical techniques have been developed, such as electrochemical devices [25], the pH meter being a well-known example and optical sensors.

1.2.2. Sensor types

The field of electrochemical sensors includes techniques such as ion-selective electrodes, voltammetry, conductimetry, amperometry and potentiometry and are commonly used in the determination of heavy metals [26, 27]. The concentration of a chemical species is obtained by measuring changes in an electrical quantity such as current as a result of applied voltage with respect to time at electrodes plunged in the sample solution. Faraday's Law is used, whereby the charge is directly proportional to the amount of chemical species undergoing a redox reaction.

For instance, in a potentiometric sensor, the signal measured is the potential difference between the working electrode and the reference electrode under zero current flow. The potential of the working electrode depends on the concentration of the analyte while the reference electrode serves to provide a reference potential. Potentiometric sensors are usually used in gas sensing instead of aqueous ions as water is an electrolyte. Selectivity and stability of the

sensor may be enhanced by use of a non-conducting membrane at the working electrode.

A heavy metal ion sensor based on conductometry was reported by S.M. Lee and W.-Y. Lee using urease to produce a measurable enzymatic activity [28]. The conductometric sensor does not require a reference electrode but uses only one electrode upon which the urease is immobilised using sol-gel. The electrode measures the admittance of the sample solution before and after addition of the analyte. The detection limit was 5 μM and 900 μM for mercury (II) and lead (II) ions respectively.

A voltammetric technique reported by Yantasee and co-workers achieved a detection limit of 0.5 ppb and 3 ppb for Pb^{2+} and Hg^{2+} respectively but required a preconcentration time of 20 minutes to reach these detection limits [29]. Whilst detection limits of electrochemical sensors are in general around the ppb level, challenges remain, especially in the area of selectivity [30].

Optical sensors are based on the interaction of light with the analyte. If there is no possible interaction, a chemical transducer is used to provide an optically detectable change in the presence of the analyte. The use of optical fibres renders an optical sensor more compact, portable and allows remote sensing. There are also techniques exclusive to optical fibres such as short and long period gratings and evanescent wave sensing. Since this thesis is devoted to fibre optic chemical sensing, more details will be given in the following chapters.

Before embarking on an assessment of fibre optic chemical sensors, it is worth pointing out for the sake of completeness that other types of sensors also exist. Clifford Ho and co-workers give a review of sensors for environmental monitoring [31]. Some sensors covered include nanoelectrode arrays, radioisotope sensors, grating light reflection spectroelectrochemistry and

surface acoustic wave sensors. Liu and Ji developed a hydrogel swelling microcantilever sensor for the detection of lead (II) ions [32]. The hydrogel was spiked with a lead-sensitive molecule which caused the hydrogel to absorb water and swell in the presence of lead in an aqueous sample. The swelling hydrogel caused the microcantilever to bend and its deflection was measured with a laser. A detection limit in the micromolar (μM) range could be achieved in this way.

1.2.3. Fibre Optic Sensors

Fibre optic chemical sensors (FOCS) offer the following advantages [33]:

1. Ease of miniaturisation. This is useful for invasive procedures and minute sample volumes.
2. A separate probe for referencing is not required as opposed to potentiometry where a reference electrode is used to measure the difference in potentials.
3. Immunity to electrical and magnetic interference at the probe since the signal is optical. Conversely, it does not present an electrical hazard risk.
4. Simultaneous sensing of different analytes by bundling the fibres together.
5. Excellent temperature, radiation and chemical resistance, especially when using silica fibres.
6. Large signal bandwidth.
7. Versatility in measurement scheme – intensity, lifetime, wavelength or polarization.
8. A modular design with easily replaceable parts which can be used to alter the sensor. Replacing the probe easily is useful in disposable sensors.
9. Distributed measurement via the whole length of fibre.
10. Wide choice of fibres (quartz, doped, plastic, polarization-maintaining) and materials as well as cheap compatible devices (LEDs, laser diodes, splitters, couplers) from the telecoms industry.

Some disadvantages are [33]:

1. Interference from background light
2. Membrane deterioration and leaching
3. Limited response time
4. Narrow dynamic range
5. No suitable optical transducer

Background light interference may be minimised with the use of proper sensor packaging painted black to absorb stray light. Alternatively, lock-in amplifiers may be used and requires modulation of the light source at a given frequency. In the past, a mechanical chopper was used for this purpose; nowadays, with the widespread use of LEDs and laser diodes, electronic modulation has become more widespread. Although lock-in amplifiers are able to give excellent signal-to-noise ratios, they can be relatively expensive and do not remove the need for a judicious sensor packaging as this is still needed to protect the probe from mechanical damage and dirt, especially in harsh environments.

Membranes may leach the embedded reagent over time or exhibit undesired fluorescence, especially with carbon-based material. In addition, because the reagent is embedded inside the membrane and is repeatedly exposed to strong light, it is more prone to photo-degradation effects such as photo-bleaching and photo-decomposition.

The immobilisation of a reagent within a membrane may modify it and adversely affect its sensitivity towards the analyte of interest. In fact, it is widely known that the response of a reagent towards a particular analyte will vary depending on its immediate environment, i.e. whether it is free to move in solution or immobilised within a matrix. Flamini and co-workers studied a ligand for the detection of mercury ions in both homogeneous solution and in a

polymeric sol-gel thin film [34]. He reported an enhancement in the stability of the ligand in the air when immobilised in the polymeric sl-gel film but with a slower response and a less favourable detection limit than in solution. The absorption spectrum of the ligand was also different in immobilised form and was due to around 20% in the film not contributing to the absorption but rather scattering or reflecting the radiation.

At times, the sensitivity of the reagent towards the analyte may disappear completely. This occurs if the site of binding between the reagent and the analyte is used to bind the reagent to the membrane, either in a covalent bond or in an electrostatic bond. If the reagent binds to the analyte via an electrostatic attraction, as is often the case for ionic species, then electrostatic immobilisation of the reagent on, for e.g. an ion-exchange resin, may destabilise the charge distribution on the reagent and disrupt the electrostatic attraction between it and the analyte, even if the electrostatic immobilisation of the reagent onto the resin is not done at the site of binding between the reagent and the analyte. Optical properties of fluorescent polymers cast as films were found to be not as sharp as in solution due to a lower extent of conjugation [35].

Often, the reagent is purposefully modified to make it compatible with the membrane. The chromogenic indicator Pyrocatechol Violet (PV) was used by Steinberg *et al* to produce an optical sensor membrane [36]. The hydrophilic indicator had to be lipophilised to render it compatible with the PVC polymer in which it was immobilised. Following immobilisation, PV changed colour from yellow to green with maximum absorption at 740nm following 10min exposure to copper ions.

The presence of a membrane will also slow down the time response of the sensor. Since the reagent and the indicator are in two different phases, mass transfer from one phase to another or, in other words, the extraction of the analyte into the membrane, is necessary to achieve a steady-state equilibrium. In addition to this, the membrane strongly affects the range of the sensor as it is

the amount of reagent within it that will take part in a chemical reaction or equilibrium with the analyte. The membrane can only hold a finite amount of the reagent. In comparison, electrochemical sensors display a much wider dynamic range than corresponding optical sensors. Optical pH sensor responses are sigmoidal while their electrochemical counterparts are linear [37].

The solution to avoid all these issues is to get rid of membranes completely as has been done in Chapter 5. Membranes are not required when an indicator is not necessary to optically signal the presence of the analyte if the latter already possesses some optically measurable characteristic such as absorption. Sensors based on the intrinsic properties of the analyte are called intrinsic sensors and are discussed in section 1.3.1.

Where a reagent is necessary and the use of membranes or solid supports cannot be avoided, their effect may often be minimised through the use of referencing techniques as discussed later in sections 2.4 and 3.4.3. The presence of a membrane frequently allows the sensor to become reversible as the reagent is trapped within it; otherwise once the sensor becomes a one-shot test as the reagent mixes with the sample solution and reacts with the analyte. The probe developed in Chapter 5 is an example.

The use of membranes is also advantageous when multi-analyte sensors are being developed. In an optical fibre configuration, membranes containing different reagents could be separately coated along the length of the fibre to exploit the evanescent wave interaction.

Kieslinger *et al* designed a capillary waveguide sensor to measure three different analytes in a single capillary tube [38]. The capillary tube was first coated with a polymer layer which was subsequently removed except for a segment in the middle. The other two ends of the tube were similar coated to result in a capillary tube with three separate segments of polymers doped with

reagents. Detection is performed by measuring the emission fluorescence propagating along the capillary waveguide. If the emission from each reagent is at a different wavelength, then it is possible to analyse each individually. Capillary sensors are discussed in Chapter 5.

Elsewhere, Malins and co-workers developed a multi-analyte optical chemical sensor to simultaneously sense for oxygen and carbon dioxide [39]. A Perspex planar waveguide was embossed with flat arrays into which single drops of sol-gel each containing a different reagent were deposited and the waveguide accelerated in a spin-coating machine. The resulting discrete pattern of sol-gel coatings was excited by means of a single LED via an evanescent wave interaction while measurement of the quenched fluorescence was performed with a CCD imaging camera. The use of sol-gel in sensors is discussed in Chapter 4.

While these two examples do not involve optical fibres, they serve to demonstrate how membranes and other solid supports may be ingeniously used to design sensors for simultaneous measurements of several analytes. Furthermore, although membranes limit the dynamic range of the sensor as discussed above, they can be used to adjust it to suit the application. A large amount of reagent doped into a membrane may render the sensor response sluggish; on the other hand, a low level of doping will give a rapid response though with a limited dynamic range. This is exemplified in work described in Chapter 3. In addition, a sharp sensor response is not always necessary if long-term monitoring is being performed.

In keeping with multiple reagents, a dual life-time referenced optical sensor membrane for the determination of copper ions was reported by Mayr *et al* [40]. This elegant technique [41] which has been patented [42] makes use of a short lifetime copper-sensitive fluorophore and an inert long lifetime reference fluorophore, both immobilised onto polymer beads and embedded in a hydrogel

membrane. The two fluorophores must have similar excitation and emission spectra so that they can be excited by the same LED and their emission measured with the same detector. While the reference fluorophore provides a constant emission intensity level, the level of emission of the other fluorophore depends on the copper concentration. The intensity being detected is a ratio of the two; thus a sinusoidally modulated excitation light will result in a phase shift at the detector level dependent on the copper concentration.

Consequently, an intensity variation has been transformed into a phase-shift measurand. While this seems advantageous a priori due to the inherent resilience against noise, the whole scheme depends heavily on the fact that the emission from the reference fluorophore is constant throughout. Any changes in the immediate environment of the two fluorophores will affect them unequally as they are different. Thus, it is hard to guarantee a stable reference level as, in the experience of the author, factors such as leaching, temperature and pH variations may interfere with the emission intensity and lead to erroneous measurements. These factors are the very reasons why referencing schemes are implemented in the first place in intensity measurement configurations.

Finally, a disadvantage of FOCS is that the sensing chemistry is the limiting factor, either in terms of selectivity or sensitivity. There might not be any suitable indicator in terms of analytical wavelength, compatibility with a membrane or selectivity available for a particular analyte [37].

It is with these advantages in mind that we select FOCS and seek to improve or limit their disadvantages for our application purposes.

The ideal sensor should have the following features:

- linear response over the whole range of interest,
- high sensitivity and selectivity,

- immediate time response,
- reversible,
- financially viable.

In practice it is impossible to meet all these demands. However, it is possible to make a reasonable compromise upon certain characteristics depending on the application required. For example, if the composition of the sample is known to consist mainly of the analyte, then the selectivity may be reduced in order to boost the sensor sensitivity. Likewise, if long-term monitoring is envisaged, rapid sensor response is not useful. Instead, the selectivity or sensitivity may be improved. The economic viability of the sensor is an important characteristic where the sensor is proposed to replace a similar existing device or is expected to be sold to a wide market. If the sensor is to be used in a niche application, and where its performance is exceptional, these will override the financial aspect.

Some applications of fibre optic chemical sensors include glucose sensors for the medical field, e. coli detector in blood diagnostic [43] as a rapid alternative to conventional analytical techniques, health and safety in industrial settings via the measurement of leaking depots of organic solvents [44] and water-soluble products [45]. Sensors for pH measurement are also very common [46]; gas sensors have been developed for oxygen, carbon dioxide, methane and ammonia among many others [39, 47-49]. In the field of environmental monitoring, many chemical species, especially ions known to have adverse environmental effects, have been potential targets of fibre optic sensors. This is the focus of this thesis.

1.3. FOCS systems

1.3.1. Sensor classification

Fibre optic chemical sensors (FOCS) may be classified as intrinsic and extrinsic sensors. The former rely on the optical properties of the analyte, such as absorption or fluorescence. For e.g. methane has a strong absorption line at 1300nm. Noda *et al* exploited this characteristic to produce a methane gas sensor operating in this infrared region [50]. The researchers showed that methane gas concentration is proportional to absorbance in the range 5-90% by volume. Because water vapour also absorbs strongly in the infrared region, a combination of silica gel and calcium chloride was used to remove humidity before taking any measurements.

Where the analyte has no useful optical properties, an extrinsic sensor is necessary. The extrinsic sensor is made up of a chemical indicator which serves to convert the concentration of the analyte into an optically measurable quantity. Intrinsic sensors are theoretically more robust and exhibit a faster time response than extrinsic sensors which rely on an indicator within a membrane leading to leaching or photo-degradation. Intrinsic sensors can also be used as fully distributed sensors. On the other hand, extrinsic sensors may display better sensitivity and selectivity as they are carefully tailored to detect the analyte. Most fibre optic ion sensors are extrinsic since ions usually have no characteristics that may be directly detected by optical methods.

1.3.2 Absorbance-based sensors

In designing a FOCS, an optical parameter must be exploited to relate the analyte concentration to the measurand. The most popular type of sensor is based on absorption measurements. If the analyte does not absorb light, a chromogenic indicator is necessary. This indicator will change colour in response to the presence of the analyte. Most metal ions require the use of a

chromogenic indicator for absorption measurements. Some indicators may be unsuitable for FOCS due to their unfavourable analytical wavelengths, poor photostability or low molar absorptivity leading to low sensitivity. The absorption of a species is governed by the Beer-Lambert law which is covered in section 3.2.

An ammonia sensor was designed by by Fneer *et al* based on the absorption of phenol red at 565nm [51]. The sensor made use of a specially designed absorption cell ended with a mirror for absorption measurements. The mirror effectively doubled the optical pathlength to improve sensitivity.

Absorption measurements are also popular in gas sensing as gases, unlike metal ions, have unique absorption spectra and do not require the use of an indicator. Gas detection based on optical correlation spectroscopy compares the absorption of a target gas of unknown concentration in a measurement cell with the same gas of known concentration in a reference cell [52]. A modulated interrogating light signal, usually of broadband spectrum to capture a wide range of the absorption lines of the target gas, is sent through the reference cell. The emerging light which has been partly absorbed by the gaseous species is combined with the interrogating signal shifted by 180˚ and whose intensity is reduced such that superposition of the two out-of-phase signal results in a zero output. This combined signal is sent to the measurement cell where only the shifted signal component will be absorbed as the in-phase signal has already experienced absorption through the reference cell. The net intensity modulation signal is now no longer zero and depends on the concentration of the target gas.

1.3.3 Reflectance-based sensors

Reflectance-based sensors measure the light scattered off non-uniform surfaces. They are actually based on absorption since what is not scattered is

absorbed by the surface coating. However, the advantage here is that no mirror coating is required to guide the light back into the fibre. This type of sensor is looked at in more detail in Chapter 3.

1.3.4 Fluorescence intensity measurements

Fluorescence sensors may measure either the emission intensity, the quenching effect of the analyte on the fluorescence intensity or the lifetime changes in the fluorescence emission intensity. The fluorophore may be the analyte itself, as in an intrinsic sensor, or more commonly, a chemical reagent whose purpose is solely to provide fluorescence. This fluorescence may increase as a result of an increase in the analyte concentration; it may be quenched by the analyte or the lifetime of the fluorescence may increase or decrease depending on the effect of the analyte. Fluorescence mechanism is given a detailed treatment in Chapter 4.

The main advantage of fluorescence sensing over absorption sensing is that measurement is made over a dark background. Lifetime measurement sensing is favoured over fluorescence intensity measurements because the lifetime is not subject to interfering radiation, provided the intensity is strong enough. However, a ratiometric measurement of fluorescent intensity is also quite robust.

Parker and co-workers designed a fibre optic sensor for pH and carbon dioxide using fluorescence intensity ratio measurements [53]. They showed that taking the ratio of the intensity of the base peak to the intensity of the isosbestic point rendered the sensor insensitive to photo-bleaching and variation in excitation intensity. A hydrogel was used to contain the dye and placed at the distal end of the fibre while excitation radiation was provided by a green LED.

1.3.5 Fluorescence lifetime – time domain

There are two approaches to fluorescence lifetime measurement. In the time domain, a short pulsed excitation signal is sent to the fluorophore resulting in an exponentially decaying emission signal. Istratov and Vyvenko have given an in-depth review of the exponential analysis and a comprehensive overview of the numerical algorithms used [54]. If a fluorophore is excited with an impulse function, the rate of decay $\frac{dI(t)}{dt}$ of the resulting emission radiation $I(t)$ is given by

$$\frac{dI(t)}{dt} = -\frac{1}{\tau} I(t) \tag{1.1}$$

Where τ is the lifetime also known as the inverse of the decay rate constant. The observed decay signal is the solution to this differential equation given by [55, 56]

$$I(t) = I_0 \exp\left(-\frac{t}{\tau}\right) + B \tag{1.2}$$

Where I_0 is the intensity at time $t = 0$ and B is the baseline offset, a time-constant noise component in the detected signal due to electronic and background noise. Taking the logarithm of (1.2) yields

$$\ln I(t) = -\frac{t}{\tau} + \ln B \tag{1.3}$$

Plotting $\ln I(t)$ versus t will give a straight line and the fluorescence lifetime may be determined by calculating this gradient.

Birch *et al* used lifetime measurements in the time domain to detect copper ions in water [57]. The fluorophore was rhodamine 800 embedded in the ion exchange membrane Nafion and excited at 670nm with a diode laser. Increasing concentrations of copper ions would cause a quenching effect on the fluorescence and result in a shorter fluorescence lifetime. In fact, one of the advantages of using lifetime measurements in sensing is to measure dynamic quenching. This is explained in section 4.2.2.

1.3.6 Fluorescence lifetime – frequency domain

The other technique to measure lifetime is in the frequency domain by excitation of the fluorophore with a sinusoidally modulated signal.

The emission response is forced to follow the excitation signal at the same modulation frequency but lags behind with a phase shift ϕ which is related to the lifetime τ of the fluorophore by [42]

$$\tan\phi = \omega\tau \tag{1.4}$$

Where ω is the modulation frequency which is chosen to be comparable to the reciprocal of the lifetime. At lower frequencies, the phase shift decreases.

The presence of this finite time response of the fluorophore also causes a decrease in the peak-to-peak of the emission signal relative to that of the excitation signal. This modulation of the emission signal occurs because some of the fluorophores, having been excited at the peak of the excitation signal, continue to emit at minimum excitation [42]. The modulation m is related to the lifetime by

$$m = \frac{1}{\sqrt{1+\omega^2\tau^2}} \tag{1.5}$$

At very high modulation frequencies, the modulation m decreases significantly. The measurement of either phase shift or modulation will reveal the lifetime. This approach is independent of signal offset but requires a lock-in technique and is very sensitive to excitation light leakage at the detector.

Grattan and co-researchers designed a fibre optic fluorescence temperature sensor based on phase shift measurements [58]. A small piece of ruby crystal was sinusoidally excited with a green LED and the phase shift between the LED signal and the emission was measured.

Rosso and Fernicola reviewed the various techniques used in time and frequency domain lifetime measurements [59] and showed that the relative differences between the two approaches are less than 0.2% for some data sets. The comparison between the various processing methods was carried out on experimentally obtained data from a fibre optic temperature probe using a fluorescent chromium doped crystal.

To make lifetime measurements on fluorophores with very short lifetime, very fast electronics is required: the pulse period or sine period must be comparable to the exponential decay time. It is well-known that the lifetime of organic fluorophores is in the nanoseconds and picoseconds [42, 60]. This translates into frequencies of gigahertz and beyond and instruments that are able to cope at this speed. These instruments are expensive and often bulky. On the other hand, judicious sensor design using the same fluorophore with an LED and a detector to make ratiometric measurements will yield satisfactory results [61].

1.3.7 Evanescent wave sensors

Evanescent wave sensing exploits the long length of fibre for greater interaction with the analyte and therefore improved sensitivity. It is based on the fact that

upon internal reflection of light at the core-cladding boundary, a small amount of light penetrates the cladding. This region constitutes the evanescent field and is typically around 100nm deep. If the analyte is within that evanescent field, it is able to modulate the optical signal. Absorbent and fluorescent dyes may be combined with this technique. Evanescent wave sensors are looked at in more detail in Chapter 5.

1.3.8 Refractometric sensors

Because light transmission in an optical fibre is based on the laws of refraction, FOCS may measure changes in refractive index. This is done by removing the cladding to expose the core. If the analyte or the indicator is able to change refractive index, then the core-cladding boundary is modified and light transmission is affected. The problem with this technique is that it is non-selective. Any process that causes a change in refractive index will affect measurements, be it changes in air humidity or smudges on the fibre. Cherif *et al* designed a refractometric sensor with multimode fibres for the detection of toluene in water [62]. The cladding was removed and replaced with a sol-gel to facilitate exposure to the analyte. Light launched in the coated fibre would suffer losses as the refractive index of the sol-gel increased when the amount of toluene present also increased. While a 1% detection limit was achieved, no mention was made of the selectivity of the sensor.

Surface plasmon resonance (SPR) sensors based on optical fibres operate by sensing a change in external refractive index. The cladding is removed to expose the core which is then coated with a thin layer of gold or silver upon which a chemical reaction will take place involving the analyte. Optical radiation in the fibre core excites surface plasma waves in the metal dielectric medium which are then modified by the presence of the analyte. Propagation of these waves occur over a very short distance due to the high loss in the metal layer [63]. So similar to evanescent wave sensing, light in the fibre core via an SPR

interaction is affected by the external environment just beyond the fibre but unlike it, increasing the length of the metal layer will not improve the sensitivity.

Multimode fibres have been used in SPR sensors but intermodal coupling, polarization conversion and modal noise affected the sensor output [64]. Single-mode fibres were used instead as hey support only one mode of propagation; further progress was made using polarisation-maintaining fibres. Other improvements included a side-polished single-mode fibre in an SPR sensor developed by Homola [65].

SPR sensors are mostly popular for biosensing applications – Homola *et al* reported that more than 75% of SPR research papers dealt with optical biosensing [63].

1.3.9. Hydrogel capabilities

Hydrogels are an active field [66] and becoming attractive to fibre optics sensor implementation. A tutorial review by Linden and co-researchers describe the mechanism of stimulus-sensitive hydrogels and their wide field of applications as sensors and actuators, including artificial muscles [67]. The hydrogel is a polymer matrix made up of backbone chains held together by crosslinks which effectively prevent them from dissolving away. The family of stimulus-sensitive hydrogels may be divided into two groups: temperature-sensitive hydrogels and pH-sensitive hydrogel which is the one of interest to ion-sensing.

The ionizable monomers making up the backbone chains will dissociate as a function of pH and the resulting free ions in the hydrogel exchange from salt ions in the solution. Within the hydrogel, the counterion concentration will increase and cause an osmotic pressure difference between the gel and the solution that appears as a drastic swelling in volume of the gel. The swelling ceases when the elastic forces inside the hydrogel are in equilibrium with the

osmotic forces. The hydrogel may give off protons to the solution but to maintain electroneutrality, it has to take up counterions from the solution [67].

If a transducer element such as crown ethers as discussed later in section 4.2.2 is incorporated into the backbone chains, it will selectively pick counterions from the solution, resulting in an ion-sensitive hydrogel [66]. This is what has been performed in the work of Liu described earlier [32]. pH-sensitive hydrogels suffer from low selectivity as they respond to any counterion present but the incorporation of a molecular recognition unit for metal ion detection overcomes that problem and so ion-sensitive hydrogels display better selectivity than the more primitive pH-sensitive gels.

Different types of transduction methods have been explored to measure the change in volume of a hydrogel [67] such as optical, conductometric, amperometric and mechanical methods. Of interest to this work are the optical and mechanical methods which may be adapted to optical fibres.

Mechanical methods convert the swelling capability of the gel into an optically-measurable quantity. Asher and Holtz have reported a novel optical technique to visually detect metal ions in solution [68, 69]. Crystalline colloidal array (CCA) photonic material embedded in a hydrogel display Bragg diffraction and are brightly coloured. Swelling of the hydrogel doped with a metal ion recognition unit changes the spacing of the CCA and leads to a change in colour. For more accurate measurements, reflectance measurements with a spectrophotometer were proposed and detection limits in the micromolar range were achieved for a range of metal ions. This scheme may be easily adapted to an optical fibre system by fixing the hydrogel to the distal end of a fibre, resulting in a small, compact and portable probe.

Optical methods directly exploit changes in optical characteristics of the gels. Changes in the reflectance [70, 71] of hydrogels which is a function of their

volume has been reported. As the hydrogel membrane absorbs water and swells, its transparency increases, leading to a drop in reflected light intensity. The membrane may be positioned at the end of a fibre to make a small compact probe. The change in fluorescence intensity of a hydrogel has been exploited to build a fibre optic glucose sensor [72]. The hydrogel was doped with a fluorophore and a glucose-sensitive enzyme and affixed to the distal end of a fibre. Swelling of the gel caused changes in the fluorescence intensity. Further exploitation of the effect of hydrogels onto optical fibres is described in the next section by first introducing the idea of fibre gratings.

1.3.10. Fibre gratings

Fibre gratings, either of the fibre Bragg grating (FBG) or LPG, have been actively studied and reviewed in recent years [73-75]. Fibre gratings are essentially a series of periodic changes in the refractive index of the fibre core. The length of the period defines either an FBG, typically a few millimetres long or an LPG, typically a centimetre or more in length. The main advantage of these gratings lies in the fact that they convert a change imposed upon the fibre into a wavelength shift of the optical signal propagating through the core, making such measurements more robust against intensity losses. The gratings respond to strain and temperature and LPGs in addition respond well to changes in refractive index and bend radius and were thus exploited to measure these parameters [76-81].

The swelling effect of polymer gels were coupled to FBGs to produce a relative humidity (RH) sensor [82]. The gel was coated onto a short length of fibre into which an FBG was inscribed. Swelling of the gel imposed a small strain on the fibre which was picked up by the grating and translated into a wavelength shift, making this class of sensors resistant to light intensity fluctuations.

It should be mentioned that hydrogels also change refractive index upon swelling. This, combined with LPG sensitivity to external refractive index [83],

led to an RH sensor by Liu *et al* [84], effectively a variation of the RH sensor described above. The measurement of changes in the index of refraction of hydrogels upon swelling using LPGs has been exploited in other sensors as well [85, 86].

These examples serve to demonstrate the close association of hydrogels and optical fibres in different ways, either by mechanical methods which translate volume changes of the gels into strain applied onto the fibre or by optical methods focussing on refractive index changes. Fibre gratings have been used in a wide variety of physical sensors which are outside the scope of this thesis but the combination of hydrogels and fibre gratings constitute the few cases where fibre gratings have been used as chemical sensors.

1.4. Aims and Objectives

The aim of this thesis is to design and build two fibre optics chemical sensors, based on the dithizone reagent and a novel fluorophore molecule, both sensitive to lead ions. The optical sensors are then evaluated for their response and performance to solutions of lead ions. The novelty of this work is the first reported fibre optic chemical sensor for lead ions based on fluorescence detection in a capillary probe. In addition, the referencing technique and probe configuration used in conjunction with the sensor build around the dithizone reagent for lead sensing also builds on existing work in the field. The importance of monitoring heavy metals and lead in particular has been highlighted at the beginning of this chapter and provides a motivation for the sensing of lead ions.

In order to address the aims described above, the following objectives have been set:

- To adapt a well-established chromogenic reagent into a fibre probe configuration and thereby develop an understanding of the instrumentation, techniques and issues involved in assembling a fibre optic sensor system.
- To implement referencing and measurement techniques that complement each other and that can be done at the software level instead of instrumental modification.
- To identify a highly-selective reagent for lead sensing that has not been used previously in a FOCS and which is different from the first reagent, i.e. not chromogenic. The characteristics of the selected reagent will be studied with a view to build a FOCS based on its properties.
- To build and test a fibre optic probe based on the results of the study of the new reagent.

1.5. Structure of this thesis

Chapter 2 is devoted to the instrumentation and measurement techniques used throughout the subsequent chapters. The FOCS system is broken down into its components and discussed; each major device and component is described and finally brought together in the experimental set-up adopted.

In Chapter 3, a reflectance sensor based on the colour change of an indicator is described and evaluated. The nature and chemistry of the indicator is first described. Following this, a FOCS is built around its colour change in the presence of lead. The probe is built for better functionality and a reference scheme incorporated into the sensor at the software layer.

The characteristics of a novel fluorophore is next investigated in Chapter 4 for implementation in a FOCS. The reasons for choosing this new fluorophore are laid out and its fluorescence mechanism studied. Based on its binding

configuration, the sol-gel approach is selected as matrix support for use in a FOCS. Tests reveal that this is not successful.

Chapter 5 deals with a capillary probe built around the fluorophore described earlier. Since the fluorophore was not immobilised, it was decided to exploit its characteristics in the medium where it works well. The capillary effect is used together with Pasteur pipettes to create a successful disposable probe.

A summary of the work carried out is presented in Chapter 6. A conclusion based on the experience gained in this field is included and with recommendations for some further work.

1.6. References

1. WHO, *Guidelines for drinking water quality*. 2006, WHO.
2. E. Hansen and C. Lassen, *Lead Review*, in *Report prepared by COWI for the Nordic Council of Ministers. January*. 2003.
3. N.T. Program, *11th Report on carcinogens: lead and lead compounds*. 2004, National Toxicology Program.
4. M.W. Shannon, D. Best, H.J. Binns, J.J. Kim, L.J. Mazur, W.B. Weil Jr, C.L. Johnson, D.W. Reynolds, and J.R. Roberts, Lead Exposure in Children: Prevention, Detection, and Management, Pediatrics 116 (2005) 1036-1046.
5. www.epa.gov.uk.
6. www.who.int/watersanitationhealth/industrypollution.
7. F. Lo Coco, P. Monotti, S. Rizzotti, and L. Ceccon, Determination of lead in oil products by derivative potentiometric stripping analysis, Analytica Chimica Acta 386 (1999) 41-46.
8. M.F. Gard, S. Electron, and O.H. Perry, A status report on environmental monitoring, Instrumentation and Measurement, IEEE Transactions on 51 (2002) 782-785.
9. K.P. Raven, J.W. Reynolds, and R.H. Loeppert, Trace element analyses of fertilizers and soil amendments by axial-view inductively-coupled plasma atomic emission spectrophotometry, Communications in soil science and plant analysis 28 (1997) 237-257.
10. www.cosmeticsdesign-europe.com.
11. European Directive 2002/96/EC, Official Journal of the European Union L37 (2003) 24-38.
12. European Directive 88/378/EEC, Official Journal of the European Community L187 (1988) 1-13.
13. Regulation (EC) No 1907/2006, Official Journal of the European Union L396 (2006) 1-849.

14. European Directive 98/70/EC, Official Journal of the European Community L350 (1998) 58-67.
15. European Directive 1999/31/EC, Official Journal of the European Community L182 (1999) 1-19.
16. *Brussels rules OK*, in *The Economist*. 20th Sept 2007.
17. A.I. Vogel and G.H. Jeffery, Vogel's textbook of quantitative chemical analysis. Longman Scientific & Technical Harlow, Essex, England,1989.
18. D.C. Harris, Quantitative Chemical Analysis. W H Freeman and Company, New York,1995.
19. S. Rapsomanikis, O.F.X. Donard, and J.H. Weber, Speciation of lead and methyllead ions in water by chromatography/atomic absorption spectrometry after ethylation with sodium tetraethylborate, Analytical Chemistry 58 (1986) 35-38.
20. M. McCarrick, B. Wu, S.J. Harris, D. Diamond, G. Barrett, and M.A. McKervey, Chromogenic ligands for lithium based on calix [4] arene tetraesters bearing nitrophenol residues, Journal of the Chemical Society, Perkin Transactions 2 1993 (1993) 1963-1968.
21. R. Jenkins, X-ray fluorescence spectrometry. Wiley New York,1999.
22. D.S. Forsyth, R.W. Dabeka, and C. Cleroux, Ionic Alkyl-Lead, Tetra-Alkyl-Lead and Total Lead in Fish from the Great-Lakes, Applied Organometallic Chemistry 4 (1990) 591-597.
23. M.S. Fragueiro, F. Alava-Moreno, I. Lavilla, and C. Bendicho, Determination of tetraethyllead by solid phase microextraction–thermal desorption–quartz furnace atomic absorption spectrometry, J. Anal. At. Spectrom 15 (2000) 705-709.
24. G. O'Connor, L. Ebdon, and E.H. Evans, Qualitative and quantitative determination of tetraethyllead in fuel using low pressure ICP-MS, J. Anal. At. Spectrom 14 (1999) 1303–1306.
25. A.J. Bard and L.R. Faulkner, Electrochemical methods: fundamental and applications. Wiley-India,1980.

26. A.S. Baranski and H. Quon, Potentiometric stripping determination of heavy metals with carbon fiber and gold microelectrodes, Analytical Chemistry 58 (1986) 407-412.
27. G. Sanna, M.I. Pilo, P.C. Piu, A. Tapparo, and R. Seeber, Determination of heavy metals in honey by anodic stripping voltammetry at microelectrodes, Analytica Chimica Acta 415 (2000) 165-173.
28. S.M. Lee and W.Y. Lee, Determination of heavy metal ions using conductometric biosensor based on sol-gel-immobilized urease, Bull. Korean Chem. Soc 23 (2002) 1169-1172.
29. W. Yantasee, Y. Lin, T.S. Zemanian, and G.E. Fryxell, Voltammetric detection of lead (ii) and mercury (ii) using a carbon paste electrode modified with thiol self-assembled monolayer on mesoporous silica (SAMMS), The Analyst 128 (2003) 467-472.
30. M. Lerchi, E. Bakker, B. Rusterholz, and W. Simon, Lead-selective bulk optodes based on neutral ionophores with subnanomolar detection limits, Analytical Chemistry 64 (1992) 1534-1540.
31. C.K. Ho, A. Robinson, D.R. Miller, and M.J. Davis, Overview of Sensors and Needs for Environmental Monitoring, Sensors 5 (2005) 4-37.
32. K. Liu and H.F. Ji, Detection of Pb 2+ Using a Hydrogel Swelling Microcantilever Sensor, Analytical Sciences 20 (2004) 9-11.
33. M. Zevin, R. Reisfeld, I. Oehme, and O.S. Wolfbeis, Sol-gel-derived optical coatings for determination of chromate, Sensors and actuators. B, Chemical 39 (1997) 235-238.
34. A. Flamini and A. Panusa, Development of optochemical sensors for Hg (II), based on immobilized 2-(5-amino-3, 4-dicyano-2H-pyrrol-2-ylidene)-1, 1, 2-tricyanoethanide, Sensors and Actuators B: Chemical 42 (1997) 39-46.
35. B. Wang and M.R. Wasielewski, Design and synthesis of metal ion-recognition-induced conjugated polymers: an approach to metal ion sensory materials, J. Am. Chem. Soc 119 (1997) 12-21.

36. I.M. Steinberg, A. Lobnik, and O.S. Wolfbeis, Characterisation of an optical sensor membrane based on the metal ion indicator Pyrocatechol Violet, Sensors & Actuators: B. Chemical 90 (2003) 230-235.
37. O. Wolfbeis, Fibre Optic Chemical Sensors and Biosensors, vol 1. CRC Press,1991, p 65.
38. D. Kieslinger, S. Draxler, K. Trznadel, and M.E. Lippitsch, Lifetime-based capillary waveguide sensor instrumentation, Sensors and Actuators. B, Chemical 39 (1997) 300-304.
39. C. Malins, M. Niggemann, and B.D. MacCraith, Multi-analyte optical chemical sensor employing a plastic substrate, Measurement Science and Technology 11 (2000) 1105-1110.
40. T. Mayr, I. Klimant, O.S. Wolfbeis, and T. Werner, Dual lifetime referenced optical sensor membrane for the determination of copper (II) ions, Analytica Chimica Acta 462 (2002) 1-10.
41. C. Huber, I. Klimant, C. Krause, and O.S. Wolfbeis, Dual lifetime referencing as applied to a chloride optical sensor, Anal. Chem 73 (2001) 2097-2103.
42. J.R. Lakowicz, Principles of Fluorescence Spectroscopy, 3rd ed.,Springer, 2006.
43. L.L. Salins, E.S. Goldsmith, M.C. Ensor, and S. Daunert, A fluorescence-based sensing system for the environmental monitoring of nickel using the nickel binding protein from Escherichia coli, Analytical and Bioanalytical Chemistry 372 (2002) 174-180.
44. A. MacLean, C. Moran, W. Johnstone, B. Culshaw, D. Marsh, and P. Parker, Detection of hydrocarbon fuel spills using a distributed fibre optic sensor, Sensors & Actuators: A. Physical 109 (2003) 60-67.
45. W.C. Michie, B. Culshaw, M. Konstantaki, I. McKenzie, S. Kelly, N.B. Graham, and C. Moran, Distributed pH and water detection using fiber-optic sensors andhydrogels, Lightwave Technology, Journal of 13 (1995) 1415-1420.

46. J. Rayss and G. Sudolski, Ion adsorption in the porous sol–gel silica layer in the fibre optic pH sensor, Sensors & Actuators: B. Chemical 87 (2002) 397-405.
47. T. Grady, T. Butler, B.D. MacCraith, D. Diamond, and M.A. McKervey, Optical Sensor for Gaseous Ammonia With Tuneable Sensitivity, The Analyst 122 (1997) 803-806.
48. G. Whitenett, G. Stewart, K. Atherton, B. Culshaw, and W. Johnstone, Optical fibre instrumentation for environmental monitoring applications, J. Opt. A: Pure Appl. Opt 5 (2003) S140-S145.
49. A. Cheung, W. Johnstone, and D. Moodie, Detection of acetylene gas using optical correlation spectroscopy, Proc. SPIE 5855 (2005) 475-478.
50. K. Noda, M. Takahashi, R. Ohba, and S. Kakuma, Measurement of methane gas concentration by detecting absorption at 1300 nm using a laser diode wavelength-sweep technique, Optical Engineering 44 (2005) 014301 - 014301-6.
51. M. Fneer, J. Kurata, W.J.O. Boyle, and K.T.V. Grattan, Optical fibre ammonia sensor for water quality measurements, 11th Proceedings of Optical Fibre Sensors (1996) 438-441.
52. A. Cheung, W. Johnstone, and D. Moodie, Gas detection based on optical correlation spectroscopy using a single light source, Meas. Sci. Tech 17 (2006) 1107-1112.
53. A. Beeby, D. Parker, and J.A.G. Williams, Photochemical investigations of functionalised 1, 4, 7, 10-tetraazacyclododecane ligands incorporating naphthyl chromophores, J. Chem. Soc., Perkin Trans. 2 (1996) 1565-1579.
54. A.A. Istratov and O.F. Vyvenko, Exponential analysis in physical phenomena, Review of Scientific Instruments 70 (1999) 1233-1257.
55. Z. Zhang, K.T.V. Grattan, Y. Hu, A.W. Palmer, and B.T. Meggitt, Prony's method for exponential lifetime estimations in fluorescence-based thermometers, Review of Scientific Instruments 67 (1996) 2590-2594.

56. L.J. Dowell and G.T. Gillies, Errors caused by baseline offset and noise in the estimation of exponential lifetimes, Review of Scientific Instruments 62 (1991) 242-243.
57. D.J.S. Birch, O.J. Rolinski, and D. Hatrick, Fluorescence lifetime sensor of copper ions in water, Review of Scientific Instruments 67 (1996) 2732-2737.
58. K.T.V. Grattan, R.K. Selli, and A.W. Palmer, Ruby decay-time fluorescence thermometer in a fiber-optic configuration, Review of Scientific Instruments 59 (1988) 1328-1335.
59. L. Rosso and V.C. Fernicola, Time-and frequency-domain analyses of fluorescence lifetime for temperature sensing, Review of Scientific Instruments 77 (2006) 034901 - 034901-6.
60. N.I. Nijegorodov and W.S. Downey, The Influence of Planarity and Rigidity on the Absorption and Fluorescence Parameters and Intersystem Crossing Rate Constant in Aromatic Molecules, The Journal of Physical Chemistry 98 (1994) 5639-5643.
61. S.F. Collins, G.W. Baxter, S.A. Wade, T. Sun, K.T.V. Grattan, Z.Y. Zhang, and A.W. Palmer, Comparison of fluorescence-based temperature sensor schemes: Theoretical analysis and experimental validation, Journal of Applied Physics 84 (1998) 4649-4654.
62. K. Cherif, S. Hleli, A. Abdelghani, N. Jaffrezic-Renault, and V. Matejec, Chemical detection in liquid media with a refractometric sensor based on a multimode optical fibre, Sensors 2 (2002) 195-204.
63. J. Homola, S.S. Yee, and G. Gauglitz, Surface plasmon resonance sensors: review, Sensors & Actuators: B. Chemical 54 (1999) 3-15.
64. J. Homola, Surface Plasmon Resonance Based Sensors, vol 4. Springer, Berlin,2006, p 251.
65. J. Homola, Optical fiber sensor based on surface plasmon excitation, Sensors & Actuators: B. Chemical 29 (1995) 401-405.

66. T. Tanaka, C. Wang, V. Pande, A.Y. Grosberg, A. English, S. Masamune, H. Gold, R. Levy, and K. King, Polymer gels that can recognize and recover molecules, Faraday Discussions 101 (1996) 201-206.
67. H.J. Linden, S. Herber, W. Olthuis, and P. Bergveld, Stimulus-sensitive hydrogels and their applications in chemical (micro) analysis, The Analyst 128 (2003) 325-331.
68. J.H. Holtz and S.A. Asher, Polymerized colloidal crystal hydrogel films as intelligent chemical sensing materials, Nature 389 (1997) 829-832.
69. S.A. Asher, A.C. Sharma, A.V. Goponenko, and M.M. Ward, Photonic crystal aqueous metal cation sensing materials, Anal. Chem 75 (2003) 1676-1683.
70. Z. Shakhsher, W.R. Seitz, and K.D. Legg, Single Fiber-Optic pH Sensor Based on Changes in Reflection Accompanying Polymer Swelling, Analytical Chemistry 66 (1994) 1731-1735.
71. L. Zhang, M.E. Langmuir, M. Bai, and W. Rudolf Seitz, A sensor for pH based on an optical reflective device coupled to the swelling of an aminated polystyrene membrane, Talanta 44 (1997) 1691-1698.
72. M.F. McCurley, An optical biosensor using a fluorescent, swelling sensing element, Biosensors & bioelectronics 9 (1994) 527-533.
73. T. Erdogan, Fiber grating spectra, Lightwave Technology, Journal of 15 (1997) 1277-1294.
74. K.O. Hill, G. Meltz, C.R. Center, and O. Ottawa, Fiber Bragg grating technology fundamentals and overview, Lightwave Technology, Journal of 15 (1997) 1263-1276.
75. V. Mizrahi and J.E. Sipe, Optical properties of photosensitive fiber phase gratings, Lightwave Technology, Journal of 11 (1993) 1513-1517.
76. V. Bhatia, Applications of long-period gratings to single and multi-parameter sensing, Optics Express 4 (1999) 457-466.
77. J.H. Chang, Y.M. Choi, and Y.K. Shin, A Significant Fluorescence Quenching of Anthrylaminobenzocrown Ethers by Paramagnetic Metal Cations, Bull. Korean Chem. Soc 22 (2001) 527-530.

78. R. Hou, Z. Ghassemlooy, A. Hassan, C. Lu, and K.P. Dowker, Modelling of long-period fibre grating response to refractive index higher than that of cladding, Measurement Science and Technology 12 (2001) 1709-1713.
79. S.W. James and R.P. Tatam, Optical fibre long-period grating sensors: characteristics and application, Meas. Sci. Technol 14 (2003) R49-R61.
80. A.M. Vengsarkar, P.J. Lemaire, J.B. Judkins, V. Bhatia, T. Erdogan, and J.E. Sipe, Long-period fiber gratings as band-rejection filters, Lightwave Technology, Journal of 14 (1996) 58-65.
81. Y.J. Rao, M.R. Cooper, D.A. Jackson, C.N. Pannell, and L. Reekie, Absolute strain measurement using an in-fibre-Bragg-grating-basedFabry-Perot sensor, Electronics Letters 36 (2000) 708-709.
82. T.L. Yeo, T. Sun, K.T.V. Grattan, D. Parry, R. Lade, and B.D. Powell, Characterisation of a polymer-coated fibre Bragg grating sensor for relative humidity sensing, Sensors & Actuators: B. Chemical 110 (2005) 148-156.
83. H.J. Patrick, A.D. Kersey, and F. Bucholtz, Analysis of the response of long period fiber gratings to externalindex of refraction, Lightwave Technology, Journal of 16 (1998) 1606-1612.
84. Y. Liu, L. Wang, M. Zhang, D. Tu, X. Mao, and Y. Liao, Long-Period Grating Relative Humidity Sensor With Hydrogel Coating, Photonics Technology Letters, IEEE 19 (2007) 880-882.
85. J.L. Elster, J.A. Greene, M.E. Jones, T.A. Bailey, S.M. Lenahan, and I. Perez, Optical Fiber-Based Corrosion Sensors for Aging Aircraft, DoD/FAA/NASA Conference on Aging Aircraft, Williamsburg, VA (1998).
86. J.L. Elster, J.A. Greene, M.E. Jones, T.A. Bailey, S.M. Lenahan, W.H. Velander, R. VanTassell, W. Hodges, and I.M. Perez, Optical-fiber-based chemical sensors for detection of corrosion precursors and by-products, Proceedings of SPIE 3540 (2003) 251-257.

Chapter 2

Instrumentation and Measurements

2.1. Introduction

In this chapter I describe in detail the major components making up a fibre optic chemical sensor (FOCS). For each component, the choices available on the market are considered and the selection of a particular component in subsequent experiments justified. In addition, the design and assembly of a filter holder, a crucial component in fluorescence experiments carried out in this work, is described.

The set-up of the experiments that have been performed for this research and which are described in later chapters is shown diagrammatically in this chapter. Examples of existing set-ups used in published work are provided and all the set-ups are shown to be of the same generic type.

Finally, the chapter ends with the reference schemes used here. No robust sensors for field applications can be designed without incorporating a safeguard against undesired signal modification by external parameters. We show that implementation of a reference scheme need not be complex and demanding if this is done at the software layer.

2.2. FOCS major components

A fibre optic chemical sensor consists of three main units:

- The light transducer
- The light detector
- The light source

2.2.1. The transducer

The transducer is the chemical substance that will change a parameter of the optical signal from the light source as a function of the concentration of another chemical substance (analyte). It is also known as the indicator or reagent in chemical sensing. The analyte may be the hydrogen ion, thus leading to pH measurement or other ions. It can also be a molecule to be detected, the most popular being glucose since it is an important physiological component and has important implications in both high and low amounts in the human body [1, 2].

The optical parameter to be modulated by the indicator may be the intensity, the wavelength, the phase or the polarisation of the light wave. We restrict our investigation to the intensity as this is the parameter affected by the reagents used in this thesis. The chemical transducers or indicators used are discussed in more detail in later chapters.

2.2.2. The detector

The purpose of the detector is to measure the changes in the optical parameter being measured. To know that a change has occurred, knowledge of the parameter before said modification is required.

Silicon photodiodes are low-cost detectors with high sensitivity in the visible wavelength regions. For higher sensitivity, avalanche photodiodes and photo-

multiplier tubes (PMT) may be used but require very high operating voltage which may be a safety hazard. The PMT detection surface is so sensitive that it must be protected from direct light otherwise it will be irreversibly damaged [3]. Any of these detectors measure the total optical intensity without regards to the wavelength at which it occurs, thus losing a large amount of information.

A better option is to measure the intensity at the wavelength at which it occurs by using a spectrometer as detector system. The spectrometer essentially breaks down the light into its wavelength constituent and measures the intensity at particular wavelength values using an array of charge-coupled devices (CCD). Because the spectrometer is an important part of the sensor and has been used throughout this work, it is worthwhile to look at its functionality to better understand the working and limitation of the sensor system.

The spectrometer used in this work is the USB2000 from Ocean [4]. This device, while not as sensitive as a photo-multiplier tube (PMT), feature several advantages over it:

1. Its small size and compactness makes it highly portable.
2. Its USB connection makes it a ‘plug and play’ device – easy and quick – and obtains its operational power supply directly from the PC or laptop. No external power supply is needed.
3. It contains no moving mechanical parts, making it rugged and adapted to field use if necessary.
4. It may be operated using the LabVIEW software, harnessing all the powerful attributes of that programming language: data acquisition and data processing in an easy to use graphical environment [5].

An illustration of how the spectrometer operates is given in Fig. 2.1 to help explain its main features and options available.

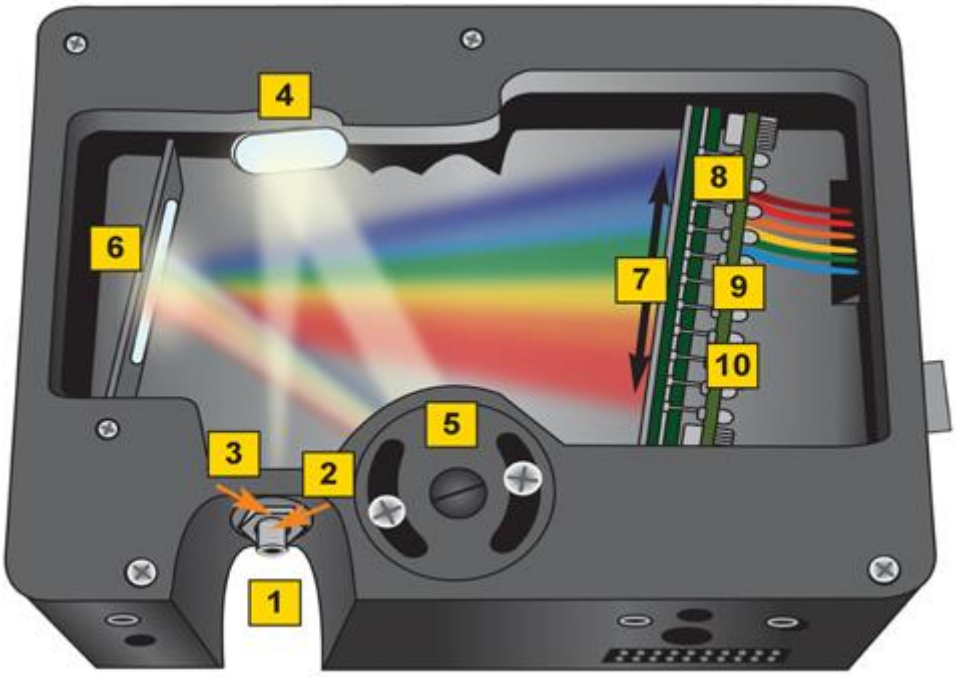

Fig. 2.1. The interior of the compact spectrometer from Ocean Optics [4].

The optical bench is designed to minimise stray light inside the device by painting it a dull black to absorb stray light and has side protrusions added to its geometrical design to trap the stray light as well.

1. The SMA connector holds the fixed slit and the long-pass filter in position

2. The fixed slit is a 1mm high rectangular window which affects the sensitivity and resolution of the spectrometer. A narrow slit (min 5μm, max

200μm) allows only very little light through. Since we are interested in intensity measurement, the maximum slit size of 200 μm is used.

3. A longpass filter may be included at this point to restrict the light to within a certain range. This option renders the sensor system more compact if a filter needs to be included. This option was not used as it can only be modified by the manufacturer and does not provide flexibility with the set-up at this experimental stage.

4. Once the light guided by the fibre passes through the rectangular slit, it is incident upon the mirror #4 which reflects it into a collimated beam of light. The mirror may be made UV-absorbing. This is useful if a UV excitation light is used in a fluorescence measurement set-up where some excitation light may enter the spectrometer and cause second and third order effects.

5. The grating is installed at this location and may be rotated to select the starting wavelength desired and then fixed into position permanently. The grating may be specified in terms of the grove density, i.e. the number of lines per cm which determines the spectral range.

6. After the light strikes the grating, it is diffracted upon mirror #6 which reflects the diffracted light towards the detector elements.

7. A cylindrical lens may be placed here to focus the light onto the detector. Each pixel is only 200μm high while the slit at the spectrometer entrance is 1000μm high. A large amount of light is wasted unless a lens is used. The lens is only useful if the fibre diameter at the entrance is greater than the pixel height. In our case, since a 6x200 μm fibre bundle or a 600 μm single fibre is used, the cylindrical lens has been incorporated.

8. The diffracted light passes through the cylindrical lens and strikes a CCD array made up of 2048 pixel elements where conversion into electrons takes place.

9. A long-pass order-sorting filter may be placed in front of the detector to block second and third order light. A band-pass interference filter is used externally in our set-up to remove any excitation light so the order-sorting filter is not needed.

10. The detector window may be replaced with quartz glass for detection of light less than 340nm. Since all measurements are made in the visible spectrum from 400-700 nm, this is not necessary.

11. The resolution of the spectrometer was 5 nm and this was adequate for the wavelength range under consideration, namely of the order of 20 nm and more.

These ten stages and options describe how the spectrometer works and how it is possible to optimise it for a particular application. In our case, it has been optimised for the detection of visible light by using a wide slit, a grating with low groove density and a collection lens at the detector to maximise light detection. Gratings with high reflectivity improves the amount of light diffracted back but also leads to more stray light within the spectrometer.

2.2.3. The light source

A light source is necessary to provide the interrogating light that will be modified by the indicator and eventually reach the detector and be converted into an electrical signal for data processing. Because of losses in the system, the interrogating light must be intense enough initially to be able to reach the

detector. Major sources of loss are during coupling of the light from the source to the fibre and especially at the transducer end.

The light source may sometimes be too intense, resulting in photo-bleaching or photo-degradation of the indicator. Photo-bleaching is usually a negative effect but has been exploited to provide information on the rate of diffusion of fluorophores in solution [6]. If a fluorophore is first irreversibly photobleached, then the rate of increase of fluorescence arising from the diffiusion of more fluorophores into the region of interest has been measured. Sensors have also been built around this effect. Hartmann *et al* have exploited the effect of oxygen on accelerating the photobleaching of a ruthenium complex to design an oxygen probe [7]. Superbright LEDs were used to produce a decrease in the emission intensity and lifetime which were found to be function of the oxygen concentration.

In sensors where intensity modulation occurs, specialised light sources with features such as polarisation, monochromaticity, coherence and tight collimated beams are not necessary. This precludes lasers which may also be high-powered, requiring external cooling systems. A current driver and temperature control to provide stable laser output are also sometimes necessary, which leads to a high financial price-tag.

As a result, the focus is on LEDs to provide the interrogating light. The coupling efficiency to fibres is low due to the mismatch in size but may be improved upon by using a system of lenses. However, as long as the LED provides sufficient intensity of light launched into the fibre, the coupling efficiency is not an issue. Nowadays, LEDs are available in a wide selection of wavelengths down to the deep UV [8] and at high optical power [9]. In all cases, the price of an LED is negligible to that of a laser, providing much of an incentive in incorporating it in a fibre optic sensor design. It is also hard for an LED to lead to the photo-degradation of an indicator.

The advantages associated with LEDs are:

- Low power consumption
- Long lifetime
- Ease of modulation
- Mechanical strength
- Small compact size

The main disadvantage is a low level of coupling to the fibre.

The disadvantages of lasers used in previous work, i.e. those that are not semi-conductor lasers, are that they are bulky devices with high power requirements and are expensive. For a sensor that aims to be small, compact and portable, lasers used in previous work are not suitable.

Admittedly, laser diodes do not suffer from these disadvantages and further offer the advantages of all lasers, namely highly collimated and monochromatic light but the wavelengths available do not cover as wide a range as LEDs. Laser diodes are currently sparse in the blue and UV region. Power level is not considered here as it can be both an advantage for lasers when high optical output is required and a disadvantage when the reagent is susceptible to photo-bleaching. The operating principles of LEDs and semiconductor lasers are covered in detail by Singh [10].

For fluorescence experiments in this work, a 435nm dominant wavelength 5mm diameter LED has been selected. Its spectral output is shown in Fig. 2.2. An operating temperature range of -30 to 80°C quoted by the supplier makes it suitable for environmental applications in harsh climates. The optical power is 10mW with a viewing angle of 28 degrees and a FWHM of 20nm. Higher power LEDs are available from Lumileds [9], for e.g., but the required wavelength is

not on offer and the viewing angle is rather large at 110 degrees, thus dispersing the optical power. The optical power output of LEDs from Lumileds is available in the hundreds of mW, which is of the same magnitude as the optical output of some laser diodes [11]. However, Wolfbeis noted that when the laser power into an optical fibre exceeded a certain limit, typically 100mW, intense stimulated Raman scatter would occur and interfere with the analytical signal [12]. Thus, high optical power causes not only photo-degradation of the indicator but also strong background noise.

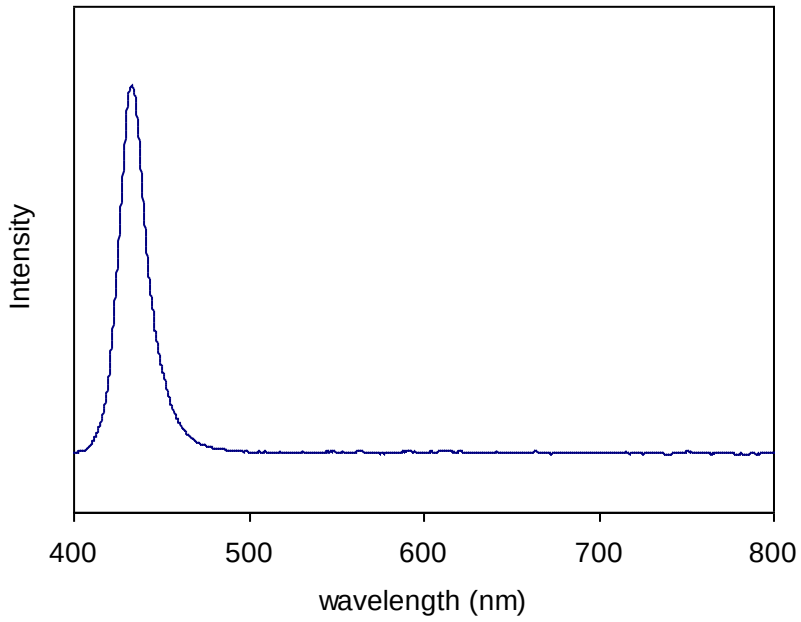

Fig. 2.2 Spectral output of the LED as seen in the visible wavelength range

The viewing angle affects the coupling efficiency of the LED output to the optical fibre. To maximise this, the selected LED has a narrow viewing angle and an LED lamp-house, supplied by Comer Optics (Cambridge) is used to focus the diverging beam from the LED onto the distal end of the fibre. The lamp-house is fitted with a system of collimating lenses for this purpose and is terminated with an SMA connector to provide a firm anchoring point for an SMA-terminated fibre. It also contains an LED-holder which may be slid in and

out of the lamp-house to adjust the focussing distance to the lenses. The LED is powered by a stable dc power supply from Thurlby Thandar Instruments.

For absorbance and reflectance measurements, a white light source is required. Although a white LED is sufficient for this task, a broadband tungsten halogen white light source complete with driver system, lens and SMA connector from Ocean Optics, model LS-1, was readily available and used for this task simply by plugging in to the mains voltage.

2.2.4. Optical fibres

Multimode fibres are usually favoured in intensity-based FOCS. Single-mode fibres, with their small core, around 5 μm diameter for standard telecoms fibre compared to up to 1mm for multimode fibres, make it difficult to collect and launch light into them. To maximise the amount of light that can be launched in a fibre, a large core with a large numerical aperture is necessary.

Multimode fibres are more affected by modal dispersion compared to single-mode fibres. However, for many sensor applications, optical fibre dispersion is not significant [13]. There are other more important factors such as indicator time response and external light scattering and absorption which will affect the performance of the sensor.

Modal dispersion is a result of modes suffering from a propagation time delay due to multiple propagation paths possible in large fibre cores. This can be understood geometrically by using the ray concept. A ray of light undergoing multiple internal reflections within the fibre core will travel a longer distance than a ray travelling parallel to the core axis. Thus, if the two light rays have been launched into the fibre at the same time, they will reach the end of the fibre at different times. Modal dispersion is a negligible source of error when a time-critical scheme is not used and especially where the fibre length is short.

Chromatic dispersion arises due to the fact the refractive index of any optical material varies with wavelength. Thus if broadband light is launched into a fibre, each wavelength will 'see' a different refractive index and propagate at a different velocity, all eventually reaching the detector at different time. Chromatic dispersion is also not critical in FOCS for the reasons mentioned above.

Rayleigh scattering is negligible in non-UV wavelength propagation. Rayleigh scattering is the dispersion of light by molecules having a diameter smaller than the wavelength of light encountering them. As Rayleigh scattering is proportional to $1/\lambda^4$, it becomes more important at shorter wavelengths. An optical fibre sensor can avoid Rayleigh scattering by operating in the visible spectrum. Light sources are also more readily available in that spectrum.

In general, intrinsic losses from optical fibres are negligible from a system design point of view compared to other external optical losses. Consider a fibre probe with a thin sol-gel coating on its distal end. If the sol-gel is doped with a fluorophore and excitation light is sent down the fibre probe, fluorescence arising from the doped sol-gel coating will be emitted in all direction. Only a fraction of this emission will be captured and propagated along the fibre to the detector. In the case of reagent-coated beads attached to the end of a fibre probe, interrogating light from the fibre probe is scattered by those beads and not all are guided back into the fibre to the detector. It is therefore useful to put into perspective such these losses alongside other intrinsic losses.

External losses such as fibre bending are non-negligible and may affect readings if the fibre is severely bent. This problem may be remedied to some extent by the use of referencing techniques discussed in section 2.4. Photosensitivity of optical fibres by nuclear or UV radiation is another example, best avoided by the use of UV-resistant fibres if operating in an environment where such radiations may occur.

All fibres used in this work were step-index multimode with a numerical aperture (NA) of 0.37 and consisting of a silica core and a hard polymer cladding. The fibre bundle consisted of a 200μm core diameter fibre on one branch and 6 fibres of the same diameter on the other branch, all joined together at the third end with the 6 fibres grouped around the fibre from the single end. Since the light from the analyte is usually a limiting factor, the six surrounding fibres are used for collection of a maximum amount of light while the central fibre is used to guide the interrogating light. The transmission profile of the fibres is shown below in Fig. 2.3. The sensor probe consists of a short length of 600μm core diameter fibre whose distal ends are polished. The diameter of the fibre probe is approximately equal to the diameter of the fibre bundle which consists of three 200μm fibres side by side.

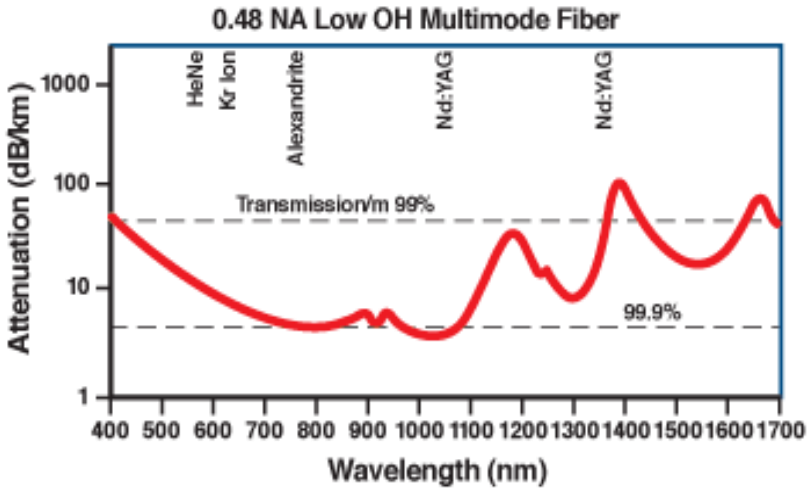

Fig. 2.3. Transmission profile of the multimode fibres used [14].

The advantage of using a fibre to stimulate fluorescence at its distal end and collect it at the same end is that there is an almost perfect geometrical overlap of excitation light and emission light cones, resulting in high efficiency. This is

depicted diagrammatically in Fig. 2.4. A fluorophore molecule within the numerical aperture of the fibre is able to get excited and emit light, some of which will get propagated along the fibre. Any fluorophore *outside* the numerical aperture will *not* undergo excitation nor will any emission be propagated along the fibre, in the case of chemiluminescence. The refractive indices of the core and cladding will be smaller for longer wavelength fluorescence but this can be negligible within real-life applications for fluorescence with short Stokes shift, as is the case in this work. This is set out below.

The NA is defined as

$$NA = n_{air} \sin\theta = \sqrt{n_{core}^2 - n_{clad}^2} \tag{2.1}$$

Where n_{air}, n_{core} and n_{clad} are the refractive index of air, core and cladding respectively and θ is the angle from the normal as shown in Fig. 2.4.

The core refractive indices at 700nm and 808nm are 1.455 and 1.453 respectively [14] and the cladding index is constant at 1.398. Refractive index values at the excitation and emission wavelengths used later in this work are around 70nm apart. Here we have selected values 100nm apart as a worse-case scenario.

Using the relationship in (1), the NA may be calculated at 700nm and 808nm respectively. Assuming the external refractive index to be that of water in the case of an aqueous sample and constant at 1.33, there is a decrease of less than 2% in the value of θ when moving from 700nm to 808nm. Taking into consideration the fact that the refractive index of water is smaller at 808nm than at 700nm, yields a larger value of θ at 808nm, making the change in angle even smaller.

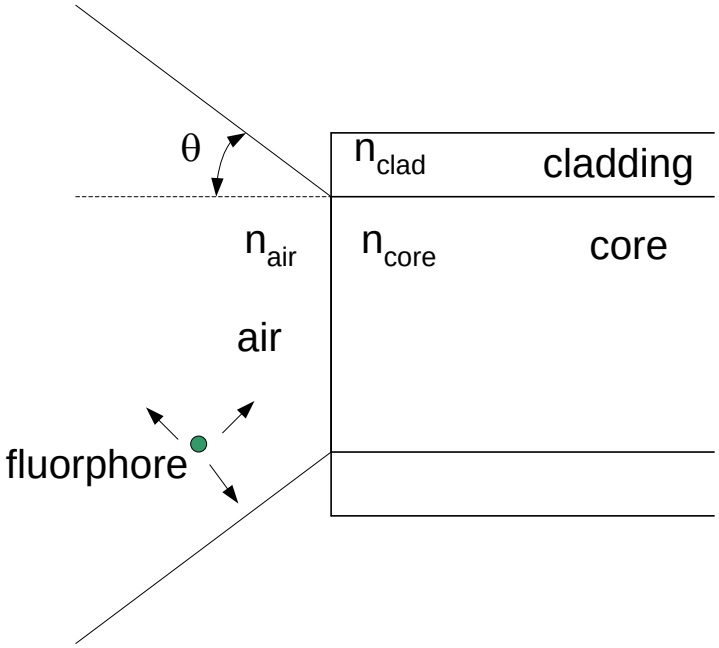

Fig. 2.4. Geometrical overlap of excitation and emission light cones

Single fibres are not a good choice in reflectometry because the fibre efficiently collects specularly reflected light in addition to diffusely scattered light [12]. It was noticed from the work described in the next chapter that a single probe connected to the end of a fibre bundle would give rise to a large amount of total internal reflection at the distal end, thus swamping the reflected signal. This internal reflection was confirmed by coating the end surface with index-matching gel which effectively destroyed the plane surface which acted as a mirror. No reflection was then detected.

In double fibre configurations, Louch *et al* found that an angle of 20 degrees between the two fibres gave an optimum SNR [15]. It is not convenient in practice, however, to work with fibres set at this angle, especially when a miniaturised probe is required.

2.3. Experimental set-up

The overall general experimental arrangement is shown below in Fig. 2.5 and Fig.2.6, modified slightly depending on the objectives. For reflectance measurement, a white light source is used and the interference filter removed. For fluorescence measurement, an appropriate LED in its lamp-house as shown here in the figure is used.

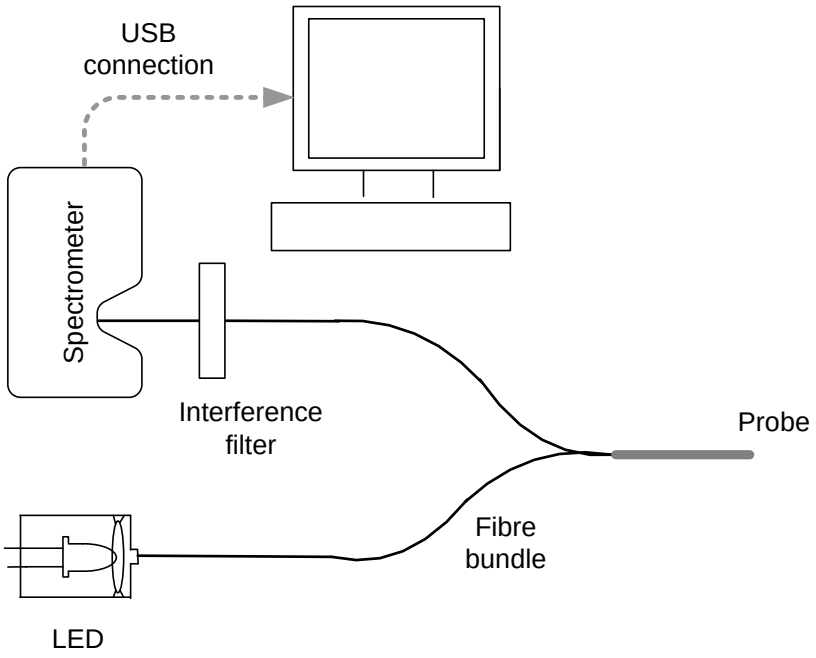

Fig. 2.5. Layout of the main components. The light source sends an interrogating light down the fibre bundle to the probe where it is modulated and guided back to the spectrometer which will measure its intensity. The computer collects and processes the data from the spectrometer using the LabVIEW software. The interference filter may be used to separate excitation light from emission in the case of fluorescence measurements.

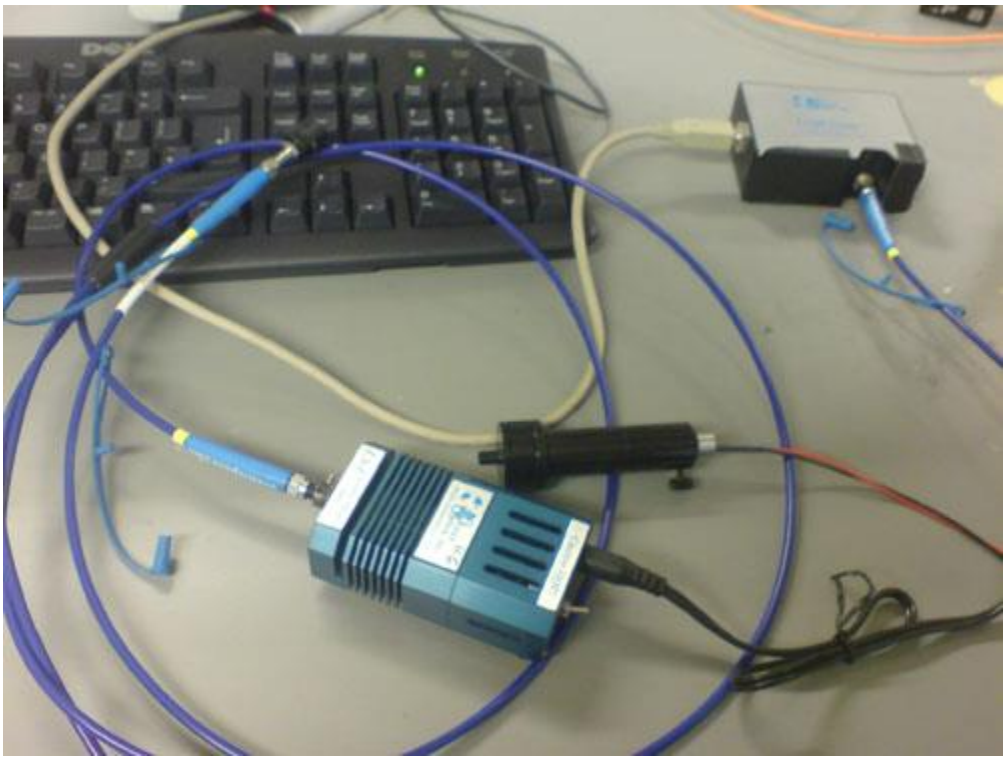

Fig. 2.6. Picture of the main components showing the white light source in blue in the centre, the LED housing in black to its right, the fibre bundle in a blue jacket, the spectrometer at the top right of the picture and connected to the computer (not shown) via the white USB cable seen here.

The light from the light source is focused onto the fibre bundle end by means of a lens incorporated within the light source unit. The branch of the fibre bundle made up of 1 fibre is used to guide the interrogating light from the light source to the probe and the branch made of 6 fibres is used to collect light from the probe end to the spectrometer. This is because we want to detect as much light as possible and therefore use a large collection of fibre at the probe end to maximise the amount of light guided to the spectrometer. Given that there are 7 fibres connected to the probe and that light will be equally propagated within each of the 7 fibres, 6/7 of the propagated light intensity ends up at the detector where it will be measured. If the fibre bundle connections had been reversed

with a single fibre connected to the spectrometer end, then only 1/7 of the propagated light intensity would have ended up at the spectrometer.

The spectrometer measures the light intensity and is connected to the computer via a USB connection to give an output. The LabVIEW software is used to process and present the data from the spectrometer. The data from the spectrometer is essentially an array of intensity and wavelength fed to the computer in real time. It is therefore possible to extract various pieces of information from this array of data for analysis by simply modifying the LabVIEW programme. Such information can be the peak intensity with time, the wavelength of the peak intensity, the summation of the intensity over a specified range of wavelength or the plot of intensities at specific wavelength versus time. The ratio of one intensity to another can also be performed easily within LabVIEW. The LabVIEW VIs (Virtual Instruments) for each experiment run are shown in Chapters 3 and 4 respectively.

An interference filter is added in front of the spectrometer in the case of fluorescence measurements to remove the excitation light. A broadband band-pass interference filter from Comar Optics with centre wavelength at 500nm and FWHM of 40 nm was selected for this.

An expanded view of the filter holder used in conjunction with the interference filter is shown in Fig. 2.7. All parts including lenses were purchased from Comar Optics. The filter holder is designed to be used in line with optical fibres. It is made up of a ball lens at either end to collimate the light from the fibre which acts as a diverging point source and focus the parallel beam of filtered light onto the other fibre end. Once the lenses have been positioned, it is only a matter of unscrewing open the holder in the middle as shown to change filters if desired, without having to move or adjust the lenses. SMA adaptors at both ends provide connection points to the fibres. Due to the way the filter is held

into place by screwing together both halves as shown in the diagram, no stray light is able to go through the other side of the holder.

Ball lenses are used instead of biconvex lenses because the latter has a much longer focal length, usually around tens of *cm* which would make it impractical to build the filter holder. The lenses used here have a focal length of 7.34 mm for a diameter of 10mm, resulting in a back focal length of 2.34 mm. It is important to position the fibre and lens at the right focal length to capture maximum light intensity. To measure accurately that distance, a digital displacement meter from Mitutoyo was employed. The Digimatic Indicator is able to measure displacement up to 3 decimal places in mm which is adequate for our task.

The distance was measured as follows using the half casing on the right in Fig. 2.7 for description purposes. The SMA adaptor with a fibre connected to it was screwed onto the casing. A driving tool was used to screw the lens adaptor close to the end of the holder casing with the ball lens placed to its right until the lens was flush with the fibre end at the SMA adaptor. The fibre was then removed and the tip of the displacement meter inserted into the SMA cavity to make contact with the ball lens. Prior to this the tip of the meter was covered with a plastic covering to protect the lens from scratches. The displacement meter was set to zero in that position and the lens adaptor was slowly unscrewed with the driving tool until the meter read a displacement of 2.34 mm which corresponds to the back focal length of the ball lens. The meter and SMA adaptor were removed, another lens adaptor screwed to the right of the ball lens to fix the latter into place and the SMA adaptor replaced. The whole process was repeated for the other half of the casing.

With this type of assembly, the whole unit is highly modular and flexible. The SMA adaptor may be screwed in or removed and the interference filter changed as necessary without having to disturb the ball lens arrangement. The holder is

also easily connected in-line to optical fibres or removed from the optical path as necessary.

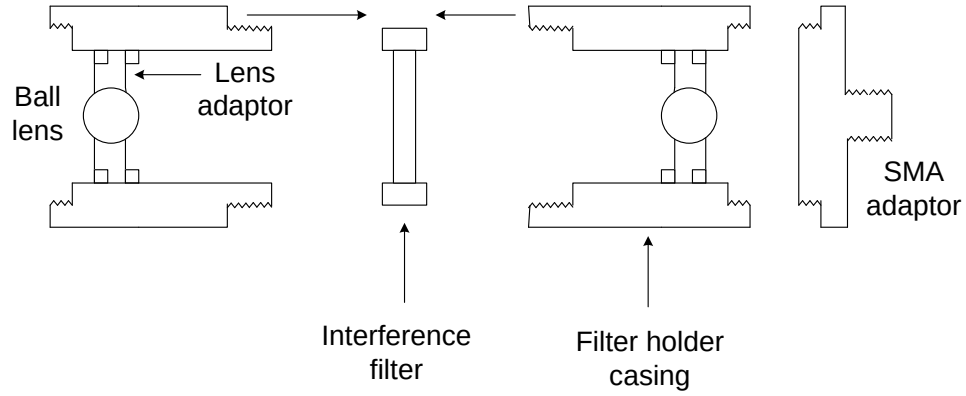

Fig. 2.7. Expanded view of the assembly of the cylindrical filter holder

2.4. Examples of instrumentation and sensor configuration

Before venturing any further, it is helpful to see how the technology described here may be used to greatly simplify a sensor construction.

Stanley and co-researchers have developed an intrinsic optical sensor based on the UV absorption of the nitrate ion [16]. A deuterium lamp was used to provide radiation in the UV spectrum which was then guided to an absorption cell via Fibreguide Industries superguide G UV-transmitting fibres. The researchers used these fibres as UV-resistant fibres are necessary due to the effect of solarisation on ordinary fibres. Detection was made using a photomultiplier tube (PMT) with measurements made at 210nm where nitrate ion absorbs strongly. To cancel the effect of absorption by other species at this

wavelength, a reference absorption measurement was taken at 275nm, a wavelength where the analyte does not absorb. Light at the two wavelengths was made available at separate time period using a filter wheel placed in front of the light source. To record measurements at the two wavelengths, a sample-and-hold amplifier (SHA) synchronised to the rotating filter wheel was used at the output of the amplified PMT signal. The SHA was in turn connected to a PC to take a ratio of the two quantities and enable correlation of the nitrate ion concentration.

This is how the set-up could be simplified using today's easily available technology. A compact CCD spectrometer can be used to measure the intensity over a whole range of wavelengths, including the ones we are interested in. There is also the addition of a software layer (LabVIEW [5]) to do the data processing. The software will take the output of the spectrometer at the two wavelengths and produce a ratio in real time. Because the spectrometer is able to provide the intensity at 210 and 275nm simultaneously, no SHA or rotating filter wheel is necessary. An LED emitting at 210 nm is not yet commercially available so the Deuterium lamp cannot be replaced with an LED.

Klinteberg and coworkers have exploited current modern technology to produce a compact medical fluorosensor described in a recent paper [17]. The point-measuring sensor uses fluorescence as well as white light for tissue characterisation; as such, it consists of two light sources – a nitrogen laser for fluorescence excitation in the near UV and a broadband white light source from Ocean Optics, similar to the one described earlier. A set of filters is mounted on a motorised rotation stage to select the appropriate excitation filter, emission filter or no filter in the case of white light studies.

A schematic diagram and a picture of the set-up are shown in Fig. 2.8. A beam splitter is used to separate excitation radiation from the emission. Optical fibres

guide light between the various optical components; in particular, the probe is made of a plain clear-cut polished fibre end to excite the tissue and capture radiation. The whole unit is computer controlled via LabVIEW which also provides a simple graphical user interface able to be used by non-specialists.

What comes across initially as a complex system is in effect no different from the set-up adopted here. It consisted of two light sources; the detector was a miniaturised CCD spectrometer from Oriel and a set of optical components were used for light coupling. Optical fibres of 600μm diameter were used as light guide and for the non-invasive probe. LabVIEW was also used as interface to facilitate and speed up data processing.

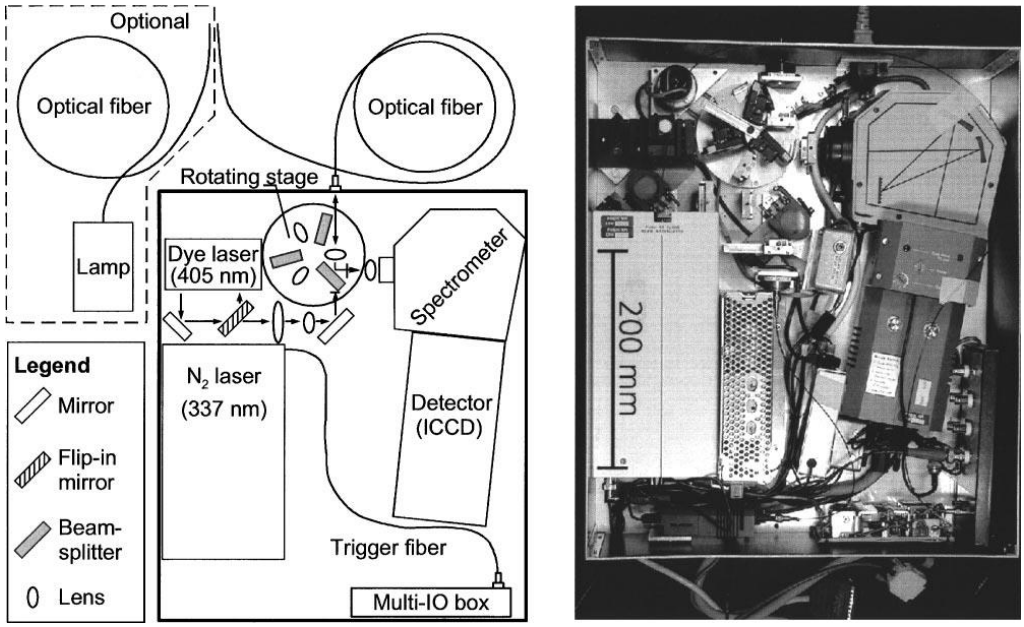

Fig.2.8. Experimental set-up adopted by Klinteberg *et al* [17].

2.5. Measurement technique and reference scheme

Point measurement of the intensity at a particular wavelength is prone to significant background noise level. While it may be assumed that background noise is uniformly distributed, this is not always the case. Sunlight reflected onto a blue piece of material will increase the background intensity in the blue region if leaked into the optical system detection. Mercury discharge lamps are made up of several distinct and very strong intensity spikes at defined wavelengths. If the analyte intensity happens to be at or near these peaks, its measurement will be severely corrupted.

One way to avoid this issue is to measure the change of intensity with time. Plotting the analyte intensity against time and measuring the gradient will directly yield this parameter which may then be correlated with the analyte intensity. Because the gradient is a straight line, its measurement may be done at any point along the line to get the same value.

Another way is to integrate the analyte intensity across a range of wavelength. If the range contains a strong background noise component, its effect over that range is minimised. This is because the analyte intensity measured over a range of wavelengths weakly corrupted by noise is greater than the intensity measured at a particular wavelength subject to strong noise effects, resulting in a better signal to noise ratio.

In the fluorescence measurement experiments, it was initially found that the spectrometer gave a fluctuating dark noise level, i.e. the instrument's electronic noise level was drifting. This is shown in Fig. 2.9a. To correct this significant problem with minimum hardware modification and costs, LabVIEW and the system design was exploited to provide the following solution. The passband interference filter blocks all the light in the region of 390-460nm and displays the instrument dark noise level. We can then measure this dark noise and

subtract it in real-time from the raw intensity measurement made in the passband region, taking care to ensure that the wavelength range taken in the stopband equals that in the passband. A LabVIEW program was written to carry out these desired data manipulations. The new analyte intensity is shown as an inset in Fig. 2.9b.

The constant intensity level of the corrected analyte intensity demonstrates that the LED output is not subject to fluctuations and therefore a reference scheme for that is not necessary.

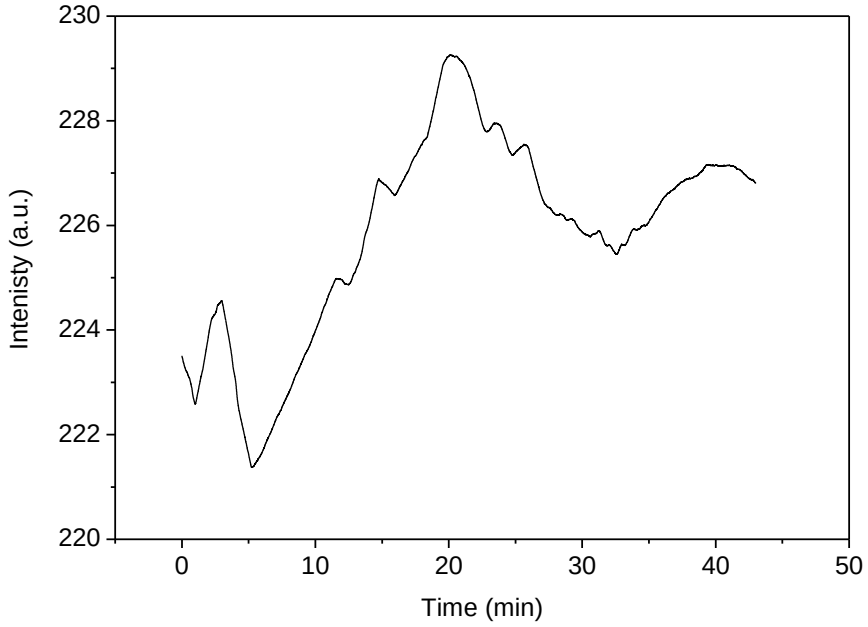

Fig. 2.9a. The graph shows the intensity output of the spectrometer in the absence of light – the dark noise - drifting as a resulting of the instrument noise.

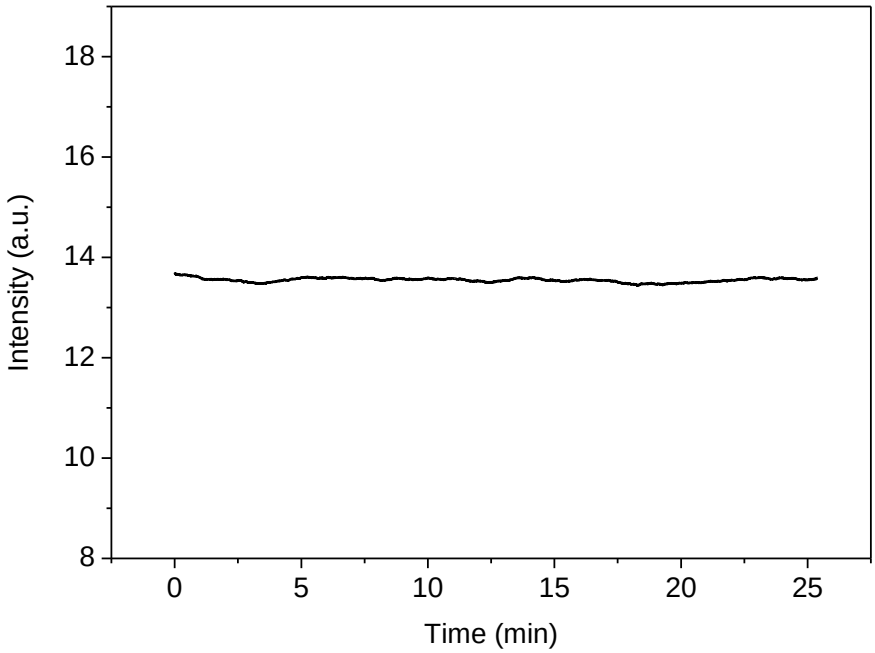

Fig. 2.9b. The corrected dark noise of the spectrometer obtained by subtracting instrument noise of one wavelength range from another. Both graphs are scaled similarly on the vertical axes to enable comparison of the variation in intensity before and after.

It is readily acknowledged that the current set-up involving the bench-top power supply used to drive the LED is not suited to field applications. If the stable power supply is not used, then the LED output is likely to be unstable and a reference scheme would be necessary. A suggested reference technique would be to connect an additional LED in series with the first one to provide the reference intensity. This second LED can be chosen to emit at around 700nm and need not be high power. Any modifications will take place at the software layer using LabVIEW to make ratiometric calculations.

An example of a ratiometric measurement is that of an optical fibre sensor for the measurement of pH designed by Grattan and co-researchers using a dual wavelength referencing scheme [18]. In this work, two LEDs were used, one to

provide radiation for absorption measurements, the other as reference intensity at a wavelength insensitive to the pH dye. Both LEDs were driven from the same current source in parallel so that any fluctuations in the power source will appear across both LEDs. Furthermore, only one detector was used so that any variation in performance will be applicable to both signal and reference wavelength and will be eliminated by applying a ratiometric measurement on the two channels.

More details on referencing are covered in the following chapter where a specific referencing scheme is implemented in a sensor.

2.6. Summary

The major components making up a fibre optic chemical sensor system have been examined, namely, the light source, the detection unit and the optical fibre. The transducer is examined in later chapters. The choice of light source lies in the optical power and wavelength suitable for the transducer while optical fibres must be able to capture and guide the optical signal at a given wavelength with minimal loss. The detector must match the characteristics of the transducer in terms of spectral range; in addition, the operation of the spectrometer and possible modifications to optimise its performance for this experimental work were described. The cost and robustness of the overall sensor is an important factor if it is to compete with other more established techniques so these were considered while selecting the components.

The use of referencing schemes was suggested such that they are compatible with the measurement techniques and both easily implemented via LabVIEW. Implementation or adaptation of the measurement and referencing techniques at the software layer rather than modifying the instrumentation leads to a less expensive solution and to easier and rapid modification in the future.

2.7. References

1. L. Zhu, Y. Li, and G. Zhu, A novel flow through optical fiber biosensor for glucose based on luminol electrochemiluminescence, Sensors & Actuators: B. Chemical 86 (2002) 209-214.
2. O.S. Wolfbeis, M. Schäferling, and A. Dürkop, Reversible Optical Sensor Membrane for Hydrogen Peroxide Using an Immobilized Fluorescent Probe, and its Application to a Glucose Biosensor, Microchimica Acta 143 (2003) 221-227.
3. www.hamamatsu.com.
4. www.oceanoptics.com.
5. www.ni.com/labview.
6. J.R. Lakowicz, Principles of Fluorescence Spectroscopy, Springer 2006.
7. P. Hartmann, M.J.P. Leiner, and P. Kohlbacher, Photobleaching of a ruthenium complex in polymers used for oxygen optodes and its inhibition by singlet oxygen quenchers, Sensors & Actuators: B. Chemical 51 (1998) 196-202.
8. www.roithner-laser.com
9. www.lumileds.com.
10. J. Singh, Optoelectronics: An Introduction to Materials and Devices. McGraw-Hill,1996.
11. www.laser2000.co.uk.
12. O. Wolfbeis, Fibre Optic Chemical Sensors and Biosensors, vol 1. CRC Press,1991, p 65.
13. K.T.V. Grattan and B.T. Meggitt, eds. *Optical Fiber Sensor Technology*. ed. K.T.V. Grattan, Chapman & Hall 1995
14. www.thorlabs.com.

15. J. Louch and J.D. Ingle Jr, Experimental comparison of single-and double-fiber configurations for remote fiber-optic fluorescence sensing, Analytical Chemistry 60 (1988) 2537-2540.
16. M.A. Stanley, J. Maxwell, M. Forrestal, A.P. Doherty, B.D. Maccraith, D. Diamond, and J.G. Vos, Comparison of the analytical capabilities of an amperometric and an optical sensor for the determination of nitrate in river and well water, Analytica chimica acta 299 (1994) 81-90.
17. C. af Klinteberg, M. Andreasson, O. Sandström, S. Andersson-Engels, and S. Svanberg, Compact medical fluorosensor for minimally invasive tissue characterization, Review of Scientific Instruments 76 (2005) 034303-034309.
18. K.T.V. Grattan, Z. Mouaziz, and A.W. Palmer, Dual Wavelength Optical Fiber Sensor for pH Measurement, Biosensors 3 (1987) 17-25.

Chapter 3

A self-referenced reflectance sensor for the detection of lead and other heavy metal ions

3.1. Introduction

This chapter describes the design and evaluation of a fibre optic sensor for lead ions based on the chromogenic reagent Dithizone.

The chemistry of the reagent is laid out first to provide an understanding of how it is affected by lead ions and how it may be implemented in an optical fibre sensor. Following this, a short review of FOCS based on chromogenic indicators is given. In particular, many do not include referencing in sensors based on intensity measurements [1-5].

Since this sensor is based on reflectance measurements, the theory of reflectance measurement is discussed. The sensor performance is then evaluated and it is shown how measurement of the rate of change of light intensity with time can be used to determine the concentration of lead.

A similar sensor in the past based on the same indicator did not include any referencing [1]. It is shown here how to exploit the reflectance spectrum of the reagent together with the software program to make 2-wavelengths ratiometric measurements unaffected by light source variation and leaching. Furthermore, unlike flow-cell sensors, this sensor is adapted into a probe configuration which makes it suitable for use in small spaces and with small sample volumes.

3.2. Dithizone as a reagent

Diphenylthiocarbazone or Dithizone is a well-known spectrophotometric reagent used for the trace detection of heavy metals [6]. For example, it has been used in the determination of lead using flow-injection analysis by Klinghoffer and co-workers [7].

Dithizone is a deeply coloured compound which works by changing colour from green to red, orange or violet, depending on the heavy metal present and forms a metal dithizonate complex. The structural formula of dithizone is shown in Fig. 3.1.

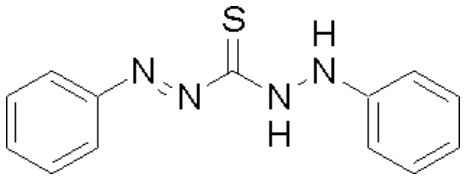

Fig. 3.1. Structural formula of the dithizone molecule

The structure of the metal dithizonate is still uncertain but it is thought that the metal ion substitutes the two hydrogen atoms bound to the nitrogen atoms to form what is called a primary dithizonate. A secondary dithizonate may be formed by the binding of another metal ion to the sulphur group in the primary dithizonate. The formation of secondary dithizonates occurs with some heavy metal ions but not with lead [8].

Dithizone and its dithizonate products are soluble in most organic solvents. In general, it is used in solution form when dissolved in carbon tetrachloride or chloroform. It is more soluble in the latter. Its solubility is greater in strongly polar organic solvents. Thus using methanol as solvent in our experiments would be a judicious choice. It will not only enable a large amount of the

indicator to be dissolved and therefore adsorbed onto the matrix support but also allow water to be used to wash away any excess methanolic solution since methanol and water are miscible while dithizone is insoluble in water.

It is helpful to look at the conventional use of this chemical indicator as it provides a starting point to adapt it to fibre sensing purposes. It is first dissolved in an organic solvent and shaken with an aqueous sample of lead. Lead in the aqueous phase will then be extracted by dithizone into the organic phase in the form of lead dithizonate. The two immiscible solvents are then separated and the organic phase retained. It is important to note the effect of the solvent at this stage. If a chloroform solution of dithizone is used, more lead will be extracted because of the greater solubility of lead dithizonate in chloroform [8].

Lead in the organic phase is tested by photospectroscopic methods as its absorbance A obeys the Beer-Lambert law [9]:

$$A = \lg\left(\frac{I_0}{I}\right) = \varepsilon l C \qquad (3.1)$$

Where I_0 and I are the light intensities at monochromatic wavelength travelling an optical pathlength l in the absence and presence of lead respectively. ε and C are the molar absorption coefficient and the concentration of the absorbing species respectively.

It follows that to extract more lead via the formation of lead dithizonate, the concentration of dithizone must be increased. This will however create departure from the Beer-Lambert relationship, typical in highly absorbing and scattering media. Calibration and a blank run are therefore important.

The extraction of lead from its aqueous sample is pH dependent. Sandell [8] showed that maximum extraction occurs at pH 9-10 and Oliveira *et al* [1]

worked at a pH of 9. Extraction of metal ions by Dithizone may be slow or fast but general observations have shown that in basic solutions, metals are extracted very rapidly [8]. This is potentially useful to achieve a fast sensor response later.

This reagent is normally used in solution but immobilizing it and subsequently regenerating it after each reaction will lead to a more rapid analysis of a larger number of samples.

There are however issues with the use of dithizone as a colourimetric agent. It oxidises to form an unreactive oxide. Under weakly oxidizing conditions, the oxide is reversible by means of a reducing agent but beyond that the oxide is irreversible. Furthermore, exposure of a chloroform or carbon tetrachloride solution of dithizone to strong light or relatively high temperatures leads to its decomposition [8]. Oliveira showed that the introduction of a passband filter to dithizone exposed to white light slowed down that photo-decomposition considerably [1].

Having discussed the features of Dithizone, we can outline its suitability as a chemical indicator for fibre optic sensing. Its deep and significant colour change makes it appropriate for reflectance-based measurements. Although soluble in the organic phase, it is able to extract lead from the aqueous phase. Its insolubility in water is advantageous as it will not be washed away by the aqueous sample. Extraction of lead is fastest and most efficient in basic solutions. Finally, care must be taken to avoid oxidation and photodecomposition.

3.2.1. Reflectance

There are two types of reflection, namely specular and diffuse reflection. For fibre optic chemical analysis, diffuse reflection is mostly encountered, usually

following the scattering of light from a non-uniform surface. If the surface of a material is coated with an indicator which absorbs light at a particular wavelength range, then when light is incident upon that surface, it will be partly absorbed by the indicator and partly scattered back or reflected. The reflected light will consist of the original light minus the absorbed light. If the absorption of the indicator is solely modified by the concentration of the analyte, then it is possible to correlate the intensity of the reflected light to the analyte concentration.

Several publications describe metal ion sensing based on reflectance at the distal end of an optical fibre. Reagents such as cupron [3], gallocynine [5], Dithizone [1], salicyclic acid [4] and chrome azurol S [10] have been immobilized on XAD type of polymer beads and their reflectance measured and plotted against the analyte concentration. They do, however, suffer from the lack of a suitable 'reference scheme' to allow for any fluctuations in the input light intensity which may be mistaken for the response of the sensor to the measurand and thus give erroneous readings. These errors can arise typically from an unstable light source, fibre bend losses and leaching which may all affect intensity measurements. A reference scheme is therefore necessary for any intensity-based optical sensor to be used in the field.

3.2.2. Effect of the Immobilization procedure

The chemical indicator may be used in conjunction with the fibre without immobilizing it. For e.g. Lee and co-researchers used a reagent in solution and measured its absorption with a fibre to relate it to the concentration of iron (III) in solution [11].

However, most FOCS immobilize the indicator to the fibre to allow interaction with the interrogating light. Immobilization of the reagent phase brings about several advantages:

1. The sensing head is compact, small and portable.
2. The reagent is protected from the external environment; for e.g. in sol-gel or PVC membranes, the reagent is entrapped in the solid support.
3. If the sensor is reversible, the reagent may be used several times as it is not washed away with the sample.
4. The selectivity may be improved; for e.g. silicone membrane is a hydrophobic polymer that is impermeable to aqueous solutions but will allow gases such as water vapour and oxygen to diffuse through, thus being useful in gas sensing.

Immobilization has some problems of its own:

1. Leaching is a common issue to all membranes. It is impossible to eradicate completely as no membrane is able to retain all the dye incorporated into it when a solvent is passed through. It is possible though to minimize the impact of leaching via referencing techniques.
2. Photo-degradation is more severe in reagents immobilised at the fibre end as they are continuously illuminated by high-intensity optical radiation. This problem is not reported in evanescent wave sensing.
3. Immobilization may cause chemical modification of the reagent either as a result of that process or to enable the process. Some non-hydrophobic dyes have to be lipophilised to render them compatible with PVC membranes and allow covalent bonding to the membrane [12-14]. Dyes electrostatically immobilised require the use of an ionic site in the reagent molecule and care must be taken that the transducing function of the molecule is not altered [2].
4. Presence of a membrane will affect the time response of the sensor as the analyte molecule must diffuse through it.

5. Intrinsic fluorescence of the membrane may occur, especially with the combined use of UV light and plasticizers in PVC membranes [15].

The solid support for the reagent must fulfill the following requirements:

- It must be optically transparent or equally reflective at all wavelengths for reflectance measurements;
- It must be chemically inert to the sensing process.

There are various ways of immobilizing an indicator and these have been described extensively in the literature [9, 15]. The choice of the immobilization matrix or polymer support determines to a large extent the overall performance of the sensor. The extent of leaching of the reagent will determine how successful the immobilisation is. The solid support of the reagent will affect significantly the time response of the sensor as it will determine how fast the analyte is able to diffuse through it and react with the reagent to produce a detectable optical change.

Oehme *et al* have investigated the effect of various polymeric supports such as hydrogels, sol-gels, PVC, polystyrene and anion-exchange resin for metal-ion sensing using the same indicator [16]. A comparative study was made in terms of leaching, sensitivity, reproducibility and stability of the membranes. Wang and co-workers have exploited a PVC membrane in developing an optode sensor for zinc [17] while Birch *et al* reported using the ion exchange membrane Nafion® in a copper ion sensor [18].

3.2.3. Reagent response to the analyte

The reaction between the reagent R and lead as the analyte A is irreversible without an external regenerating agent (the acid):

$$A + R \rightarrow AR \qquad (3.2)$$

Because only a finite amount of reagent R may be placed at the end of the fibre, it is assumed in this work that the amount of analyte is large enough so that the reaction ends when R is depleted. This assumption holds because in general, the sample volume is very large relative to the reagent. In addition, if the amount of analyte is large enough, then introduction of the sensor reagent R will not disturb its concentration equilibrium significantly.

As AR is being measured here, the signal changes with time during the reaction until R has been consumed and the reaction reaches completion whereby the signal reaches a steady state. At this point the sensor may be regenerated by means of dilute HCl. Analysis of the signal change with time will thus yield the analyte concentration.

3.2.4. Referencing scheme

It is important to provide a method of referencing to eliminate errors arising from fluctuations of the light source, bending losses and any leaching of the indicator that may occur whilst operating the sensor. LEDs are subject to unstable optical output; instead of coupling a cheap LED to a more expensive current driver and temperature control to achieve a stable optical output, a cheaper but just as effective solution resides in improving the system design. This involves making use of a suitable reference scheme which will compare the reference intensity to the analyte intensity.

There are various techniques of referencing, the simplest method of which involves measuring the reference intensity at the light source itself and taking the ratio of the light source intensity and analyte intensity. Thus if light from the source drops, the analyte intensity will drop consequently but the ratio of the

two will stay constant. The disadvantage with this method is that the reference intensity is not measured along the same optical path, and optical losses are not identical. Furthermore, there may also be leaching of the indicator which will result in a drop in the analyte intensity. An alternative would be to use two light sources emitting at different wavelengths, one to interact with the analyte and the other insensitive to the analyte and to be used as reference intensity. If the two light sources are LEDs driven by the same current, they will be subject to the same current fluctuations. Detection is made using a single spectrometer for both analyte and reference wavelengths, and the ratio of the two will therefore cancel out instrument noise. Moreover, the reference intensity follows the same optical path as the analyte intensity. A downfall with this method is that the two LEDs are not identical and may be subject to manufacturing defects or imperfections. Reference techniques are discussed in more details by Grattan [19] and Wolfbeis [9].

3.3. Experimental setup

The setup is shown in Fig. 3.2. A tungsten halogen white light source from Ocean Optics is used as to provide the interrogating signal over the visible wavelengths. The interrogating light is guided down one arm of the fibre bundle made up of a single fibre to the probe to be modulated by the reagent in the presence of lead. The modulated light is guided back up the fibre bundle along the arm made up of 6 fibres to the spectrometer input where its intensity is analysed.

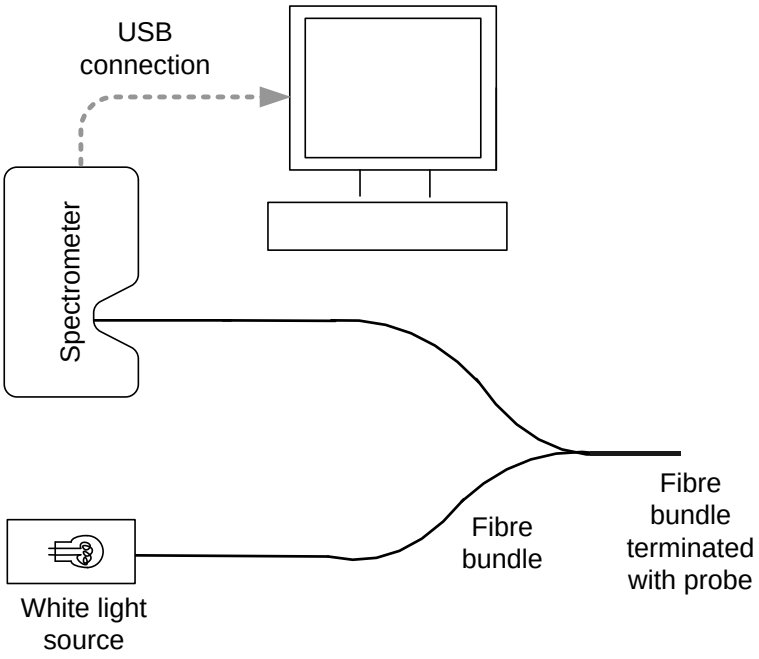

Fig. 3.2. Experimental set-up to evaluate the dithizone reagent. The main components are the tungsten halogen white light source from ocean Optica, the spectrometer also from Ocean optics, the fibre bundle used for the propagation of the optical signal and a computer to run the LabVIEW software for data analysis.

A LabVIEW program was written to process the data output from the spectrometer. The spectrometer essentially measures the intensity over a range of wavelengths and presents this data in an array containing the intensity and corresponding wavelength values. This array is fed to the computer as often as the spectrometer updates it; the time interval between two updates is called the integration period. Throughout this work, an integration of 100 mS was used, thus providing 10 new array values per second. The LabVIEW program may be written to extract the peak intensity value, the wavelength corresponding to that peak intensity, the rate of change of intensity at a given wavelength, the ratio of two intensities at specific wavelengths and so on. Fig. 3.3a and 3.3b show the front and back panel respectively of the LabVIEW VI (virtual instrument). Data may be saved by clicking the relevant button I nthe

front panel while the experiment is running or at the end of the experiment to save all data.

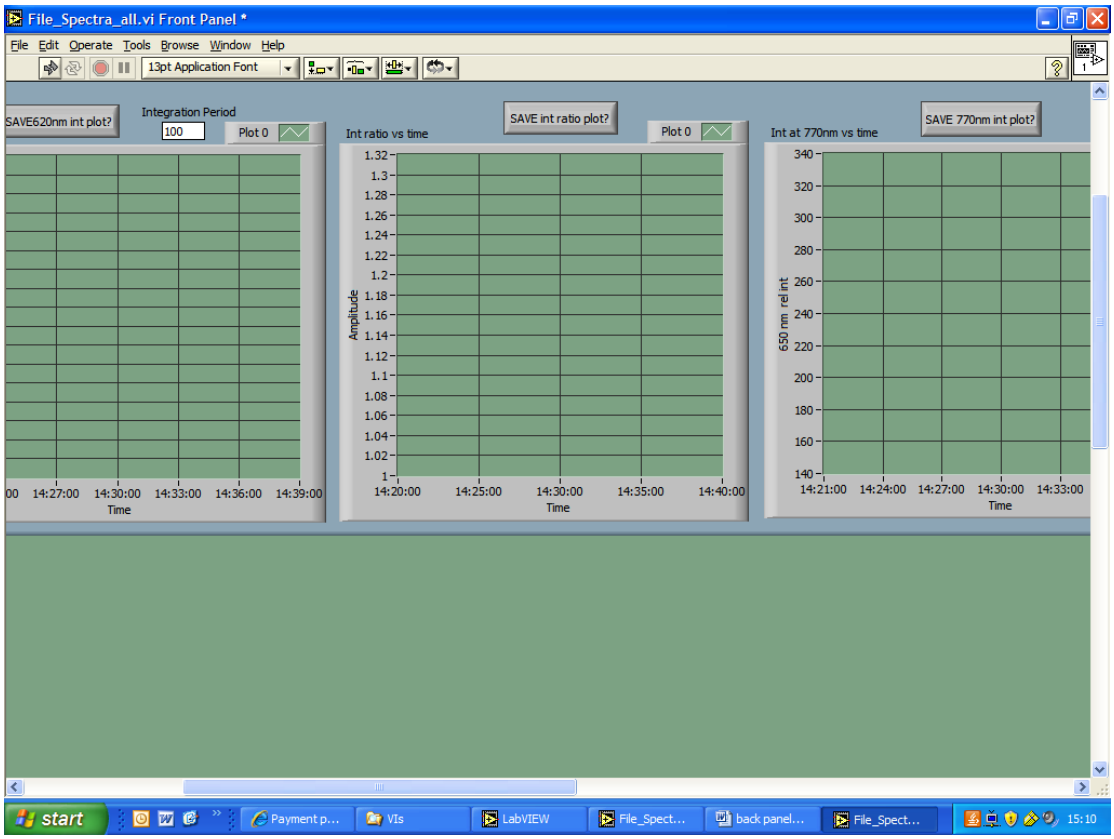

Fig. 3.3a. Front panel of the LabVIEW VI used to gather and analyse data from the spectrometer output. The first graph will display the intensity at 620 nm, the last graph the reference intensity at 770 nm and the middle graph will display the ratio of the intensities from the 2 graphs in real time. The horizontal axes are all in real time.

The back panel is used to make all the connections between the sub-VIs. Data from the spectrometer array is split into two: the intensity and the wavelength values. A clock is added to provide the time, giving a third variable. Calculations such as extracting the peak values, taking ratios and filtering are all performed by selecting the appropriate sub-VIs and connecting them together such that the data signal flows from left to right, from the output of one block into the input

of another block. Outputs from the VI are displayed graphically and the data are saved as arrays which can later be plotted again.

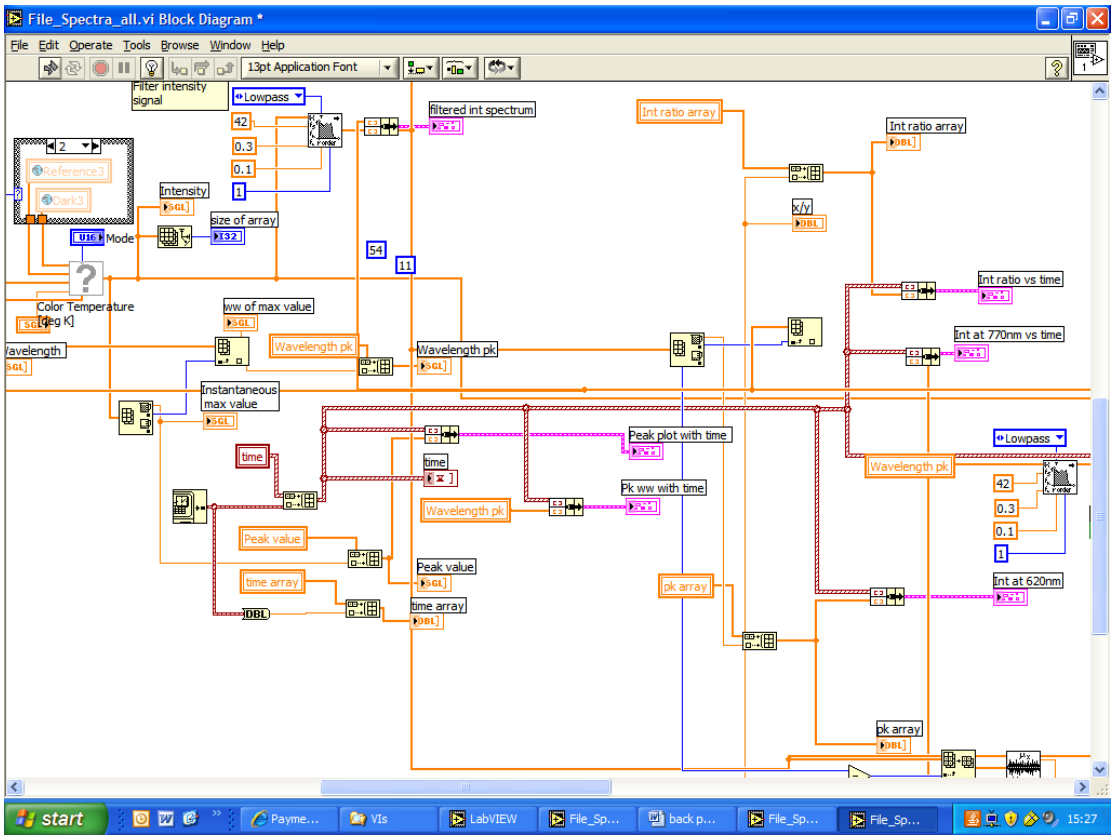

Fig. 3.3b. Back panel of the LabVIEW VI used to gather and analyse the spectrometer output. The spectrometer device here is depicted as a question mark in the top left of the VI; a lowpass filter to remove high frequency noise is visible in the top left; the clock providing synchronisation is seen at the bottom left.

The probe itself was specially designed and developed for this application and consisted of a thin layer of immobilised indicator at the end of the fibre bundle as depicted in Fig. 3.4a and Fig. 3.4b. A nylon membrane separated the immobilized indicator from the solution, held by a demountable rubber ring connector in this configuration.

The interrogating light is guided into the central fibre from the light source and is incident upon the beads where the dithizone layer absorbs part of the spectrum, depending on its colour. The rest of the spectrum covering the visible wavelength is reflected back in all directions due to the non-uniform surface presented by the beads. Light that is reflected back to the six fibres surrounding the central fibre and that is within the numerical aperture of these six fibres are able to be propagated along the fibres down to the spectrometer for intensity measurements.

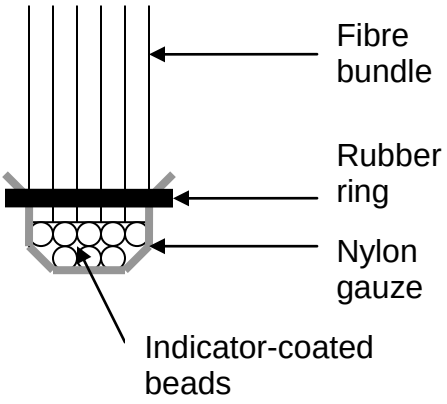

Fig. 3.4a. Probe construction

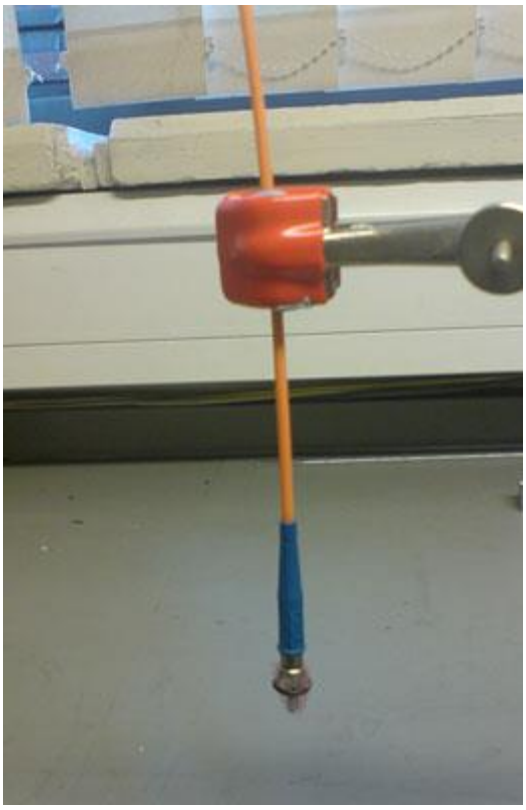

Fig. 3.4b. Picture of the probe constructed with XAD beads coated with the dithizone reagent and held together by means of the nylon gauze and rubber O-ring.

This sort of probe construction is very common in reflectance sensors using resin beads. The membrane must not be made of absorbing material that will retain traces of the sample even after washing. Nylon membranes are a good choice as they are also unreactive. Metal meshes might react with the metal-sensitive indicator or with the acid used for regeneration. Fig. 3.5 below shows the construction of a probe for a similar type of reflectance sensor by Yusof [5]. In this case, a relatively thick layer of beads have been placed at the fibre end. No mention is made of the bead size but it would be sufficiently large so as not to impede the flow of aqueous sample.

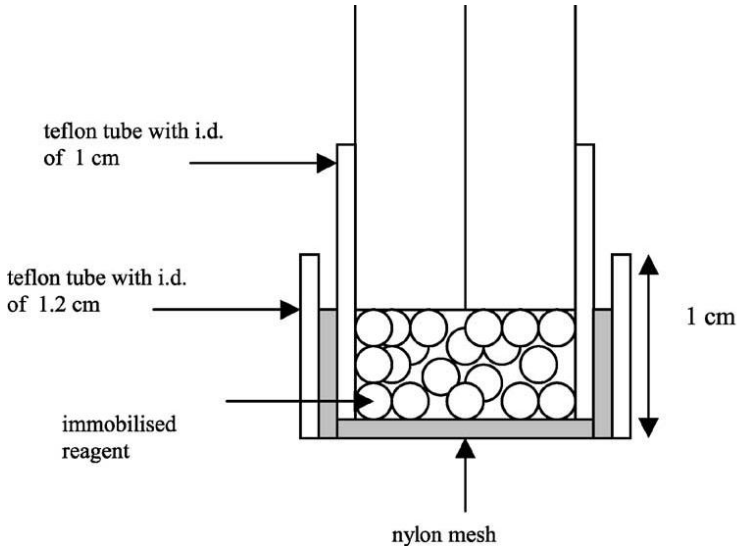

Fig. 3.5 Probe construction for a reflectance sensor by Yusof *et al* [5]

3.3.1. Reagents

All chemicals used in this work were of analytical grade purchased from Sigma-Aldrich. Deionized water was used throughout. The buffer solution was made up of 0.01 M hydroxylamine hydrochloride and 0.05 M ammonium citrate dibasic in water. Hydroxylamine hydrochloride will prevent the oxidation of dithizone while citrate is used to prevent precipitation of insoluble lead hydroxide. Ammonium hydroxide is added to adjust the pH to a value of 9 as lead is most efficiently extracted from its aqueous solution at this pH value [8].

Lead nitrate salt was weighed and dissolved in the buffer solution to produce a stock solution of known concentration. This was further diluted with the buffer to produce different concentrations of buffered lead ion solution. The dithizone solution was prepared by dissolving dithizone into methanol.

3.3.2. Immobilization

Following the previous work reported by de Oliveira *et al* [1], Amberlite XAD-4 resin, a porous non-ionic co-polymer, was chosen as a suitable matrix on which

to covalently bind dithizone. The resin was ground to reduce its particle size and washed in water, dilute hydrochloric acid and distilled water to remove any chemicals such as sodium chloride and then finally rinsed with methanol.

3.3.3. Probe Fabrication

A small amount of the green dithizone-coated resin was removed from its acid solution and attached to the distal end of a fibre bundle by means of an arrangement using a nylon gauze and a small rubber ring which previously had been washed in dilute acid. The probe was rinsed in the buffer solution and dipped in an optically isolated measuring cell containing an excess of lead ions solution relative to the immobilised reagent. The spectrometer monitored the spectral changes of the light reflected from the beads in real time.

3.4. Results and discussion

3.4.1. Response to lead ions

The response of the probe to lead ions was evaluated by immersing the probe in the measuring cell containing aqueous solutions of lead at various concentrations. Changes in the reflectance spectrum upon addition of a 30ppm concentration of lead are shown in Fig. 3.6.

Prior to the addition of lead, the spectrum shows a minimum intensity at 620 nm due to strong absorption by the reagent at that wavelength. The peak absorption of dithizone dissolved in carbon tetrachloride occurs at 620 nm [8] and our results are in agreement with that, also highlighting the fact that immobilization and use of an aqueous solution do not change the peak absorption wavelength.

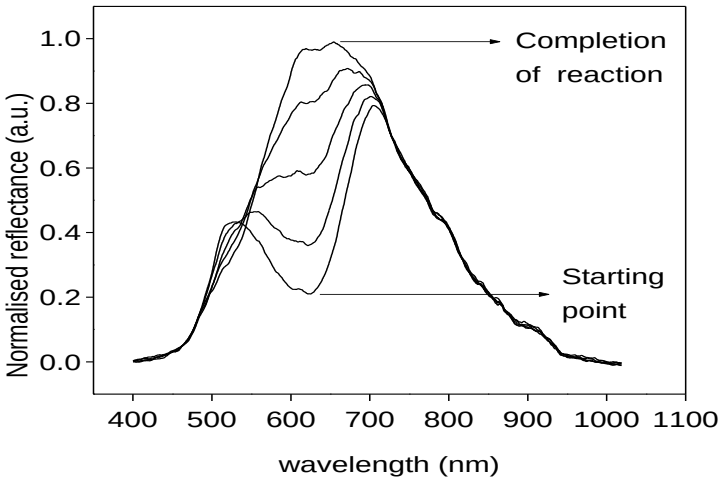

Fig. 3.6. Normalized reflectance as a function of wavelength showing the observed change in reflectance spectrum as the lead ions react with the reagent. This change in reflectance occurs as the chemical reaction proceeds from the starting point to the completion of the reaction over 20 min.

In the presence of lead ions, the spectrum changes gradually to a peak at the same wavelength. At higher lead concentrations, the reaction proceeds faster so the rate of change of the spectrum intensity was measured to give a quantitative measure of the amount of lead present. Since the largest change in intensity occurs at 620 nm, measurement at this wavelength is considered to be the most sensitive to measure lead ion concentration.

3.4.2. Analyte measurement

In this reflectance measurement, to avoid the problem of two non-identical LEDs for referencing, a reference intensity from the light which follows the same path as that used to probe the analyte intensity and thus being subject to the same deleterious effects is used. The reference intensity is chosen at a wavelength not subject to the measurand-induced changes while the analyte intensity is that at 620 nm which responds best to the presence of lead [20]. It can be seen from Fig. 3.6 that part of the observed optical spectrum from the

probe (beyond a wavelength of approximately 720 nm) is essentially insensitive to any changes in the lead concentration. This spectral region provides an excellent means to choose a wavelength for this ‘reference intensity’ and for convenience a wavelength of 770 nm is chosen – the intensity of light at this wavelength is readily detected by the detector. The ratio of the analyte intensity to the reference intensity is used to represent the measurand-sensitive signal and is used subsequently in this work.

This ratio represents a ‘relative’ measurement, i.e. the intensity at 620 nm relative to the intensity at 770 nm. To show the need for and value of the referencing scheme applied in the work, an experiment was performed by measuring the analyte intensity and reference intensity separately over the same time period while the probe was placed in its acid solution so that no reaction takes place. Figure 3.75a illustrates the results from the probe. The analyte intensity is first plotted with no referencing scheme: this represents the raw measurement. The signal is seen to oscillate and thus cannot be used alone to determine the quantities needed – the measurement is subject to a number of loss mechanisms such as photodecomposition, leaching, power fluctuations and fibre bending, for example.

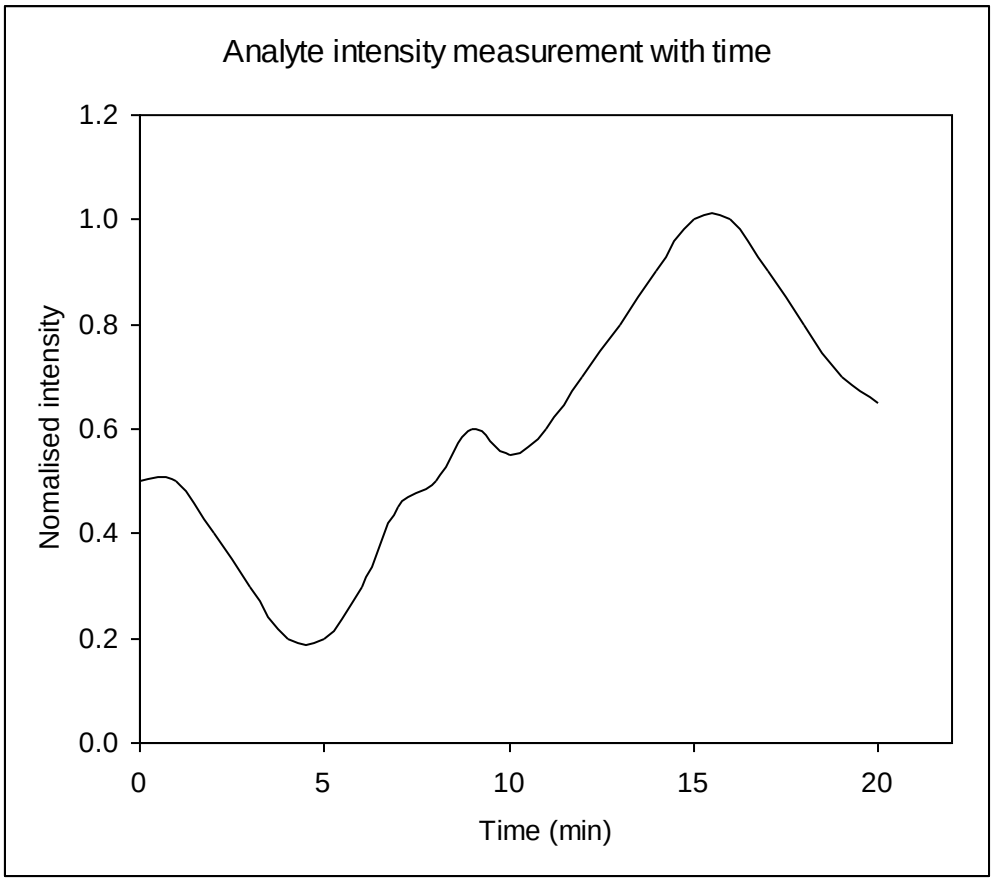

Figure 3.7a Measurement of the normalized optical intensity at 620 nm without the referencing scheme in place. The probe is placed in dilute acid so that no reaction takes place. A constant signal level is expected but the variable light intensity output of the white light source masks this.

By contrast Fig. 3.7b shows the same data divided by the reference intensity collected at the same time. Because the intensity at 770 nm is subject to the same losses e.g. the unstable power output of the lamp, making a measurement of one intensity value relative to another completely eliminates this instability and the signal obtained immediately becomes one that is meaningful in terms of the required analysis, i.e. no reaction is taking place as expected.

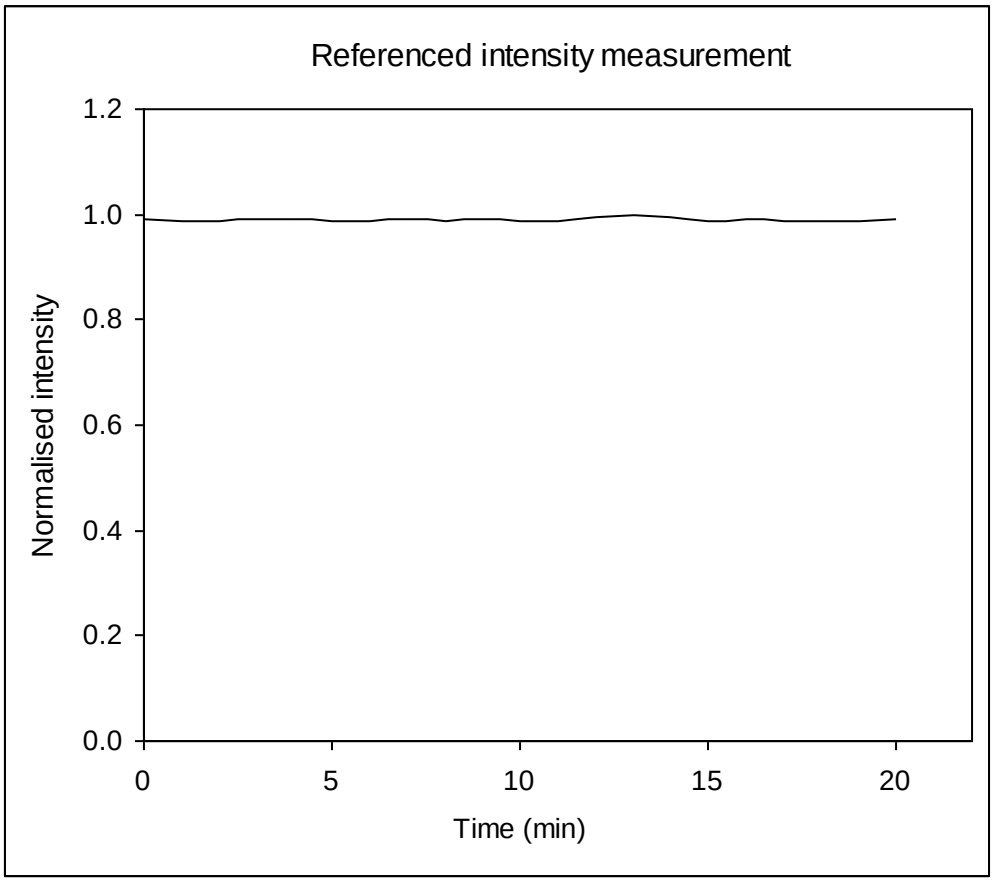

Fig. 3.7b. Using the same analyte intensity data in Fig. 3.7a and dividing by the reference intensity at 770 nm yields a more constant signal level as expected when no reaction is taking place at the probe.

By measuring the change in the above intensity ratio with time using different concentrations of lead ions, the plots in Fig. 3.8 are obtained. The reagent complexes with lead ions from the solution until all the reagent is depleted and the signal reaches saturation. Thus, regardless of the initial concentration of lead ions used, all the plots in Fig. 3.8 reach the same final reflectance intensity ratio, although a higher lead concentration causes the reaction to reach completion more quickly. The initial slope of all the plots is strictly linear and allows the information on the concentration of the analyte to be obtained by calculating the corresponding slope. This concept has been explained by

Oehme and Wolfbeis [21] and is illustrated in a copper sensor by Oehme *et al* [16].

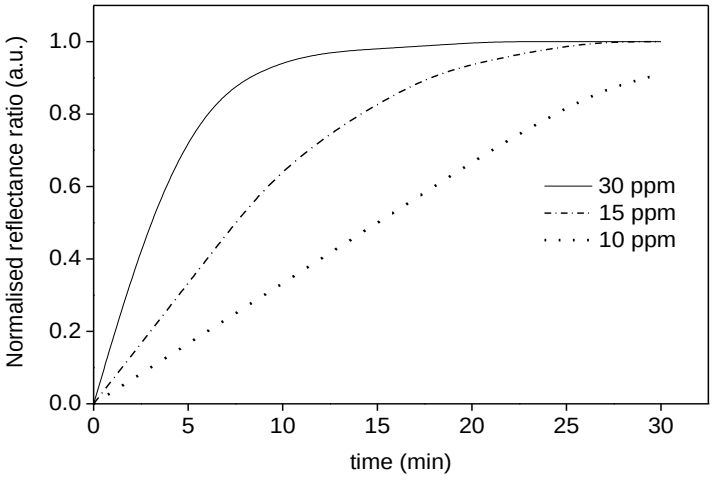

Fig. 3.8 Normalized reflectance as a function of time showing analytical information from the slope of the plot. The vertical axis represents the intensity ratio of 620 nm to 770 nm and is normalised at the largest value.

3.4.3. The selected matrix support for the reagent

Amberlite™ XAD-4 resin is a polymeric adsorbent available as white insoluble porous beads. It is a non-ionic cross-linked polymer which derives its adsorptive properties from its high surface area and the aromatic nature of its surface. This structure gives Amberlite™ XAD-4 resin polymeric adsorbent excellent physical, chemical and thermal stability. It is normally used in chromatography separation techniques in column or batch modes, to adsorb hydrophobic molecules from polar solvents or volatile organic compounds from vapour streams. Its characteristic pore size distribution makes it an excellent choice for the adsorption of organic substances of relatively low molecular weight [22].

Such polymeric adsorbents are highly porous structures whose internal surfaces can adsorb and then desorb a wide variety of different species

depending on the environment in which they are used. For example, in polar solvents such as water, polymeric adsorbents exhibit non-polar or hydrophobic behaviour and so can adsorb organic species that are sparingly soluble. This hydrophobicity is most pronounced with the styrenic adsorbents. In non-polar solvents, such as hydrocarbons, etc. most adsorbents exhibit slightly polar or hydrophilic properties and so will adsorb species with some degree of polarity. This polarity is most pronounced with the acrylic adsorbents and the phenolic adsorbents [22].

There are other polymeric adsorbents of the same class, namely XAD-2 and XAD-7. XAD-2 and XAD-4 are nonpolar and are useful in sensitive analytical procedures for the detection and identification of narcotics and environmental organic contaminants. XAD-7 has intermediate polarity and adsorbs phenols from water or hexane; it can adsorb either hydrophobic materials from water or hydrophilic materials from nonaqueous systems [23]. De Oliveira et al made a comparative study of all three types of resin and determined that Amberlite XAD-4 yielded the best results with dithizone and selected it as the immobilisation matrix. XAD-4 provides a porous, large surface-area structure of hydrophobic nature which is well-suited to the dithizone molecule. Once adsorbed, the molecule is not washed away with water due to this very hydrophobicity. This makes it ideal for testing lead ions in aqueous solutions.

The structural formula of the repeat unit of the XAD-4 polymer is shown below:

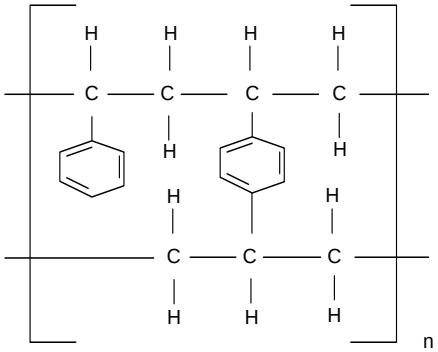

3.4.4. Factors which affects the sensor response

The most important step in the development of this sensor system is the probe fabrication as it affects the sensitivity, response time and dynamic range of the system. In the preliminary work carried out, it was found that it was not possible to reproduce exactly the same amount and distribution of the resin attached at the fibre end every time and thus the results presented reflect this particular aspect of the sensor system performance and focus mostly on the qualitative aspects. The main factors which affect the sensor response are described in Table 3.1 below.

Factors	Parameters
Amount of reagent adsorbed onto beads	Concentration of reagent
	Volume of reagent solution
	Time allowed for adsorption (soaking time)
Resin size	Individual resin diameter
	Amount of resin at probe end

Table 3.1. Factors affecting the amount of reagent adsorbed.

In able to be able to optimize the factors in the left column experimentally, one parameter at a time in the right column must be varied while all the others are kept constant. To simplify the adsorption process, the amount of reagent was always in excess relative to the amount of resin present which was fixed at 130 mg. This ensures that there is more than enough reagent for adsorption onto the surface area presented by the porous resin beads.

The concentration of reagent used was a saturated solution at room temperature. This was prepared by adding solid dithizone powder gradually into the methanol solvent and dissolving gradually until no more solid will dissolve. The excess solid was then filtered off and the solution retained. Having fixed

the reagent concentration, to make sure that the reagent is in excess relative to the amount of resin during the adsorption process as described just above, the volume of the reagent solution must therefore be in excess. From Table 1, the only parameter left to vary in order to optimize the quantity of reagent on the resin beads *after* adsorption is the time allowed for soaking during this adsorption process. The reagent concentration was chosen to be very high in order to keep this soaking time short.

3.4.5. Determining the volume of reagent solution

To ensure that the volume of reagent solution used during the adsorption process is large enough to provide sufficient reagent molecules for adsorption onto the surface of the porous resin, different volumes deemed to be in excess were tested on the resin. 130 mg samples of the resin were added to various sample volumes of the solution and allowed to soak for 10 min in a beaker. The resin was then removed, washed with the buffered solution and immediately tested with 100 ml of 100 ppm aqueous lead in a beaker to determine how fast the colour changed from green to red in the presence of lead ions. As this experiment was only to provide a guide of what volume of reagent solution make up an excess quantity to 130 mg of resin, no accuracy was required and the colour change was measured visually. The data are presented in Table 3.2 below.

Volume of reagent solution (ml)	**Time taken to visually change colour to red by 90% approximately (min)**
10	25
20	25
30	25

Table 3.2. Determining an excess volume of reagent

Since there is no noticeable increase in the time taken to change colour as the volume of reagent solution is increased, 10ml already contains an excess of reagent for this mass of resin. As an extra precaution, 20 ml of reagent solution were used in future experiments with the confidence that any inaccuracy in the visual detection of the colour change will not affect the reagent-to-resin excess relation. Referring back to Table 1, the concentration of reagent solution and its volume have been determined and are summarized below in Table 3.3 below.

Parameter	Quantity
Concentration of reagent	Saturated
Volume of reagent solution	20 ml
Mass of resin beads	130 mg

Table 3.3. Summary of quantities

Before moving on to determine the appropriate period of time allowed for the adsorption process to find the optimum amount of reagent to be adsorbed onto the solid support, the resin particle size must be considered.

3.4.6. Resin size

So far in the all above experiments, the resin size used was as sold, i.e. with a mean diameter size of around 0.6 mm. To determine the influence of the bead diameter onto the probe response, different sizes were prepared by crushing the beads in a crucible and filtering them through sieves of aperture size 0.500 mm, 0.354 mm, 0.250 mm and 0.125 mm sequentially. Three sizes were kept with nominal dimensions as presented in Table 3.4.

Size	Nominal dimensions (mm)
Small	<0.125
Medium	0.250-0.354
Large	>0.50

Table 3.4. Bead diameters

The reagent was then adsorbed onto the resin using the parameters set in Table 3 with a soaking time of 10 minutes after which the resin was immediately removed and washed with the buffer solution. Equal samples, each having bead diameters small, medium and large, were placed in beakers containing 100 ml of 100 ppm aqueous lead solution and the colour change from green to red monitored visually. The results are shown below in Table 3.5.

Size	Time taken to change colour to to red by 90% (min)
Small	5
Medium	15
Large	30

Table 3.5. Relation between bead diameter and time taken to change colour.

By using XAD-4 beads of small diameter (around 0.1 mm and less), the reaction time can be significantly reduced compared to that with larger beads (0.5 mm diameter). This arises because beads of small diameter require lead

ions to diffuse through a shorter distance inside the pores to react with all the reagent.

Fresh samples for each diameter size were then taken and affixed to the end of an optical fibre probe which was then placed in 100 ppm of aqueous lead solution which had a volume large enough that the depletion of lead ions in the solution could be considered negligible. It was not possible to measure and place an exact reproducible amount of coated beads at the end of the fibre but an amount considered large was used each time. The optical signal reflected at the fibre end was strong and well-defined due to the thick coating at the end. The observed signal for the probe consisting of medium-sized beads is shown in Fig. 3.9.

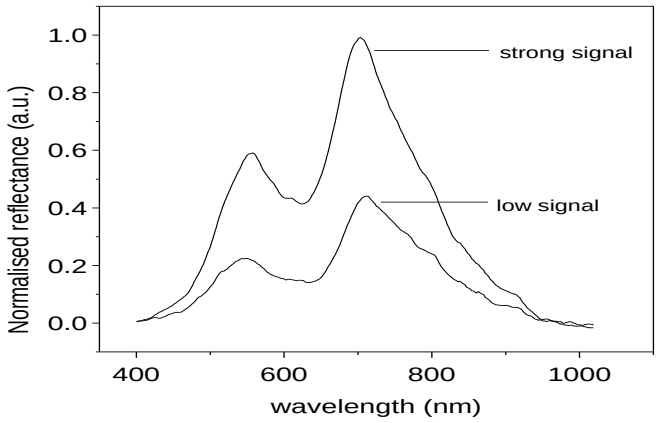

Fig. 3.9. Increase in signal, about 2.5 times greater, with a large amount of resin of medium size (strong signal) at probe end compared to a smaller quantity (low signal)

However, the reaction with lead never reached completion as the final curve, similar to that shown in Fig. 3.6, was never achieved. This was confirmed when the nylon gauze was removed and the beads examined. While the outer beads exposed to the analyte solution had changed colour to red, the beads in the middle were still green and completely dry despite having been left in the analyte solution for more than 4 hours. All the probes with their respective bead

size were left up to 4 hours in the analyte solution and all of them failed to react completely with lead, albeit with different degrees of completion. Fig. 3.10 shows the final reflectance signal after 4 hours for each probe and equivalent bead size within.

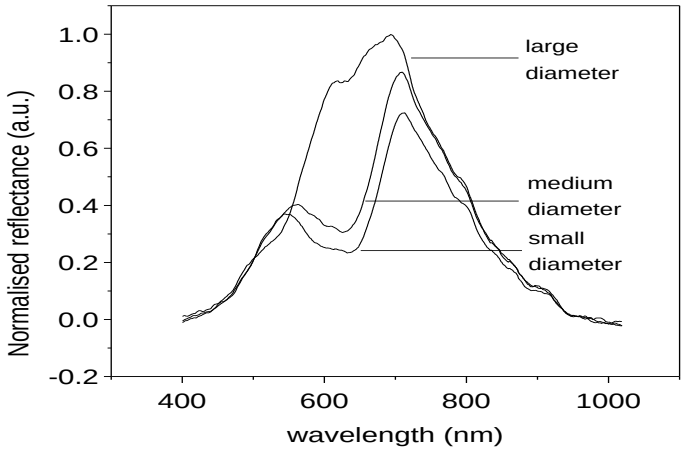

Fig. 3.10 Relation between bead diameter and completion of reaction

In the case of the probe consisting of small beads, no reaction was actually detected by the probe as the resin in contact with the surface of the optical fibre was not exposed to the analyte solution at all, although the external surface did change colour. The probe with medium-sized beads detected a small change in the spectrum due to the analyte solution being able to reach deeper into the resin layer. In the case of the large beads, the reaction is nearly complete, confirming that the larger beads have more space between them and do not impede the flow of analyte solution.

It can be concluded that a large amount of resin attached to the probe end, although providing a strong and well-resolved signal, does not allow the free flow of the analyte solution through it. Furthermore, the smaller the resin beads, the more compact a barrier they represent and further impede the flow of

analyte solution through them, ultimately preventing any flow of analyte solution.

As a result of this, a similar experiment was repeated with all three bead sizes but by placing a minimal amount of resin sample at the distal end of the probe, just sufficient to cover it completely. The resultant signal for the probe consisting of medium-sized beads is shown in Fig. 3.9 and provides a useful comparison with the signal from a probe of same bead size but with a larger amount. The signal in the case of a minimal amount of resin at the probe end is much weaker as the signal reflected from the resin is lower; however, there is sufficient detail in the spectrum to allow for measurements. The three probes thus assembled with the three different bead sizes were then placed in an excess volume of 100 ppm of aqueous lead solution and the reflected signal monitored. The results are shown in Fig. 3.11.

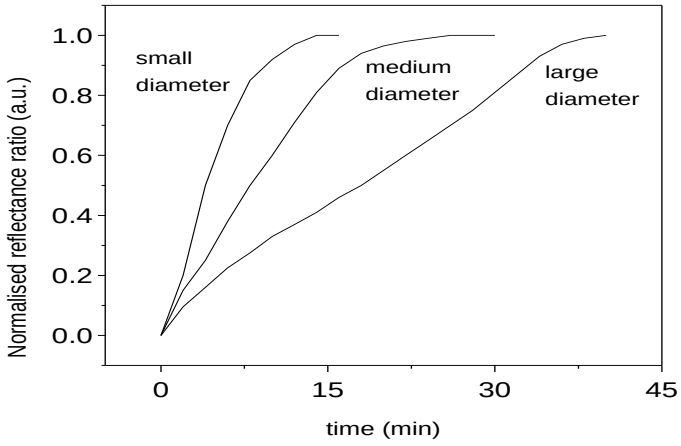

Fig. 3.11. Time taken for beads of different sizes to complete reaction

In this situation, the beads of largest dimensions take the longest time to react completely and change colour. The results are comparable to that obtained in Table 5 and in general the beads take slightly less time to react when they are

free to move within a vessel as they are then surrounded by the solution equally on all sides.

Based on these results, it was decided to continue further experiments using a medium bead diameter as it provides a satisfactory compromise between too rapid a reaction time and an incomplete reaction with lead. A minimum number of beads was also used to just cover the tip of the fibre and in this way it was found to provide an adequate level of reflected signal at the detection system. Klimant *et al* [2] have reported similar observations regarding the effect of bead size. Their response time of 2 min for a reflectance sensor using an anion-exchange resin was attributed to the rate of diffusion of lead ions through the pores of the resin. The particle size used was less than 0.1 mm.

3.4.7. Time allowed for adsorption

The last parameter to examine from Table 2 is the time allowed for adsorption. This parameter will “fine-tune” the amount of reagent adsorbed onto the matrix support to ultimately determine the performance of the probe. It has already been shown in the previous section how the bead diameter greatly affects the response time and how the amount of resin, in relation to its size impedes the flow of analyte solution and therefore slows down its response. Having solved these issues, we are now in a position to optimize the probe response based on the soaking time.

Ideally, we would want a solid support with an infinite amount of reagent that would be able to react with an infinite amount of lead ions. However, large quantities of the reagent will result in a long time to reach completion of reaction, thus affecting the response time of the sensor. In practice, a compromise between the response time and the response range needs to be found. By varying the soaking time, the amount of reagent on the resin is varied and the loaded resin can be tested at the fibre end for the probe response time.

A number of resin samples were prepared using the parameters described in Table 4 with beads of medium diameter as described in Table 5 and with a soaking time varied as described in Table 6 below. After adsorption, the resin was removed from the solution, washed with the buffer solution and immobilised to the fibre end using a minimal amount to sufficiently cover the distal end as described in Section 3.4.6. Each probe thus built was then tested by placing it in 100 ml of various concentrations of lead. The results are summarized in Table 6 where the time taken is measured at 90% of its final value.

It is important to realize that each soaking time tested corresponds to a different probe assembled. This in itself is a source of error known as the reproducibility of the probe and described later in Section 3.4.9. The response time of each probe may therefore not be comparable with each other without avoiding and compounding this type of error. Consequently, the response times in Table 3.6 should be viewed as a guide to select the most convenient soaking time.

Soaking time (min)	**Probe response time (min)**		
	100 ppm	**10 ppm**	**1 ppm**
60	150	n/a	n/a
30	32	n/a	n/a
15	22	n/a	n/a
5	9	53	n/a
1	0.75	8.5	15
0	n/a	n/a	3.5

Table 3.6. Relationship between soaking time and probe response time

The aim was to get a sensor response under 30 min for low lead concentrations. Thus where a long response time was achieved at high lead concentration, the experiment was not repeated with a lower lead concentration as the response time would have been even longer and therefore unsuitable for a probe. A soaking time of zero represents the resin placed in the reagent solution and immediately removed and washed with the buffer solution. It can be seen that the longer the soaking time, the longer response time of the probe. Thus for a given lead concentration, a desired response time for the probe may be achieved by selecting an appropriate length of time for the adsorption process. This means that if the sensor must give an output within 10 minutes for a given range of lead concentration, the soaking time may be adjusted for that.

A soaking time of 1 min for the adsorption process was selected. There are no right or wrong values; rather, the value chosen represented a good compromise between measuring low and high concentrations of lead ions within a response time of around 30 minutes. A longer soaking time effectively causes more of the reagent to be immobilised; when tested at the fibre end, the immobilised reagent will take more time to react with lead and change colour. This is because its local concentration is very high compared to the ppm level of lead ions. A large amount of lead ions is then required to accumulate at the site of the reagent to cause a detectable colour change. Similar findings have been reported by Ahmad *et al* [24] and Arnold *et al* [25].

A typical calibration plot showing the measurand (normalized slope) as a function of the lead concentration for a probe assembled as described here with a soaking time of 1 minute for the resin beads is depicted in Fig. 3.9.

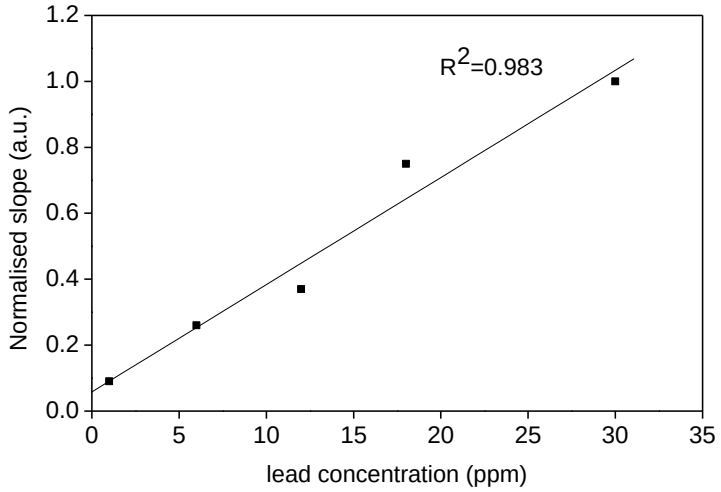

Fig. 3.9 Calibration plot showing normalized slope as a function of lead ion concentration

The time taken for the signal to reach steady-state varies with the concentration of lead from around 3-4 min for a 50 ppm lead solution to 15 min for a 1 ppm solution. The limit of detection, defined as the concentration of lead corresponding to the signal of a 'blank' plus three times its standard deviation, is 500 ppb. The dynamic range may be increased by increasing the amount of dithizone available to complex with the lead present in the solution. This is achieved at the expense of sensitivity and response time of the sensor as the immobilised reagent will take a much longer time to change colour, as has been explained earlier.

In a similar sensor configuration based on reflectance measurements for heavy metal ions, Malcik *et al* [26] obtained sub-ppm detection limits for a range of heavy metals with a limited linear range of 1-10 ppm due to a small amount of reagent immobilized on the resin. In this work, the linear dynamic range is found within the range 1 ppm to 30 ppm although this may be increased to suit the application needed as mentioned above.

3.4.3. Effects of photodecomposition

The extent of photodecomposition of the immobilized dithizone was studied by placing the probe in a solution of dilute acid and exposing it to the light source in the absence of lead ions and the signal reflected was monitored by a detector.

A linear increase in intensity with time was seen over a period of 2 hours. The limit of detection (LOD) at 500 ppb determined above is set by this photodecomposition. The photodecomposition is, however, constant and will only introduce a systematic error that can be taken into account.

The use of an appropriate bandpass filter will reduce photodecomposition as it removes all light except that of the wavelength under measurement but it will also remove the signal at the reference wavelength of 770 nm if not chosen correctly. It should be noted that the referencing scheme in use in this work requires no additional hardware and is very effective at canceling the deleterious effects of leaching and the inevitable fluctuations present from the light source.

In this work, with the configuration used, the only effect of the photodecomposition is to impose an LOD on the sensor and the figure determined above of 500 ppb was deemed acceptable in light of typical figures from published work [26] for a sensor system that is robust, optically referenced and relatively inexpensive by minimizing the hardware used. The use of filters will not guarantee the removal of this photodecomposition effect and at the same time will not guarantee a significant improvement in the LOD observed.

3.4.4. Repeatability and regeneration of the probe

Following each measurement, the probe was regenerated by placing it in a solution of 0.1 M HCl. According to Sandell, mineral acid can be used as

reversion reagent for lead [8]. The baseline performance of the probe was reached within 2 minutes and the probe was then rinsed in the buffer solution prior to being used for the next measurement. In the experimental work carried out, it was found that the sensor could be regenerated up to five times without any effect on performance.

The repeatability of the sensor was studied by using the same probe to measure the concentration of a known 30 ppm lead solution several times and Fig. 3.10 shows the results obtained from this series of measurements. Using these results, the repeatability of the sensor yielded a relative standard deviation (r.s.d) of 11%, which compares well with a value of 7% obtained from previous work [1] using a flow-cell arrangement which is more stable.

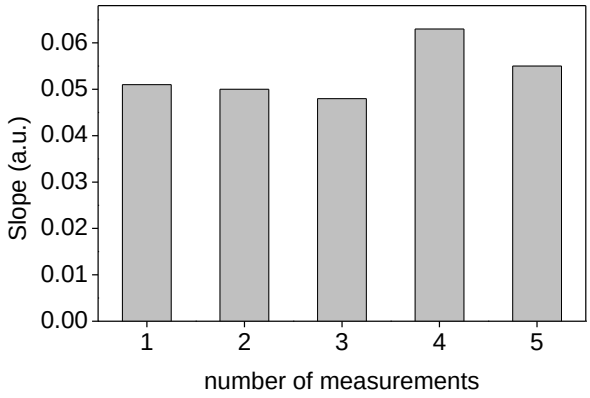

Fig. 3.10. Repeatability measurements

Data on the reproducibility of a series of probes prepared using the same technique were obtained by measuring the response of several such sensors constructed using different resin batches but exposed to the same lead concentration. The result, depicted in Fig. 3.11, gives an r.s.d of 14%. This is a relatively high figure but can be attributed to variations in the amount and distribution of the resin in the sensor construction process which cannot easily

be controlled using the techniques applied. Several other researchers have mentioned similar limitations and have extensively commented on them [2, 10].

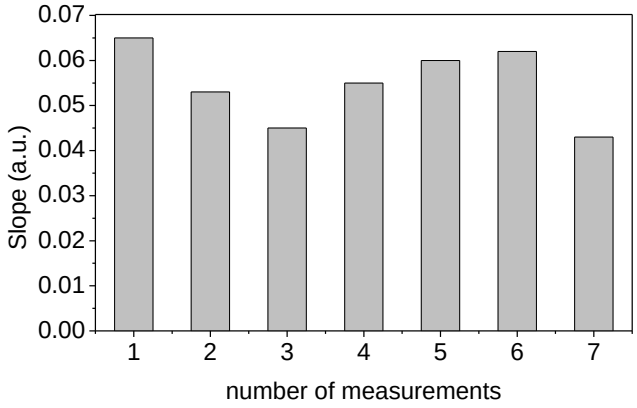

Fig. 3.11. Reproducibility measurements

3.4.5. Efficiency

The efficiency of the experimental setup was measured using the spectrometer. Due to its physical shape and adaptor, it can only be connected to a fibre terminated with a fibre connector. Therefore it is not possible to connect the light source directly to it. Instead, the light exiting from the branch of the fibre bundle connected to the light source was measured. Then, using the same light source intensity, the probe was fixed to the fibre bundle and dipped into a 30 ppm lead solution and the reaction allowed to reach completion by monitoring the optical signal on the spectrometer. The ratio of the optical signal at completion of reaction to the light source measurement yielded an efficiency of 11.2% over the wavelength range 600 nm to 800 nm.

3.5. Summary

A fibre optic sensor to measure aqueous lead ion concentration based on the use of immobilized dithizone has been developed, its design and performance described and results obtained reported. The sensor measures the reflectance of a reagent chosen so that it changes colour in the presence of lead and from which the concentration of the analyte can be related to the rate of change of the intensity of the reflectance signal from the probe.

The reagent dithizone, which is used in this work, reacts to a wide range of heavy metals. Selectivity to the ion in question i.e. lead is imparted by working at a specific pH or by using an appropriate masking agent. As an alternative the probe could be configured to provide a measure of the total heavy metal ion content in a sample [2].

The work has shown the value of the referencing scheme which has been incorporated, utilizing no major experimental modification or expensive hardware. The technique was modified from the previous arrangement [1] and does not need a flow-cell arrangement, making it more compact and easier to use without the need for a pump, flow-cell and tubing.

Applications of sensors of this type lie particularly in environmental monitoring. For example, fertilizers are a much overlooked source of heavy metals which can easily enter the food chain and also expose farm workers, the concentration of heavy metals in fertilizers being typically in the ppm range [27]. A sensor of the type described here could be used to measure the amount of heavy metals entering rivers and ground water from agricultural lands.

3.6. References

1. W.A. De Oliveira and R. Narayanaswamy, A flow-cell optosensor for lead based on immobilized dithizone, Talanta(Oxford) 39 (1992) 1499-1503.
2. I. Klimant and M. Otto, A fiber optical sensor for heavy metal ions based on immobilized xylenol orange, Microchimica Acta 108 (1992) 11-17.
3. N. Mahendra, P. Gangaiya, S. Sotheeswaran, and R. Narayanaswamy, Investigation of a fibre optic copper sensor based on immobilised a-benzoinoxime (cupron), Sensors & Actuators: B. Chemical 90 (2003) 118-123.
4. R. Sundari, M. Ahmad, and L.Y. Heng, Development of an optical fibre reflectance sensor for copper(II) detection based on immobilised salicylic acid, Sensors and Actuators B 113 (2006) 201-206.
5. N.A. Yusof and M. Ahmad, A flow-through optical fibre reflectance sensor for the detection of lead ion based on immobilised gallocynine, Sensors and Actuators B: Chemical 94 (2003) 201-209.
6. A.I. Vogel and G.H. Jeffery, Vogel's textbook of quantitative chemical analysis. Longman Scientific & Technical Harlow, Essex, England,1989.
7. O. Klinghoffer, J. Ruzicka, and E.H. Hansen, Flow-Injection analysis of Traces of Lead and Cadmium by Solvent Extraction with Dithizone, Talanta 27 (1980) 169-175.
8. E.B. Sandell, Colorimetric determination of traces of metals. Interscience Publ.,1965.
9. O. Wolfbeis, Fibre Optic Chemical Sensors and Biosensors, vol 1. CRC Press,1991, p 65.
10. M. Ahmad and R. Narayanaswamy, Development of an optical fibre Al (III) sensor based on immobilised chrome azurol S, Talanta 42 (1995) 1337-1344.
11. S.T. Lee, P.S. Kumar, K.P. Unnikrishnan, V.P.N. Nampoori, C.P.G. Vallabhan, S. Sugunan, and P. Radhakrishnan, Evanescent wave fibre

optic sensors for trace analysis of Fe in water, Measurement Science and Technology 14 (2003) 858-861.

12. K. Wang, K. Seiler, B. Rusterholz, and W. Simon, Characterization of an optode membrane for zinc (II) incorporating a lipophilized analogue of the dye 4-(2-pyridylazo) resorcinol, The Analyst 117 (1992) 57-60.
13. E. Wang, K. Ohashi, and S. Kamata, Optical Sensing Properties of PVC Membrane Incorporating Lipophilic 8-Hydroxyquinoline Derivative, Chemistry Letters 21 (1992) 939-942.
14. M. Lerchi, E. Bakker, B. Rusterholz, and W. Simon, Lead-selective bulk optodes based on neutral ionophores with subnanomolar detection limits, Analytical Chemistry 64 (1992) 1534-1540.
15. G. Boisdé and A. Harmer, Chemical and biochemical sensing with optical fibers and waveguides. Artech House Boston,1996.
16. I. Oehme, S. Prattes, O.S. Wolfbeis, and G.J. Mohr, The effect of polymeric supports and methods of immobilization on the performance of an optical copper (II)-sensitive membrane based on the colourimetric reagent Zincon, Talanta 47 (1998) 595-604.
17. B. Wang and M.R. Wasielewski, Design and synthesis of metal ion-recognition-induced conjugated polymers: an approach to metal ion sensory materials, J. Am. Chem. Soc 119 (1997) 12-21.
18. D.J.S. Birch, O.J. Rolinski, and D. Hatrick, Fluorescence lifetime sensor of copper ions in water, Review of Scientific Instruments 67 (1996) 2732-2737.
19. K.T.V. Grattan and B.T. Meggitt, eds. *Optical Fiber Sensor Technology*. ed. K.T.V. Grattan. 1995, Chapman & Hall
20. W.R. Seitz and M.J. Sepamak, Chemical Sensors Based on Immobilized Indicators and Fiber Optics, Critical Reviews in Analytical Chemistry 19 (1988) 135-173.
21. I. Oehme and O.S. Wolfbeis, Optical sensors for determination of heavy metal ions, Microchimica Acta 126 (1997) 177-192.
22. www.rohmhaas.com.

23. www.sigmaaldrich.com.
24. M. Ahmad and R. Narayanaswamy, Optical fibre Al (III) sensor based on solid surface fluorescence measurement, Sensors & Actuators: B. Chemical 81 (2002) 259-266.
25. M.A. Arnold and T.J. Ostler, Fiber optic ammonia gas sensing probe, Analytical Chemistry 58 (1986) 1137-1140.
26. N. Malcik, O. Oktar, M.E. Ozser, P. Caglar, L. Bushby, A. Vaughan, B. Kuswandi, and R. Narayanaswamy, Immobilised reagents for optical heavy metal ions sensing, Sensors & Actuators: B. Chemical 53 (1998) 211-221.
27. K.P. Raven, J.W. Reynolds, and R.H. Loeppert, Trace element analyses of fertilizers and soil amendments by axial-view inductively-coupled plasma atomic emission spectrophotometry, Communications in soil science and plant analysis 28 (1997) 237-257.

Chapter 4

Feasibility studies of thin sol-gel films doped with a novel fluorophore

4.1. Introduction

There are few reported FOCS for lead based on fluorescence. Most of them are based on chromogenic reagents, leading to absorption or reflectance-based measurement schemes. Yusof and Ahmad briefly reviewed reagents that have been used for the determination of lead using FOCS but no fluorescent indicator was mentioned [1]. However, Casay *et al* devised a metal ion sensor based on the fluorescence of a reagent and were able to detect lead but selectivity was low as the sensor also detected cadmium, alkali and alkali earth metal ions to a low ppm range [2]. This lack of fluorescent FOCS for lead implies that there are few fluorescent reagents and those few reported in the literature exhibit low selectivity and have only been used in solution [3-5]. The task of the FOCS designer is thus to find a suitable way to immobilise these reagents on a solid support for fibre optic sensing.

In this work, a novel fluorescent reagent with high selectivity to lead ions has been chosen to be adapted to optical fibre sensing. This fluorophore was chosen based on the following properties [6]:

1. High sensitivity and selectivity to lead. The quantum yield is reported to be approximately 0.35 and emission is visible to the naked eye.

2. Excitation and emission spectra in the visible spectrum where fibre transmittivity is high. Many organic fluorophores must be excited in the UV which leads to problems such as high background fluorescence and Rayleigh scattering.

This chapter will present an explanation of the fluorescence mechanism behind the molecule followed by a study of its properties for adaptation to an optical fibre system based on sol-gel chemistry. A series of experiments were carried out to optimise the sol-gel probe and study the performance of the sol-gel probe.

4.2. Fluorescence

4.2.1. Principles of Fluorescence

The mechanisms of fluorescence are best explained with the use of a Jablonski diagram [7] as shown in Fig. 4.1 to illustrate the energy levels involved. The ground, the first and the second electronic states are denoted by S_0, S_1 and S_2 respectively. Within each of these electronic energy levels, a fluorophore may exist in various vibrational energy levels, denoted in the diagram by the closely-spaced lines at each electronic energy level. Transitions between energy states are depicted by vertical lines to illustrate the instantaneous nature of absorption and emission of light.

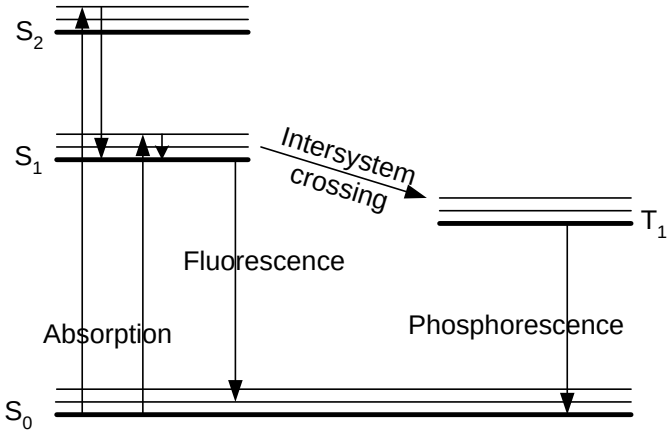

Fig. 4.1. Jablonski diagram depicting the fluorescence mechanism in terms of fluorescence level [7].

Consider an electron in the ground state. If a photon of energy greater or equal to the energy level of a vibrational state at S_1 or S_2 is incident upon that electron, the photon energy will be absorbed, transferring the energy level of the electron to the corresponding vibrational energy state, say, the second vibrational energy level of S_2 as illustrated in Fig. 1. A very rapid relaxation of this state sends the energy level to the lowest vibrational state of S_1.This process is called internal conversion [7]. From the electronic energy state S_1, the energy level drops in a finite time to a higher excited vibrational *ground* state, releasing a photon in the process. This finite time represents the fluorescence lifetime of the fluorophore.

At the S_1 state, a spin conversion of the electron may send the molecule to the state T_1 in a process called intersystem crossing [7]. The electron in this excited state has the same spin orientation as its paired electron in the ground state, thus forbidding a return to the ground state and resulting in slow emission rates so that the lifetime is several orders of magnitude longer than the fluorescence lifetime. This long lifetime is called phosphorescence and the emission energy

in that process is also lower as the energy level of T_1 is closer to the ground state than S_1, resulting in emission of longer wavelengths compared to fluorescence.

Any excited energy level that does not lose its energy by emission of photon does so in a radiationless process such as heat. For example, after a transition of energy level from S_1 to a higher vibrational energy state of S_0 with the emission of a photon, the molecule finally returns to the lowest vibrational energy level of S_0 by a radiationless process. The large energy difference between S_1 and S_0 means that thermal energy cannot be used to promote an electron to this higher energy level. Consequently, light and not heat is used for fluorescence excitation.

UV light is commonly used for fluorescence excitation but as it is of very high energy, it also leads to high background fluorescence as other molecules are then also capable of fluorescing under such intense excitation radiation. In the design of fluorescent sensors, it is usually a good idea to select a fluorescent indicator having the lowest excitation energy required so that fewer interfering species may be excited under these conditions.

The distinct presence of vibrational energy levels is often observed as individual maxima in the absorption and emission spectra, often leading to a mirror image of each other. The two spectra sit side by side as a result of a phenomenon called the Stokes shift, an important and distinct characteristic of fluorescence that arises as a result of the radiationless emission during the excited state, for example internal conversion.

4.2.2 Characteristics of fluorescence

The Stokes shift is explained using the Jablonski diagram as a transition in energy level to the ground state, for example from S_1 to S_0, which is shorter than the transition to a higher excited state such as S_0 to S_2. The result is the emission of a photon of lower energy than that which has been absorbed. In practice, the Stokes shift appears as the emission of light of longer wavelength than the excitation light and is usually measured as the difference in wavelength between the peak absorption spectrum and the peak emission spectrum. The presence of this Stokes shift allows the detection of fluorescence on a low background noise, thereby improving the detection sensitivity.

The solvent relaxation effect, or solvatochromic effect, also contributes to the Stokes shift. It usually occurs in polar solvents where the solvent molecules have a dipole moment. They are able to reorient themselves around the fluorophore molecule already in the excited state and lower its energy level. Upon return to the ground state, the emitted photon thus has less energy. In general, the more polar the solvent, the greater the Stokes shift due to a greater solvent relaxation effect [7].

The quantum yield of a fluorophore determines how efficient it is at emitting light given a certain amount of excitation energy. The quantum yield is formally defined as the ratio of emitted photons to absorbed photons; in an ideal situation the ratio is 1. Some fluorophores have quantum yield approaching unity and are as such very bright; examples are rhodamines and fluorescein [5].

The lifetime of a fluorophore is an important feature that can be used in sensing. It is defined as the average time the molecule spends in the excited

state prior to returning in the ground state [7]. If Γ and k_{nr} are defined as the emissive rate and the radiationless decay rate respectively of the fluorophore, then it follows that the fluorophore lifetime τ is

$$\tau = \frac{1}{\Gamma + k_{nr}} \tag{4.1}$$

Because emission is a random process, not all the photons are emitted spontaneously at time $t = \tau$. The lifetime indicates the average time spent in the excited state and for a single-exponentially decaying fluorescence signal, 63% of the molecule will have decayed before $t = \tau$ and the rest at $t > \tau$. If non-radiative processes do not apply for a given fluorophore, then its lifetime is the reciprocal of its emissive rate and is called the natural lifetime:

$$\tau_n = \frac{1}{\Gamma} \tag{4.2}$$

Organic-based molecules able to undergo fluorescence usually have a lifetime in the order of nanoseconds. This implies the use of complex and expensive instrumentation to make time-resolved measurements on this scale. However time-resolved fluorescence measurements reveal additional information at the molecular level such as the type of quenching or the type of multi-exponential decays [7]. This type of information, however, is best left to spectroscopists probing at the molecular level.

For the sensor designer only interested in relating an analyte concentration to fluorescence, the most useful feature of lifetime measurements is their robustness against noise. However, through the use of proper referencing techniques, especially the ratiometric technique which is robust and easy to implement, steady-state fluorescence measurements are just as effective and

cheaper in terms of the instrumentation required. As such, fluorescence measurements in this chapter focus on steady-state signals.

To implement a fluorescence-based sensor system, knowledge of the absorption and emission spectra is required. The point where peak absorption occurs will be used for efficient photo-excitation, in the past by lasers, nowadays more frequently by LEDs. Following the excitation of the fluorophore, emission will occur and optical detection will be performed within that spectrum, targeting the wavelength range of maximum emission. The longer the Stokes shift, the further away the emission spectrum will be from the high intensity excitation radiation so that erroneous measurement of the excitation light will not occur.

To ensure that no excitation light occurs in the emission spectrum, lasers have been traditionally used as source of excitation light, providing a very narrowband spectrum. LEDs have a wider bandwidth but may be used where the Stokes shift is large enough. In the case of broadband light sources such as Xenon lamps, excitation filters are required to provide a narrowband emission radiation.

An excitation light radiation of intensity I_0 watts travelling an optical pathlength l cm through a fluorescent solution will give rise to fluorescence of intensity F described by

$$F = 2.3 I_0 \Phi \left(\varepsilon C l \right) k \tag{4.3}$$

also known as Parker's law [4] where Φ is the quantum yield of the fluorophore, ε its molar extinction coefficient in moles per cm, C the molar concentration of the fluorophore and k is a dimensionless constant introduced to account for the fact that only a fraction of the total emission is detected. Thus

the detected fluorescence is proportional to any one of the above parameters provided the others are kept constant.

At high fluorescence concentration C, there is departure from linearity and the emitted fluorescence drops as a result of quenching from the fluorophore itself. This is known as the inner filter effect. The primary filter effect arises when the excitation light intensity is not constant throughout the optical pathlength due to strong absorption from the solution. The secondary filter effect arises when the emitted fluorescence is re-absorbed by the fluorescent solution itself.

While this appears as a disadvantage, the inner filter effect has been exploited in absorbance-based schemes by measuring this drop in fluorescence. This technique requires a fluorophore whose emissive properties are not affected by the sample composition and which is added to a chromogenic reagent. The fluorophore must have its emission or excitation spectrum overlapping the absorption spectrum of the chromogenic reagent. The fluorescence intensity will then vary with changes in the absorbance of the indicator. This scheme was used by Jordan and co-researchers in a pH sensor using phenol red as the indicator and eosin as fluorophore [8]. The advantage of this method is that measurement of the analytical signal is made at a wavelength other than that of the interrogating light, providing a much lower background noise.

Using the same line of thought, Tohda and co-researchers exploited the inner filter effect to perform absorption studies using fluorescence measurements [9]. In this work, a fluorescent dye was added to a non-fluorescent absorbing molecule. The aim was to perform optical detection measurements on the characteristics of microscopic solution volumes in the range of femtolitre.

The inner filter effect is not the only cause of fluorescence quenching. In fact, there are two main classes of quenching that optical sensors exploit: static and dynamic.

Dynamic or collisional quenching occurs when a fluorophore returns to the ground state by radiationless deactivation due to collision with a quencher whilst its excited state. The Stern-Volmer equation describes dynamic quenching as follows [10]:

$$\frac{F_0}{F} = \frac{\tau_0}{\tau} = 1 + k_q \tau_0 [Q] = 1 + K_D [Q] \qquad (4.4)$$

Where F_0, τ_0 and F, τ are the fluorescence intensities and lifetimes in the absence and presence of a quencher respectively and k_q is the bimolecular quenching constant for the dynamic reaction of the quencher with the fluorophore and $[Q]$is the quencher concentration. K_D is known as the Stern-Volmer constant.

Static quenching, on the other hand, arises as a result of the formation of a non-fluorescent complex between the fluorophore and the quencher when in the ground state. If this complex absorbs light, it immediately returns to the ground state without emission of a photon. A similar Stern-Volmer equation may be used to describe static quenching [10]:

$$\frac{F_0}{F} = 1 + K_S [Q] \qquad (4.5)$$

Where K_S is the association constant for the formation of the non-fluorescent complex.

The most efficient way to differentiate between static and dynamic quenching is via lifetime measurement as dynamic quenching occurs in the excited state and

both, the intensity and the lifetime are affected as given by (4.4) whereas the lifetime is unaffected in static quenching.

4.2.3. Crown ethers and photo-induced electron transfer

Recently, fluorophores have been given enhanced selectivity and versatility by pairing it with a new class of compounds, the crown ethers.

When Pederson synthesized crown ethers in 1967 [11] and its 3-dimensional counterpart, cryptands shortly after, a new field of chemistry was born, called Supramolecular Chemistry [12]. His subsequent award of the Nobel Prize in 1987 recognized the importance of crown ethers and cryptands in the field of ion sensing.

Crown ethers and their analogues are organic molecules which can trap ions depending on the host molecule size and the ionic radius of the guest. They perform a so-called molecular recognition function. Crown ethers are atoms of carbon and oxygen linked together in the shape of a ring. Often, a nitrogen or sulphur atom is introduced to improve the binding affinity of a particular ion to the crown ether. While crown ethers have a simple cyclic planar structure, more complex molecules have been synthesised such as calixarenes [13, 14]. Calixarenes have a 3-dimensional structure that resembles a cup as depicted in Fig. 4.2. By modifying the upper and/or lower rims, it is possible to synthesize various derivatives and tune their selectivity towards the guest ion of interest.

The affinity of crown ethers and other macrocyclic ligands towards cations is due to lone pairs of electrons from the oxygen atoms within the ring forming electrostatic bonds with a cation as it fits inside the ring. Selectivity for a particular cation increases if the host cavity diameter matches closely the guest ion diameter. A bigger ion will not be able to fit into the ring while a smaller ion,

although able to fit through easily, while not be able to form sufficiently strong electrostatic bonds.

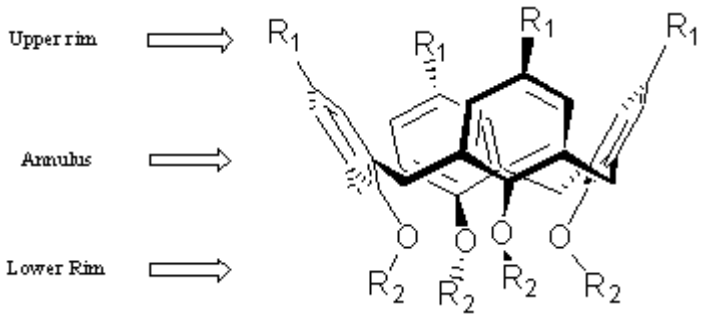

Fig. 4.2 Cone formation of a typical calixarene [15].

However useful crown ethers were initially found to be, they only serve as ion-recognition molecules [16] and do not signal a binding event. It was only later that the idea followed of attaching these ion-recognition molecules, also termed ionophores, to conventional fluorophores [17]. The end product is a fluoroionophore which is made up of an ion-recognition moiety, i.e. the crown ether incorporating a nitrogen atom, and a signal-transducing element which is the fluorophore moiety. With the advent of fluoroionophores, the use of crown ethers and the like in ion sensing became mainstream [18-21].

The sensing mechanism of fluoroionophores is based on a photo-induced electron transfer (PET) quenching process by amines. When the fluorophore is photo-excited, an electron in the Highest Occupied Molecular Orbital (HOMO) is promoted to the Lowest Unoccupied Molecular Orbital (LUMO). The lone pair of electrons from the nitrogen atom is still at the HOMO level and therefore at a higher energy state than the vacancy left behind by the excited electron. An electron from the nitrogen atom then enters this lower energy orbital, effectively quenching the fluorescence [7].

When the lone pair of electrons is involved in binding with a proton or cation, the energy of that pair is lowered, inhibiting electron transfer and deactivating the quenching process. This results in a fluorescence enhancement and signals a binding event. This is the basis of fluorescent ion sensing as pioneered by A. P. de Silva [18, 22]. The medium in which the binding event takes place is important: parameters such as the polarity of the solvent and pH affects the photophysical characteristics of the molecule and the efficiency and selectivity of binding [23].

A schematic of the structure of a fluoroionophore made up of a fluorophore and a crown ether is shown in Fig. 4.3. A spacer unit is used to join the two groups together to minimise the structural modification of either group which might hinder their performance.

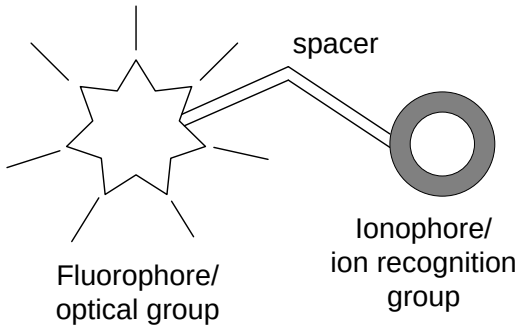

Fig. 4.3. Schematic diagram of the structure of a fluoroionophore

There are many other examples of similar chemoreceptors used to detect metal ions [24-27]. Dang and co-workers reported a newly-synthesized terbium (III) nitrate chemosensor able to selectively bind with silver ions and undergo fluorescence enhancement as a result of PET [28]. The photophysical properties of a new red-light emitting ligand made up of a combination of

calixarene and crown ether were studied and reported by Jeon and co-researchers [29].

Fery-Forgues *et al* synthesized a molecule in 1988 which detected alkaline and alkaline earth metals at the low millimolar level [30]. Ten years later, Addleman and co-workers reported the detection of lead and mercury ions at the low micromolar level [3] using the same molecule whose structure is shown in Fig. 4.4. It was shown that a combination of lower charge density for univalent ions and disparity in diameter led to a lower binding strength in the case of Group I and Group II cations.

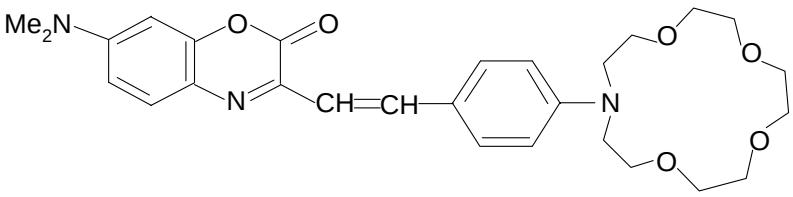

Fig. 4.4. Structure of an azacrown ether derivative [3, 30]

A fluorescent chemosensor for lead ions was reported recently in 2006 by Liu *et al* [31]. The authors first highlighted the need for inexpensive, real-time chemosensors for lead and mentioned the lack of calixarenes for heavy metal ion detection, especially for lead. The new chemosensor they synthesized had maximum absorption bands at 274 nm and 340 nm with emission peak at 410 nm. Addition of lead caused a decrease in fluorescence emission due to an electron energy transfer quenching process according to them. A 1:1 complex was formed between the ligand and lead ion and the complex displayed no sensitivity to the presence of a wide range of foreign metal ions with the exception of sodium. This ligand was capable of performing in a mixture of acetonitrile and water in the ratio 3:1 with the pH set to 5.2 for the experiments.

4.2.4. The selected lead-sensitive fluorophore

The novel fluorophorionophore used in this study and called Molecule **1** is made up of a crown ether and a coumarin moiety as shown in Fig. 4.5 below. The nitrogen atom linked to the two ethyl groups possesses a pair of lone electrons which makes it an electron-donor while the fluorophore is the electron-withdrawing group. The nitrogen atom on the crown ether also possesses a lone pair of electrons which is delocalised over the fluorophore moiety during photo-excitation, causing the PET process. These delocalized electrons act to reduce the electron-withdrawing nature of the fluorophore. In the presence of a cation, the lone pair of electrons from the nitrogen atom will bind to it, inhibiting the PET and causing a concomitant increase in emission from the fluorophore moiety.

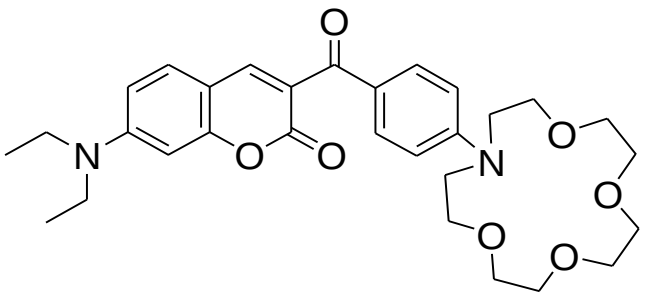

Fig. 4.5. Structural formula of the fluorescent molecule **1**

A 2:2 binding stoichiometry has been proposed [6] as depicted in Fig. 4.6, leading to two reasons for fluorescence enhancement upon binding with lead:

1. Inhibition of the PET process;
2. Conformational restriction of the **1**•Pb^{2+} sandwich complex.

Conformational restriction in general leads to fluorescence enhancement because the fluorescent molecule is no longer able to adopt a shape leading to the most stable energy level [32, 33]. Given a series of aromatic compounds, the most planar, rigid and sterically uncrowded are the most fluorescent [34].

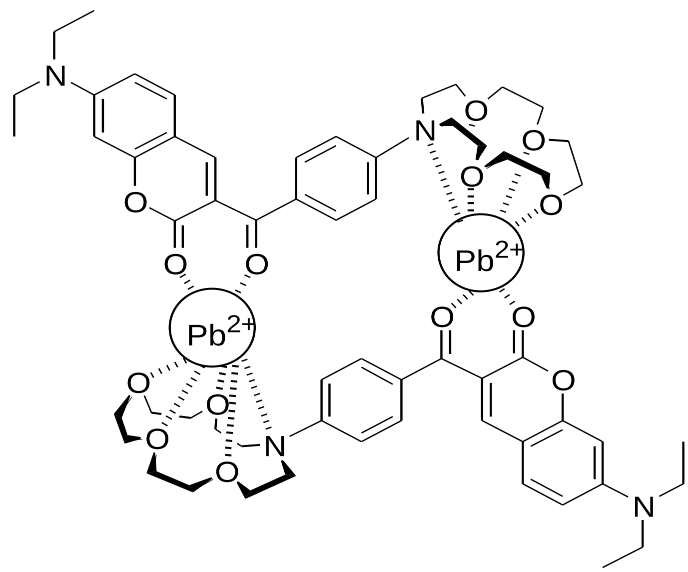

Fig. 4.6. A proposed 2:2 complex formed between **1** and Pb^{2+}

The selectivity of molecule **1** in the presence of divalent metals as reported by Chen [6] is displayed below in Fig. 4.7. It was found that univalent ions do not cause significant changes in the fluorescence spectrum.

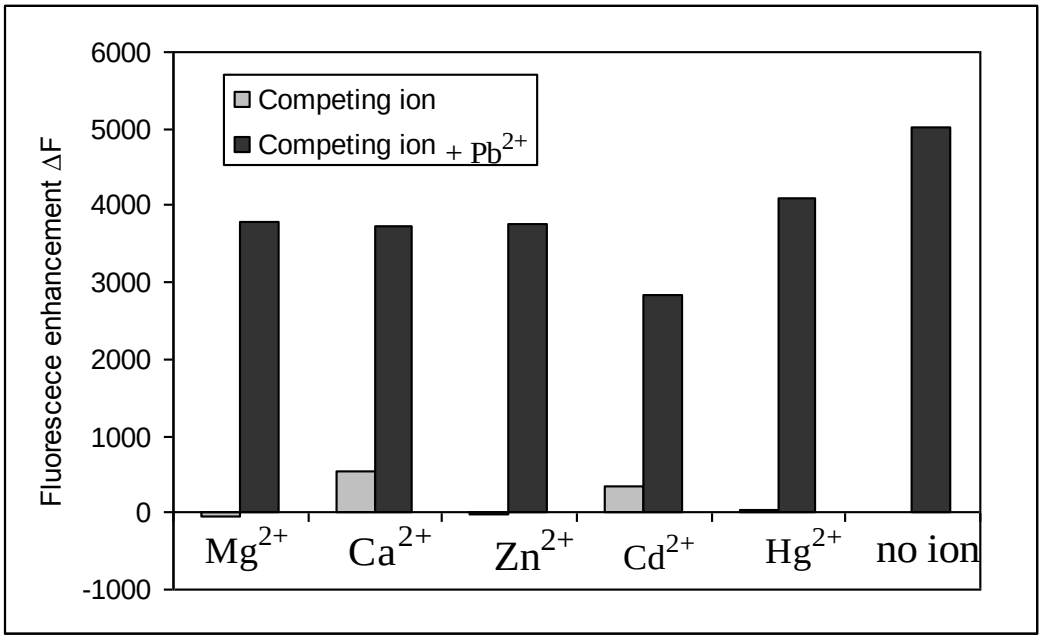

Fig. 4.7. The fluorescence increase of molecule **1** (10 μM in acetonitrile) in the presence of selected metal ions, in collaboration with the Chemistry Department, University of Taiwan [6]. Fluorescence increase with the competing ions in the absence of lead is negligible or negative. When lead ions are added to the competing ions, the fluorescence enhancement is significant.

Most of the research carried out by workers in the field of molecular recognition has been restricted to investigations in solution form. Immobilising these chemoreceptors onto a solid support will enable them to be adapted into a probe configuration and be used reversibly in sensing. Given the large number of macrocycles which have been synthesized for the detection of a wide range of metal ions, they could be adapted to fibre optic probes and enable the sensing of a range of metal ions in this new configuration. Because these ligands are synthesized, they can be tailored to fit a particular application, for e.g. a particular fluorophore of desired excitation and emission wavelength could be selected to be coupled to an ionophore with affinity for the analyte of interest.

4.3. Fluorescence studies

4.3.1. The solvatochromic effect

In order to evaluate its performance and characteristics, molecule **1** was dissolved in various solvents at a given concentration and the peak emission wavelength observed was recorded as shown in Table 1. As the polarity of the solvent increases, the bathochromic shift in the emission wavelength also increased as a result of the solvatochromic effect [22]. It is therefore important to take the nature of the solvent into consideration when measuring the fluorescence intensity at a fixed wavelength range. The fluorescence of molecule **1** in water is drastically reduced [6] due to the presence of hydrogen bonding and protons which interfere with it, making aqueous studies not viable at this stage.

Solvent	**Dielectric constant** *	**Peak emission wavelength (nm)**
Dichloromethane	9	456
Acetone	21	475
Acetonitrile	37	480

* CRC Handbook of Chemistry and Physics 67th Ed. (1986); dielectric constants quoted at 20˚C.

Table 4.1. Effect of solvent polarity on the peak fluorescence wavelength.

4.3.2. The inner filter effect

To determine the optimum wavelength for fluorescence intensity measurements on the fluorophore, its excitation and emission spectra were studied. It was found that an inner filter effect was occurring i.e. part of the emission radiation was re-absorbed by the fluorescing molecule.

To demonstrate this effect, dichloromethane was chosen as it is a non-polar solvent and the Stokes shift for the emission spectrum is small, leading to a significant spectral overlap with the absorption spectrum. This is depicted in Fig.4.8a for 30 μM of molecule **1**. The concentration of the fluorophore was varied and its peak emission intensity and corresponding peak emission wavelength plotted as a function of the concentration as shown in Fig. 4.8b and Fig. 4.8c. The results obtained show that there is an *apparent* decrease in fluorescence intensity arising from the overlap of the absorption and the emission spectra due to the re-absorption of light.

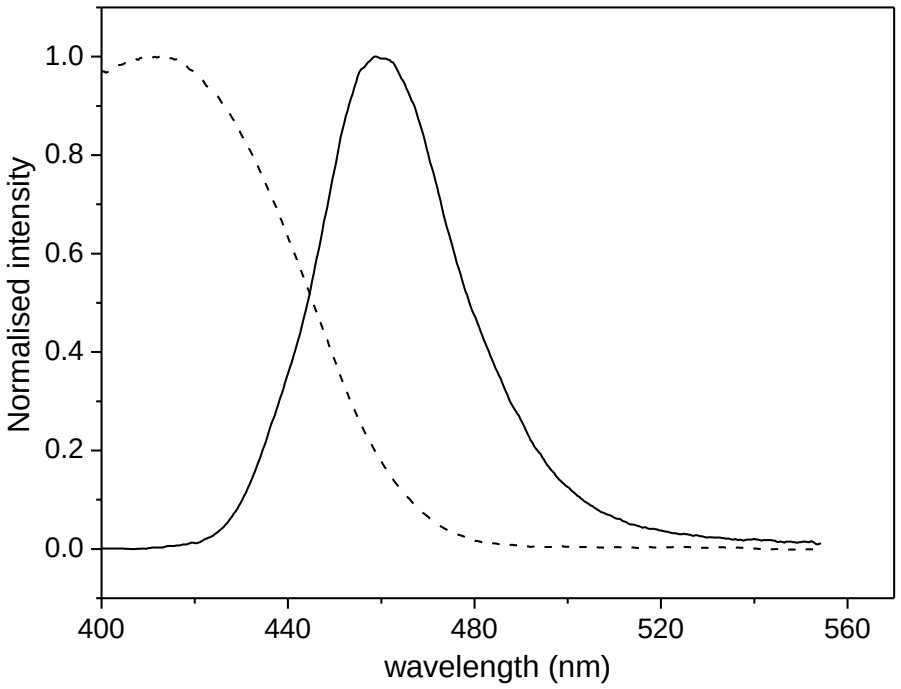

Fig. 4.8a. Absorption (dotted line) and emission spectra of 30 μM molecule **1** in dichloromethane showing spectra overlap; inset: peak emission intensity and corresponding wavelength as the concentration of the molecule **1** is varied.

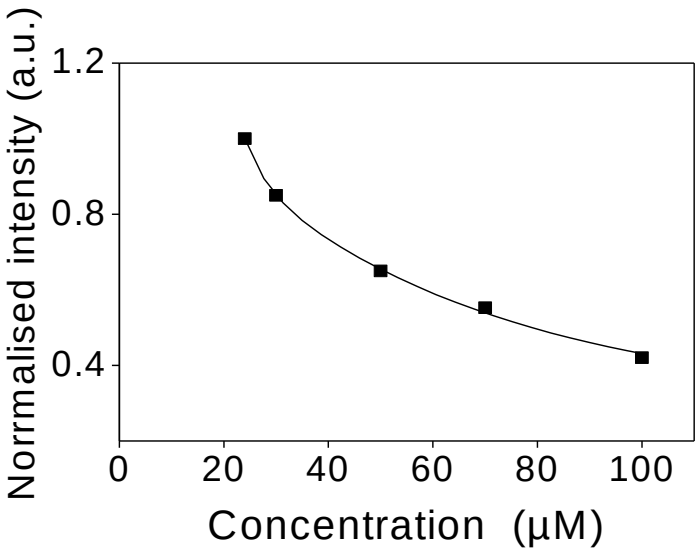

Fig. 4.8b. Peak normalised emission intensities as the concentration of molecule **1** is varied. The drop in intensity as the concentration increases is attributed to the inner filter effect.

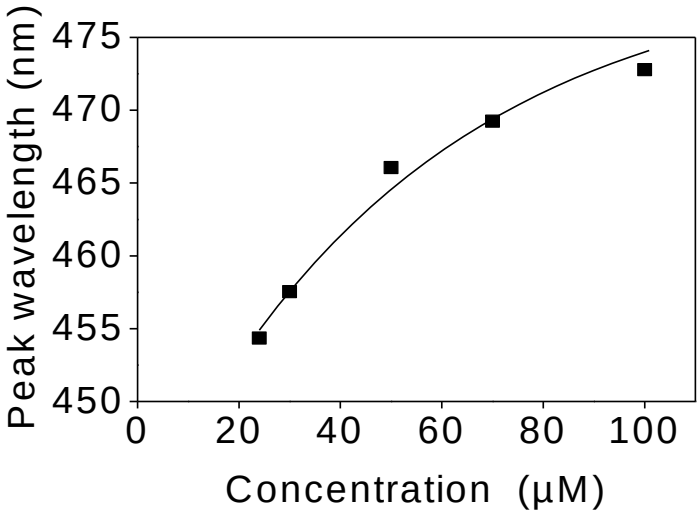

Fig. 4.8c. Corresponding wavelength of the peak emission intensities as the concentration of the molecule **1** is varied. The apparent bathochromic shift is due to the inner filter effect.

To show that in fact fluorescence increases as the fluorophore concentration is also increased, it is necessary to measure the emission intensity at wavelengths lying beyond the spectral overlap. Fig. 4.9 shows the same data used in Fig. 4.8a-c but now the emission intensity is measured at specific wavelengths and plotted as a function of fluorophore concentration. At wavelengths of 480 nm and below, the fluorescence drops as the concentration increases but at wavelengths lying at 490 nm and higher, i.e. at wavelengths beyond the absorption spectrum, the fluorescence increases smoothly until saturation. It is therefore important not to measure the fluorescent intensity below 480 nm to avoid any erroneous results as in Fig. 4.8a-c. By taking fluorescence measurements in a wavelength band that lies beyond this spectral overlap, the inner filter effect is avoided completely and the fluorescence intensity measurement can give a true picture of the concentration of the measurand. While the absorption spectrum of Molecule **1** in acetonitrile is similar to that in dichloromethane, its emission spectrum in acetonitrile is more red-shifted (see Table 4.1). Consequently, the emission and absorption spectral overlap is smaller and self-absorption effects are not expected to occur beyond 480 nm in acetonitrile solution.

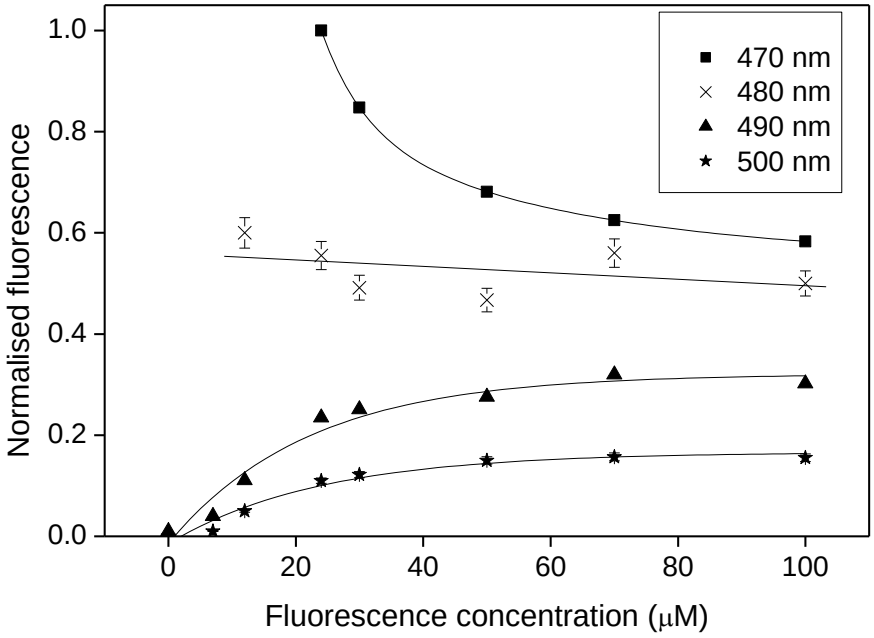

Fig. 4.9. Normalized fluorescence intensity of molecule **1** in dichloromethane at different wavelengths as a function of concentration. The fluorescence intensity is normalised at its highest value.

4.4. Sol-gel studies

Addleman and co-workers studied the fluorescent properties based on the PET of a crown ether bound to a fluorophore moiety [3]. They immobilised the reagent onto a silica surface and noticed that it became insensitive to cations, thereby concluding that surface-restricted rotation renders this particular reagent ineffective. They recommended sol-gel as a technique which might accomplish immobilisation without interfering with its PET mechanism. In the case of molecule **1**, surface immobilisation would prevent the binding molecules and lead ions from adopting the required orientation for binding in the sandwich configuration.

Elsewhere, Zhmud and co-workers performed comparative immobilisation studies on a crown ether-type molecule using silica and showed that it still

displayed fluorescence in the presence of rare-earth metals in aqueous solution [35]. However, it was found that whilst in the free state, the molecule had two crown ethers rings for binding, upon immobilisation, only one site was available. A suggested explanation for this was the strong electrostatic repulsion between multivalent ions in this constrained environment.

In the light of these results and recommendation, I decided to adopt the sol-gel route as immobilizer. The sol-gel would act as an entrapment matrix to the reagent molecules, allowing them freedom of movement essential for its fluorescence mechanism to operate whilst still keeping them captive at the fibre end. The low-temperature requirement during the manufacturing process of sol-gels will not destroy organic molecules. Furthermore, the large carbon groups in molecular recognition units render them hydrophobic, preventing them to be dissolved away in water when testing for aqueous ions, if they were to be immobilised. McCarrick and co-researchers have also shown that macrocyclic ligands in an organic phase are able to extract metal ions from an aqueous phase [36]. This means that it may be possible for a macrocyclic ligand immobilised in sol-gel to extract metal ions from their aqueous solution.

Sol-gel is a matrix or immobiliser which has received a great deal of interest in the recent years. Zevin and co-workers have used sol-gel coatings doped with diphenylcarbazide to measure the concentration of chromate ions down to 1 ppb [37]. Changes in the absorption of the dye was used in the determination of chromate ion concentration.

Elsewhere, MacCraith *et al* provide a review of the state-of-the-art optical sensors employing sol-gel coatings [38]. In particular, a pH absorption-based sensor and an oxygen fluorescence quenching sensor are described. In both cases, the cladding of a plastic-clad silica (PCS) fibre was removed and replaced by a sol-gel coating 300nm thick by dip-coating. An evanescent wave sensing approach was used. Abdelghani *et al* also used evanescent wave

sensing to detect gaseous species with sol-gel coated PCS fibres [39]. The dip-coating technique resulted in individual layers around 200nm thick which is of a similar magnitude to that obtained by MacCraith above [38].

Sol-gel is an attractive option as an immobilisation material. It is easy to prepare, essentially by mixing several precursors together and allowing hydrolysis and gelation to proceed and offers design flexibility and versatility. Layer deposition may be done by spin-coating or dip-coating which yields a thickness of a few hundreds of nm, as mentioned above while the fibre may be coated at the end or on the sides to exploit the evanescence wave.

The porous nature of sol-gel is very useful to entrap chemical molecules without modifying them so that they can interact freely with the analyte. This is an especially important point in bio-sensing where proteins and antibodies must be able to adopt the right configuration or undergo conformational changes to bind to the target molecule, as highlighted in a review by Avnir *et al* [40]. Furthermore, the sol-gel cage provides a mechanical protection to the entrapped dye.

4.5. Experimental

The optical setup for fluorescence measurements is depicted in Fig. 4.10. It incorporates the interference filter to separate residual excitation light of the 435 nm LED from the emission intensity which occurs at around 480 nm peak intensity. The broadband filter is centred at 500 nm with a full width half maximum (FWHM) of 40 nm. The branch of the fibre bundle made up of 6 fibres is used to collect the emission back to the spectrometer.

All other reagents apart from Molecule **1** were of analytical grade or better and purchased from Sigma-Aldrich. Molecule **1** was synthesized at the Department of Chemistry, National Taiwan University. Deionised water was used

throughout. Buffers were prepared using sodium acetate for pH 4, sodium dihydrogen phosphate for pH 6, Tris for pH 7 and 8 and ammonium chloride for pH 10. Nitric acid was added to sodium acetate, sodium dihydrogen phosphate and Tris respectively to lower the pH to the desired value while sodium hydroxide was used with ammonium chloride to adjust the pH to 10. pH measurements were made using a digital pH meter from Hanna Instruments. Aqueous lead ions were produced by dissolving known amounts of lead perchlorate into the buffers. Lead ions in acetonitrile were produced by dissolving known amounts of lead perchlorate.

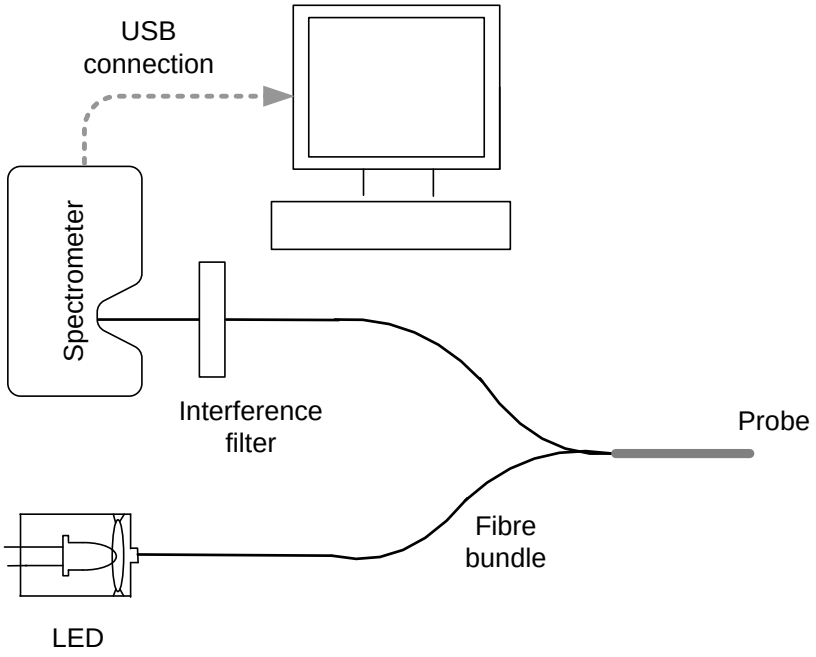

Fig. 4.10. Layout of the main components with a high intensity 435 nm LED to provide excitation light for fluorescence of the sol-gel coated probe affixed at the end of the fibre bundle. The interference filter may be used to separate excitation light from emission in the case of fluorescence measurements.

4.5.1. Sol-gel preparation

The sol-gel was prepared based on the method of Aylott *et al* [41]. 1.5 ml of TEOS was sonicated on ice with 1.5 ml of ethanol, 3.0 ml of water and 0.15 ml

of 0.05 M HCl until a homogenous solution was obtained. The sol was then stored at -20˚C for 72 hours to allow hydrolysis to reach completion. The sol was removed and 0.1 ml of the fluorescent indicator was added to 0.9 ml of the sol. The indicator was at a concentration of 4.37 mM dissolved in methanol.

To create the coated fibre optic probe, the polished fibre probe was immediately dipped into the resulting mixture to a depth of around 1 mm to ensure that the distal end surface was fully coated. After dipping, the coated fibre was allowed to dry vertically at room temperature for 24 hrs before being used.

Observation of the sol-gel coating was performed with a PRIOR microscope providing 10, 20 and 40 times magnification and adapted with optical fibre connectors. A camera (JVC, model TK-C1381) was focused onto the microscope image and the output displayed on a VDU.

4.5.2 Fluorescence measurements

The absorption spectrum of Molecule **1** immobilised in the sol-gel matrix was measured and is depicted in Fig. 4.11, showing that photo-excitation with 435 nm LED is appropriate as mentioned in Chapter 2. Fluorescence intensity measurement was made from 515-525 nm to avoid the absorption spectrum. To remove dark noise from the spectrometer, dark noise measurement was made in the stopband of the interference filter from 400-410 nm and subtracted from the fluorescence emission.

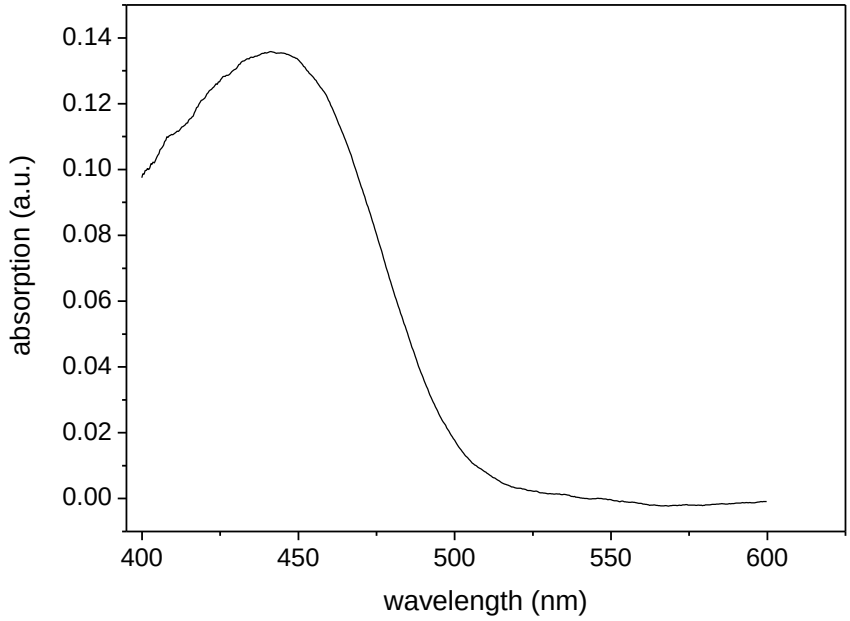

Fig. 4.11. Absorption spectrum of 4.37 mM of molecule **1** added to sol-gel.

Before any measurement of the fluorescent signal was made, the detected signal first had to be confirmed as arising from the photo-excitation of Molecule **1** and not to be resulting from noise or from other interfering species. To this end a probe was prepared with a 'blank' sol-gel coating, i.e. prepared in the exact way but containing no reagent. This was connected in turn to the end of the fibre bundle in the optical set-up and the excitation light launched along the fibre. No signal in the region of interest was detected with the blank probe.

4.6. Results and Discussions

The sol-gel was prepared with a high water/alkoxide ratio and acid concentration, both of which are known to produce a dense sol-gel and thus minimise leaching [42], [43].

Dip-coating of the optical fibre probe was performed at a moderate speed by hand as full reproducibility of the resulting coating was not seen as essential at this stage. An attempt was made to use a lab-made dipping machine to perform the coating under controlled conditions. However, in cases where crack-free coatings were obtained by hand-dipping, the use of the machine consistently resulted in coatings which showed cracks. It was believed that the slow speed (7cm/minute maximum) of the machine and the time in setting up allowed the sol-gel to start forming too early whereas the manual process was sufficiently rapid to allow the fibre to be dipped into the sol when it was still at sub-zero temperatures.

4.6.1. Effect of multiple coatings

Multiple coatings on the distal end of the probe will provide a stronger fluorescence signal; however, the probe response may become sluggish as the response time is a function of the mass transfer of the analyte within the matrix. As a result, two coatings were applied during the probe fabrication, allowing each coating to dry fully before application of the second coating.

It was observed that a sol-gel layer deposited onto another fully formed sol-gel layer had a high risk of resulting in fragmentation. Zevin *et al*, using an atomic force microscope, have taken pictures of sol-gel films showing the granulated surface on a nanometre scale [37]. This uneven surface at the microscopic level may not be suitable as a support for another sol-gel layer when compared to a highly polished silica surface.

4.6.2. Indicator concentration in sol-gel

The relative amount of the fluorescent indicator doped in the sol-gel was investigated. A high concentration of indicator was used when added to the sol to minimise the volume required and therefore disturb the composition of the

sol to a minimum. Methanol had to be used instead of ethanol as the indicator was not as highly soluble in the latter.

In all of the above experiments so far, 0.1 ml of 4.37 mM of the indicator was added to 0.9ml of the sol solution. The volume of indicator added was varied whilst the overall volume was kept constant by adjusting the volume of the sol solution. The optical response of the sol-gel thus formed was measured and the results shown in Fig. 4.12 below. A steep increase in fluorescence occurs when the volume of indicator is increased from 0.05 to 0.1 ml but any further increase in volume did not produce any more significant concomitant fluorescence increase.

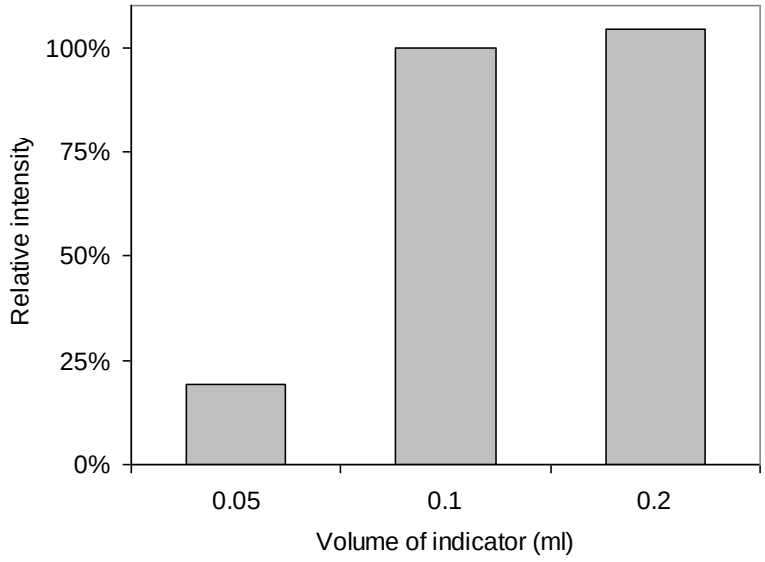

Fig. 4.12. Relative fluorescence intensity normalised to that of 0.1 ml of indicator.

The volume of indicator added to the sol mixture was not increased beyond 0.2 ml to prevent any significant departure from the composition of the sol. A 20% proportion by volume of indicator in the sol was deemed to be more than adequate. On the other hand, that proportion could be decreased to zero without affecting the sol-gel formation. However, it is clear in this graph that 0.1ml provides an adequate signal. Thus the amount of indicator added to the

sol was therefore not altered. Zevin and co-workers recommend that the amount of indicator contained in the film must be as large as possible in order to increase the sensitivity of the optical detection [37].

4.6.3. Leaching in water

An experiment to investigate the leaching characteristic of the sol-gel was performed on a probe prepared using the parameters discussed above. After the probe was ready for use, it was immediately placed in deionized water and the fluorescence intensity monitored over the following days. To ensure that any dissolved indicator in the aqueous phase did not reach equilibrium with that in the sol-gel and thus prevent further solvation, the water was replaced with a fresh batch daily. There was no measurable drop in intensity in the first hour and a decrease of 4.3 % after 4 days of continuous immersion. The constant intensity level in the first hour might be seen as indicating that all the indicator has been fully entrapped in the sol-gel. However, it is highly unlikely that there is no residue of the indicator that has not been successfully immobilised at the high concentration used. What is more likely is that the indicator is highly hydrophobic and cannot pass easily into the aqueous phase at this stage in the experiment.

4.6.4. Probe response to pH

The probe response to aqueous lead ions at different pH values was examined using freshly prepared probes. At low pH, protonation of the nitrogen on the azacrown ether is expected to occur, resulting in the disruption of the PET and yielding a fluorescence enhancement. Protonation suppresses electron transfer even more efficiently than cations [23] and may thus bind more readily to the indicator. There will therefore be strong competition with lead ion, resulting in an erroneous fluorescence enhancement.

At higher pH values, the concentration of hydroxide ions increases. Lead ions may combine with the hydroxide ions to produce insoluble lead hydroxide. This reduces the amount of lead ions in the solution free to bind with the indicator, again leading to erroneous measurements**.** It is therefore advisable to exclude from the investigation the pH effects at either end of the scale and to expect the best performance around a neutral pH value. Buet *et al* restricted the study of a fluoroionophore in aqueous solution to pH 8.5 due to hydrolysis of the molecule at higher pH values [44].

The probe response was investigated at pH values of 4, 6, 7, 8 and 10. The probe was placed in the buffer solution at the working pH value and allowed to equilibrate. It is important to allow the buffer to soak well through the sol-gel as there might be traces of acid left which could lead to a fluorescence increase. The buffer solution was then replaced with a 0.2 mM of lead solution at the same pH value. The response to both buffer and lead was monitored over 30 minutes but no change was seen in the optical signal before and after addition of lead, irrespective of the pH value. Any probe response is expected to be immediately detected, or within the first minute, due to the thin coatings applied. Lam *et al* reported changes in their work within the first 20s [45].

The 0.2 mM lead solution was later replaced with 1 mM and 5 mM lead solutions respectively to ensure that a full range is covered. The probe was rinsed in 5 mM EDTA to remove any trace of lead followed by deionized water and the experiments repeated at the different pH values but no response to lead ions was noted. It can be argued that the indicator, because of its hydrophobicity, is unable to dissolve in the aqueous solution to interact with it, thus explaining the lack of response to either buffer or lead ions. However, dithizone is an organic compound sparsely soluble in water but which has been used to detect heavy metals ions in water successfully [46].

Oehme *et al* noted that a sol-gel prepared at low pH was dense and as a result, showed insensitivity to the analyte due to its inability to pass through the matrix [43]. To address this issue and increase the porosity, a sol-gel was prepared by reducing the acid content to 0.1 ml of 5 mM HCl since a higher pH favours greater porosity [26]. When tested, this probe displayed no sensitivity to lead in buffered solution at any of the pH prepared.

The pore size of the sol-gel can thus be eliminated as a factor in the insensitivity of the probe to aqueous lead ions.

4.6.5. Probe response to lead in acetonitrile.

As the indicator is known to perform well in acetonitrile [6], lead ions dissolved in that solvent were tested with the immobilised indicator. The probe was first rinsed with EDTA followed by deionised water to remove all traces of lead and EDTA respectively and then placed in acetonitrile and the signal measured with time. The response is depicted in Fig. 4.13 showing that a steep increase occurred initially. When the signal did not rise any further, the acetonitrile solution was replaced with 0.2 mM of lead in acetonitrile but no further fluorescence increase occurred. The lead solution was subsequently increased to 0.5mM but the probe showed no increased emission even at this high lead concentration.

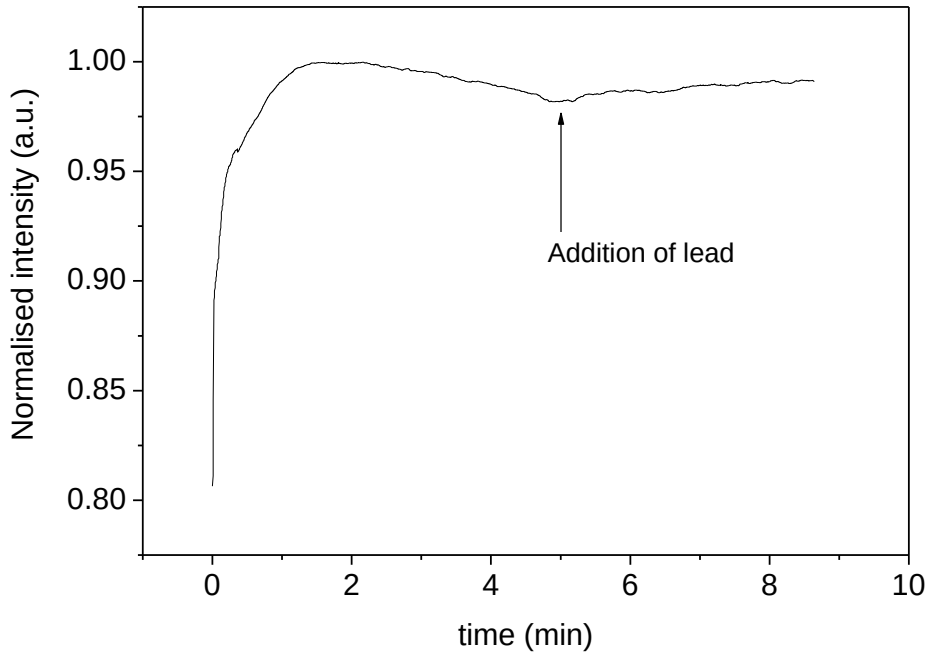

Fig. 4.13. Probe response to acetonitrile followed by lead. Signal is normalised at highest intensity.

The initial increase is probably due to acetonitrile dissolving the reagent within the pores, leading to a decrease in concentration and therefore a decrease in quenching which is typical at high fluorophore concentration. This rapid signal rise (of nearly 20 % within the first minute) demonstrates that the thin sol-gel coating is capable of responding very rapidly and confirms our earlier assumption. After reaching a peak, the fluorescence intensity starts to drop, most probably as a result of leaching given that the indicator is highly soluble in acetonitrile. This leaching effect is seen to cease upon addition of lead. This can be explained by the fact that the acetonitrile solution already contains dissolved lead. However, these changes are very small, less than 2.5 % in this graph, compared to the 20 % signal increase in the first minute.

4.6.6. Probe response to buffer and acetonitrile

It was earlier shown that the probe does not exhibit any response whatsoever in an aqueous environment while signal changes occur in a lipophilic environment, although no specific response to lead has been noted so far. Since acid is used to catalyse the sol hydrolysis, it is possible that there are traces of the catalyst left in the formed sol-gel. It has also been mentioned earlier that dilute acid is able to protonate the fluorophore and cause a fluorescence enhancement. Any subsequent addition of lead may therefore not cause a fluorescence increase if the indicator is already bound to protons. A buffer solution was used in conjunction with aqueous lead to resolve this problem but not whilst using acetonitrile earlier.

Work was undertaken to equilibrate the probe in a neutral buffer prior to immersion in acetonitrile solutions. Gojon and co-workers have shown that the polarity of the silica cage may be varied by changing the pH of the environment [47]. In her work, the absorption peaks of a benzalazine in solution and in immobilised form were found to behave in the same way at identical pH values.

The probe described here was immersed in an aqueous Tris buffer at neutral pH for ten minutes followed by acetonitrile. Once the peak fluorescence is attained, that value is noted and the probe is placed again in the buffer to neutralise the pH again, after which it is placed in an acetonitrile solution containing 0.2 mM of lead. The maximum fluorescence intensity is then compared with the value obtained in the absence of lead. No fluorescence increase was noted in the presence of lead in acetonitrile compared to a sample of acetonitrile only. The only difference is that in the presence of the aqueous buffer, the fluorescence dropped sharply but increases again in acetonitrile. Any increase in the concentration of lead to 0.5mM did not produce any effect on the probe.

4.6.7. Other solid supports

Other matrix supports were briefly considered and tested. PVC, XAD-4 resin and silicone were doped with the indicator. PVC membranes were prepared by dissolving 50mg of PVC granules in 1.0 ml of THF (tetrahydrofuran) into which the fluorophore had already been dissolved to give a concentration of 1.0 mM and adding 0.1 ml of DBS plasticizer (dibutyl sebacate) to the mixture. After mixing thoroughly, fibre probes were dipped vertically and manually into the solution to coat just the distal end of the fibre. The coated fibre was allowed to dry vertically for a day before testing for fluorescence.

As discussed above, no response was noted to aqueous lead ions due to the hydrophobic nature of the indicator. Use of acetonitrile dissolved all the indicator within a few minutes and disintegrated the thin PVC and silicone membranes. PVA was also doped with the indicator; however, the membrane was damaged after swelling in water. Use of acetonitrile did not have any effect – it is possible that the solvent is not able to penetrate the highly hydrophilic polymer. In all of the above cases, these polymer supports were not expected to be appropriate as the indicator would form covalent bonds to them, which are unsuitable here. Furthermore, silicone is waterproof and normally used in gas sensing to exploit this feature.

Sol-gel was favoured due to its ability to provide microscopic pores in which dyes are usually trapped. This feature seemed suitable for the indicator which requires mobility for a 2:2 binding stoichiometry with lead ions. In practice, what we saw was a lack of response to lead either at a neutral pH value or in acetonitrile and we showed that this was not a result of low porosity. A possible hypothesis for this is that instead of being trapped inside the pores, the indicator bonded covalently with the sol before gellification occured. Covalent bonding between the fluorophore molecules and the sol-gel structure would explain the lack of response with lead as this rigidity will not allow the sandwich configuration required for binding with lead. This would also explain how

acetonitrile was able to dissolve the indicator away gradually despite producing a dense sol-gel. Addleman has mentioned how the macrocycle depicted in Fig. 4.6 was *immobilised* onto silica by slow evaporation from the solvent and how this resulted in a lack of response to cations [3].

The transition of an indicator from a bulk solution environment to an immobilised form is not always successful. Wallington and co-researchers reported that the indicator Eriochrome Cyanine R (ECR) immobilised in sol-gel showed no significant spectral changes with aqueous Al^{3+} in the mM range [48]. ECR is known to complex strongly with Al^{3+} in bulk solution, leading to changes in the absorption spectrum [49]. Several explanations were put forward including the effect of pore-wall interactions and the conformations of the receptor molecule being constraint by the matrix.

4.7. Summary

An explanation of the mechanism behind molecular recognition and PET fluorescence enhancement have been provided at the beginning of this chapter as they form the basic functionality behind molecule **1,** the selected reagent used to detect lead ions in this work. A description of how these two mechanisms work in tandem to enable molecule **1** to detect lead is then provided followed by studies of that reagent with a view to implement it in a fibre optic probe configuration.

Following recommendations in published work and the particular 2:2 binding stoichiometry of the reagent with lead, sol-gel was selected as an encapsulating matrix for the reagent. A series of experiments were then carried out to verify the fluorescence detected from the doped sol-gel matrix and make optimisation in terms of signal strength and optical quality of the sol-gel. Experiments have revealed that despite the apparent suitability of the porosity of the sol-gel matrix to the indicator, no response to lead in various environments was detected in this immobilised state. This lack of response to lead ion suggests that molecule **1** was unable to bind to it as it did not have the degree of freedom required for the sandwich configuration with lead as illustrated in Fig. 4.6 earlier.

4.8. References

1. N.A. Yusof and M. Ahmad, A flow-through optical fibre reflectance sensor for the detection of lead ion based on immobilised gallocynine, Sensors and Actuators B: Chemical 94 (2003) 201-209.
2. G.A. Casay, N. Narayanan, L. Evans, T. Czuppon, and G. Patonay, Near-infrared tetra-substituted aluminum 2, 3-naphthalocyanine dyes for optical fiber applications, Talanta 43 (1996) 1997-2005.
3. R.S. Addleman, J. Bennett, S.H. Tweedy, S. Elshani, and C.M. Wai, Response of a benzoxainone derivative linked to monoaza-15-crown-5 with divalent heavy metals, Talanta 46 (1998) 573-581.
4. A. Beeby, D. Parker, and J.A.G. Williams, Photochemical investigations of functionalised 1, 4, 7, 10-tetraazacyclododecane ligands incorporating naphthyl chromophores, J. Chem. Soc., Perkin Trans. 2 1565 (1996) 1565-1579.
5. R.P. Haugland, Handbook of Fluorescent Probes and Research Products, Molecular Probes, Inc., Eugene, OR (2002).
6. C.T. Chen and W.P. Huang, A highly selective fluorescent chemosensor for lead ions, J. Am. Chem. Soc 124 (2002) 6246-6247.
7. J.R. Lakowicz, Principles of Fluorescence Spectroscopy, 3rd ed., Springer, 2006.
8. D.M. Jordan, D.R. Walt, and F.P. Milanovich, Physiological pH fiber-optic chemical sensor based on energy transfer, Analytical Chemistry 59 (1987) 437-439.
9. K. Tohda, H. Lu, Y. Umezawa, and M. Gratzl, Optical Detection in Microscopic Domains. 2. Inner Filter Effects for Monitoring Nonfluorescent Molecules with Fluorescence, Anal. Chem 73 (2001) 2070-2077.
10. T. Mayr, *Optical Sensors for the determination of heavy metal ions*, in *Faculty of Chemisttry and Pharmacy*. 2002, Regensburg University: Regensburg. p. 128.

11. C.J. Pedersen, Cyclic polyethers and their complexes with metal salts, Journal of the American Chemical Society 89 (1967) 7017-7036.
12. J.M. Lehn, Supramolecular Chemistry: Concepts and Perspectives. VCH New York,1995.
13. J.H. Kim, A.R. Hwang, J.I. Choe, and S.K. Chang, Chromoionophoric Recognition of Alkylamines by Nitro Derivative of Calix [4] arene-crown-5 Ether, Bulletin of the Korean Chemical Society 25 (2004) 301-303.
14. J.S. Kim and D.T. Quang, Calixarene-derived fluorescent probes, Chem. Rev 107 (2007) 3780-3799.
15. G. McMahon, S. O'Malley, K. Nolan, and D. Diamond, Important Calixarene Derivatives–their Synthesis and Applications, ARKIVOC (VII) (2003) 23–31.
16. G.E. Pacey and Y.P. Wu, Ion-pair extractions with 12-crown-4 and its analogues, Talanta(Oxford) 31 (1984) 165-168.
17. L.R. Sousa and J.M. Larson, Crown ether model systems for the study of photoexcited state response to geometrically oriented perturbers. The effect of alkali metal ions on emission from naphthalene derivatives, Journal of the American Chemical Society 99 (1977) 307-310.
18. A.P. de Silva and R. Rupasinghe, A new class of fluorescent pH indicators based on photo-induced electron transfer, J. Chem. Soc., Chem. Commun (1985) 1669-1670.
19. H.G. Loehr and F. Voegtle, Chromo-and fluoroionophores. A new class of dye reagents, Accounts of Chemical Research 18 (1985) 65-72.
20. M.V. Rusalov, S.I. Druzhinin, and B.M. Uzhinov, Intramolecular Fluorescence Quenching of Crowned 7-Aminocoumarins as Potential Fluorescent Chemosensors, Journal of Fluorescence 14 (2004) 193-202.
21. F.D. Souza, G.R. Deviprasad, and Y.Y. Hsieh, A novel porphyrin based fluorescent chemosensor using a molecular recognition approach, Chem. Commun (1997) 533-534.

22. A.P. de Silva and S.A. de Silva, Fluorescent signalling crown ethers; switching on of fluorescence by alkali metal ion recognition and binding in situ, J. Chem. Soc., Chem. Commun (1986) 1709-1710.
23. B. Valeur, in: J.R. Lakowicz (Ed.), Topics in Fluorescence Spectroscopy, J.R. Lakowicz, Editor vol. 4, Plenum Press, New York, 1994, Chapter 2, 21-28.
24. M.E. Huston, K.W. Haider, and A.W. Czarnik, Chelation-enhanced fluorescence in 9, 10-bis (TMEDA) anthracene, Journal of the American Chemical Society 110 (1988) 4460-4462.
25. J. Bourson, M.N. Borrel, and B. Valeur, Ion-responsive fluorescent compounds. III: Cation complexation with coumarin 153 linked to monoaza-15-crown-5, Analytica chimica acta 257 (1992) 189-193.
26. J.P. Malval, R. Lapouyade, J.M. Léger, and C. Jarry, Tripodal ligand incorporating dual fluorescent ionophore: a coordinative control of photoinduced electron transfer, Photochem. Photobiol. Sci 2 (2003) 259-266.
27. D.Y. Sasaki and B.E. Padilla, Dithioamide metal ion receptors on fluorescent lipid bilayers for the selective optical detection of mercuric ion, Chemical Communications 1998 (1998) 1581-1582.
28. F. Dang, K. Lei, and W. Liu, A new highly selective fluorescent Silver probe, Journal of Fluorescence 18 (2008), 149-153.
29. Y.M. Jeon, T.H. Lim, J.G. Kim, J.S. Kim, and M.S. Gong, Preparation of Red Perylene Fluoroionophore Containing Calix [4] azacrown Ether and Their Ionophoric Properties, Bulletin of the Korean Chemical Society 28 (2007) 816-820.
30. S. Fery-Forgues, M.T. Le Bris, J.P. Guette, and B. Valeur, Ion-responsive fluorescent compounds. 1. Effect of cation binding on photophysical properties of benzoxazinone derivative linked to monoaza-15-crown-5, The Journal of Physical Chemistry 92 (1988) 6233-6237.

31. J.M. Liu, J.H. Bu, Q.Y. Zheng, C.F. Chen, and Z.T. Huang, Highly selective fluorescent sensing of Pb2+ by a new calix[4]arene derivative, Tetrahedron Letters 47 (2006) 1905-1908.
32. S.A. McFarland and N.S. Finney, Fluorescent chemosensors based on conformational restriction of a biaryl fluorophore, J Am Chem Soc 123 (2001) 1260-1261.
33. N.I. Nijegorodov and W.S. Downey, The Influence of Planarity and Rigidity on the Absorption and Fluorescence Parameters and Intersystem Crossing Rate Constant in Aromatic Molecules, The Journal of Physical Chemistry 98 (1994) 5639-5643.
34. H.H. Willard, J.L.L. Merritt, and J.A. Dean, Instrumental methods of analysis. New York,1981.
35. B.V. Zhmud, A.A. Golub, and V.G. Pivovarenko, Synthesis and Study of Ion Adsorption and Fluorescent Properties of Silica-Grafted Bis (crownazo) methine, Inorganic Materials 40 (2004) 1006-1013.
36. M. McCarrick, B. Wu, S.J. Harris, D. Diamond, G. Barrett, and M.A. McKervey, Chromogenic ligands for lithium based on calix [4] arene tetraesters bearing nitrophenol residues, Journal of the Chemical Society, Perkin Transactions 2 1993 (1993) 1963-1968.
37. M. Zevin, R. Reisfeld, I. Oehme, and O.S. Wolfbeis, Sol-gel-derived optical coatings for determination of chromate, Sensors and actuators. B, Chemical 39 (1997) 235-238.
38. C. Malins, M. Niggemann, and B.D. MacCraith, Multi-analyte optical chemical sensor employing a plastic substrate, Measurement Science and Technology 11 (2000) 1105-1110.
39. A. Abdelghani, J.M. Chovelon, N. Jaffrezic-Renault, M. Lacroix, H. Gagnaire, C. Veillas, B. Berkova, M. Chomat, and V. Matejec, Optical fibre sensor coated with porous silica layers for gas and chemical vapour detection, Sensors and Actuators B: Chemical 44 (1997) 495-498.

40. D. Avnir, S. Braun, O. Lev, and M. Ottolenghi, Enzymes and Other Proteins Entrapped in Sol-Gel Materials, Chemistry of Materials 6 (1994) 1605-1614.
41. J.W. Aylott, D.J. Richardson, and D.A. Russell, Optical biosensing of gaseous nitric oxide using spin-coated sol-gel thin films, Chemistry of Materials 9 (1997) 2261-2263.
42. G.E. Badini, K.T.V. Grattan, A.C.C. Tseung, and A.W. Palmer, Sol-Gel Properties for Fiber Optic Sensor Applications, Optical Fiber Technology 2 (1996) 378-386.
43. I. Oehme, S. Prattes, O.S. Wolfbeis, and G.J. Mohr, The effect of polymeric supports and methods of immobilization on the performance of an optical copper (II)-sensitive membrane based on the colourimetric reagent Zincon, Talanta 47 (1998) 595-604.
44. P. Buet, B. Gersch, and E. Grell, Spectral Properties, Cation Selectivity, and Dynamic Efficiency of Fluorescent Alkali Ion Indicators in Aqueous Solution Around Neutral pH, Journal of Fluorescence 11 (2001) 79-87.
45. C. Lam, T.D. Jickells, D.J. Richardson, and D.A. Russell, Fluorescence-Based Siderophore Biosensor for the Determination of Bioavailable Iron in Oceanic Waters, Analytical chemistry(Washington, DC) 78 (2006) 5040-5045.
46. H. Guillemain, M. Rajarajan, T. Song, and K. Grattan, A self-referenced reflectance sensor for the detection of lead ions using optical fibres, Journal of Meas., submitted Mar 2008.
47. C. Gojon, B. Dureault, N. Hovnanian, and C. Guizard, A comparison of immobilization sol-gel methods for an optical chemical hydrazine sensor, Sensors and actuators. B, Chemical 38 (1997) 154-162.
48. S.A. Wallington, T. Labayen, A. Poppe, N. Sommerdijk, and J.D. Wright, Sol-gel entrapped materials for optical sensing of solvents and metal ions, Sensors and actuators. B, Chemical 38 (1997) 48-52.
49. Z. Marczenko, Spectrometric Determination of Elements, Willey and Sons Inc (1976) 51-53.

Chapter 5

A disposable optical fibre-based capillary probe

5.1. Introduction

Lead in organic solutions has received much less attention than lead ions in water, although it has been shown that the toxicity of lead in organic media is up to a hundred times greater than in its aqueous counterpart [1-3] and able to cross pathways and eventually result in the contamination of rivers and groundwater [4-7]. There is a host of situations where lead can occur in organic matrices: food oils, paint, hydrocarbon fuels and lubricants, polymers for the electronics industry [8] and in the emerging bio-fuel market where lead is extracted from the soil by the plant. Samples of an organic nature are highly volatile, making *in situ* detection highly desirable.

A disposable capillary-based probe using optical fibre technology to create a compact and portable configuration has been designed for sensing lead ions. It is based around a glass capillary tube pre-treated with a fluorophore which has high sensitivity and selectivity towards lead ions. The capillary tube makes use of capillary action to uptake the same sample volume for each single-shot measurement.

This preliminary work undertaken and reported is essentially a proof-of-principle for a probe design in which chemical indicators that cannot be immobilised on a solid support can still be adapted for optical fibre sensing without any chemical modification. The disposable capillary probe provides a mechanical support and

protection to the fluorophore without the use of membranes, thus avoiding problems with leaching. As far as the researcher is aware, this is the first optical fibre sensor to utilize a fluorescent indicator with high selectivity for lead. Deo and Godwin synthesized a fluorescent protein-based molecule for lead ions but immobilised it on a resin and screened it in tissue culture plates [9].

5.2. Capillary sensors

The disposable probe developed in this work consists of a long thin glass tube having its inner surface pre-treated with Molecule **1**. The tube allows the sample to make contact with the fluorophore, through capillary action. A large-core fibre inserted inside this same tube is then used both to guide the optical radiation needed for photo-excitation of the fluorophore and also to collect the emission from the sample, where the fluorescence intensity is correlated with the concentration of lead present in the sample.

The advantage of the capillary tube is that it acts as a mechanical support for the fluorophore deposited *inside* the tube and protects it from damage; in addition the capillary effect is exploited to allow the uptake of a similar volume every time. Thus the sensor acts in a way that is akin to a flow-cell by drawing in the sample without requiring a pump, making it suitable for direct sampling. Furthermore, because the sensor is inexpensive to produce it is designed to be disposable; there is thus no need to regenerate it using a different solution, nor is there a problem with lifetime deterioration during storage or usage.

Several researchers have previously used the capillary tube as an optical waveguide; for example Tao *et al* have reported on a flexible light guiding tubular waveguide as a substitute to conventional fibre to provide enhanced evanescent wave sensing over a much longer pathlength [10]. There was no need to remove the cladding as the waveguide was hollow and coated inside

with an analyte-sensitive polymer, resulting in a much more robust waveguide than the conventional fibre stripped of its buffer and cladding. Kieslinger *et al* used a capillary waveguide to collect the evanescent wave emission propagating along it while the excitation was performed from the side [11]. Further research by Dhadwal and co-workers, on the other hand, made use of a capillary waveguide for evanescent wave excitation of a fluorophore and collected the emission in a direction that was perpendicular to the tube [12].

Propagation along the capillary waveguide may be for the sole purpose of evanescent wave sensing. For example, Lippitsch *et al* coated the inside of a capillary glass tube with an analyte-sensitive dye and coupled light in and out of the waveguide from the side using index-matching oil [13]. The sensing layer acted as the waveguide and absorption gave a measure of the analyte concentration. This approach was also extended to fluorescence measurements. Weigl and co-workers have studied the best angle for coupling the light sideways in and out of the capillary tube [14]. However, using the capillary tube as waveguide is prone to errors such as contamination of the external surface due to handling, differences in refractive indices among samples and variation in the manufacture of the tubes [15]. Furthermore, light coupling is not always efficient and is a serious issue if disposable capillary probes are to be used. Further complications arise in that side illumination and emission detection requires index-matching oil and a fixed coupling angle while end detection requires some more complex or lab-made optical couplers [10, 12]. Weigl and Wolfbeis have described a capillary optical sensor using fibres to guide light sideways across the capillary tube and with this configuration, the tube could easily be substituted [14].

While several researchers have mentioned the use of capillary action for sampling [11, 14], none has actually implemented it in a fibre optic-based probe configuration. Kieslinger did implement it in a capillary waveguide sensor but no optical fibre was involved in the design [11]. His work serves to demonstrate

that such a technique is feasible and it was reported that drawing the liquid in by surface tension used a volume from 20-50 μL and as low as 1 μL for a single analyte. Thus the capillary action of the probe supplies a well-defined sample volume and lends itself easily to the design of disposable probes to allow for measurements involving similar volumes of samples. Based on the knowledge of prior research and the need for an approach that was effective in this application, the use of the capillary tube as a disposable vessel for a well-defined sample volume was pursued.

5.2.1. Theory of capillary action

Capillarity is the phenomenon by which a liquid rises into a narrow tube above or below its general level as a result of net molecular forces. Intermolecular attraction among the liquid molecules (cohesion) are overcome by molecular attraction between the liquid and the solid surface (adhesion), resulting in a rise of the liquid level.

Now, for equilibrium, the lifting force due to the surface tension is balanced by the weight of the water column in the tube [16]:

$$\pi d\left(\sigma\cos\theta\right)=\pi\left(\frac{d}{2}\right)^{2}h\left(W\right)$$

$$\therefore h=\frac{4\sigma\cos\theta}{Wd} \qquad (5.1)$$

Where h and d are the liquid height and tube diameter as shown in Fig. 5.1.

W = weight density of the liquid (i.e. density multiplied by the gravitational force).

σ = surface tension force per unit length.

θ = contact angle of the liquid surface

For pure water at 4˚C, $\theta=0$.

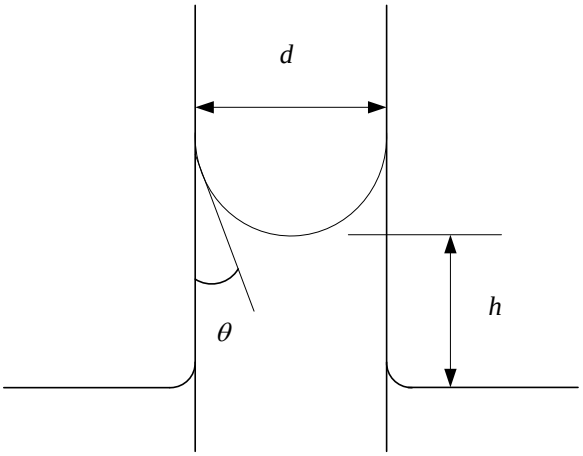

Fig. 5.1 The capillary effect is more noticeable with thin tubes

Clearly, from (5.1), for a given liquid, the narrower the tube, the higher the liquid will rise. The following illustrates some characteristics of the capillary tube.

1. For a given liquid, its density is constant, as well as θ if the solid surface is always the same. Hence the height is always constant.

2. It is important to leave the end of the capillary tube open so that air is allowed to escape as the liquid rises up otherwise the volume in the tube will not be the same.

3. The capillary tube must be used in a vertical position for consistency of the liquid volume drawn up. If the tube is at an angle, the surface tension along the tube will be balanced only by the vertical component of the liquid weight which is less than in the vertical position. Hence more liquid needs to rise in the tube to balance out the suction force

4. It is important that the glass walls be clean otherwise θ will change and will affect the height of liquid in the tube.

5. Mercury causes a capillary *depression* due to the contact angle being negative, i.e. it forms a convex meniscus. This is because the forces of attraction within the liquid are greater than the forces of adhesion between mercury and the solid surface.

5.2.2. Choice of capillary probe configuration

A brief overview is given here to show what various optical configurations are possible with a capillary probe, what has already been done in this area and the advantages or disadvantages of these configurations to justify the configuration adopted in this work.

The various optical configurations that have been used with capillary sensors have been reviewed by Dhadwal *et al* [12] and are illustrated below in Fig. 5.2. Fluorescence excitation and emission detection of the inner coating is performed by evanescent wave in Fig. 5.2a. In Fig. 5.2b, illumination and detection are performed on the side of the capillary tube utilising optical fibres as reported by Quesada *et al* [17] and in Fig. 5.2c, this is done in-line which also allows absorption measurements [14]. Excitation is performed from the side in Fig. 5.2d while the emission that propagates along the waveguide is detected but this arrangement results in non-uniform illumination along the entire capillary length [12]. In Fig. 5.2e, evanescent wave excitation causes emission that is detected from the side using an array of fibres.

In the configurations of Fig. 5.2a and 5.2d, the emission detected is that propagating along the capillary waveguide. The disadvantages of this arrangement have been discussed earlier in section 5.2, namely contamination, material quality and light coupling issues. On the other hand, those

arrangements providing excitation by evanescent wave, although subject to the same issues, will not impair the emission measurement.

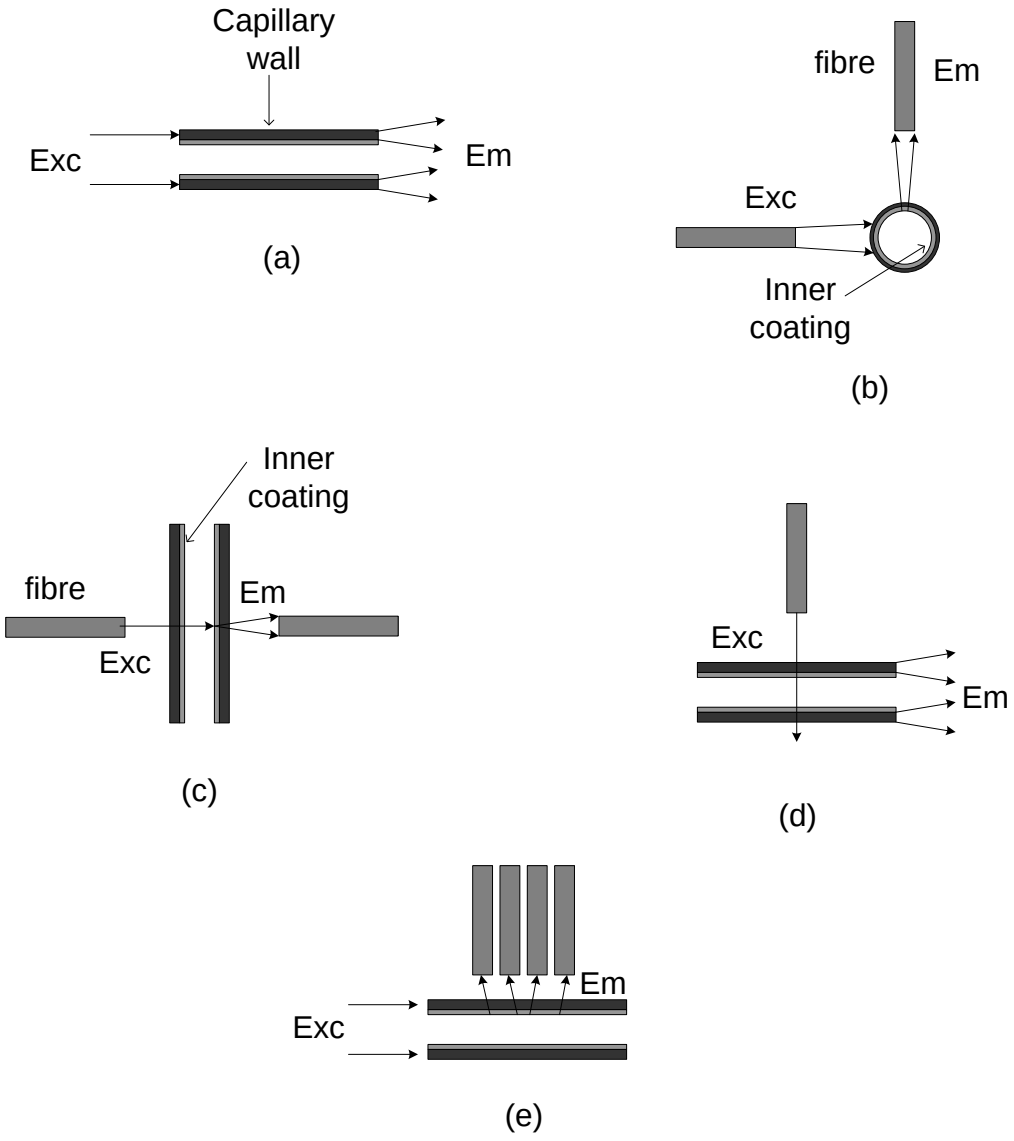

Fig. 5.2 Capillary probe configurations. Exc = excitation radiation; Em= emission radiation

Inefficient light coupling is not a problem if the intensity is high enough to lead to excitation or if a high-power light source is used. For contamination, material and manufacturing defects and any other factors which affect the light intensity,

a suitable referencing scheme may overcome them. Since the emission intensity is directly proportional to the excitation intensity – any variation in the latter will be reflected in the former but if say, a ratiometric measurement is taken, then the variations will cancel out.

This is not the case, however, if the emission intensity is affected by these same factors. Thus it is possible to use evanescent wave for excitation but it is not advisable to detect the emission in the same manner.
The configurations of Fig. 5.2 with the exception of 5.2c suffer from inefficient light excitation and emission along the length of the capillary tube. For the case of Fig. 5.2a, the evanescent wave approach cannot be optimised simultaneously for propagation of both excitation and emission radiation.

The configuration adopted in this work does not make use of the capillary tube as waveguide; instead, the fibre within the tube provides an efficient way for the excitation and collection of emission of the fluorescence, as was explained in section 2.1.4 and Fig. 2.4 whereby the geometrical overlap of the excitation and emission regions from the fibre was shown. In this way, only the emission radiation that is able to enter the fibre is actually excited in the first place.

5.3. Probe development

The experimental set-up used for this experiment is shown in Fig. 5.3. A high power 435 nm LED is used for excitation and the spectrometer in conjunction with the interference filter centred at 500 nm with FWHM of 40 nm measures the emitted light. The fluorescence emission intensity is measured over the wavelength range 480-525 nm and the instrument noise measured in the stopband of the filter from 400-445 nm is subtracted from it.

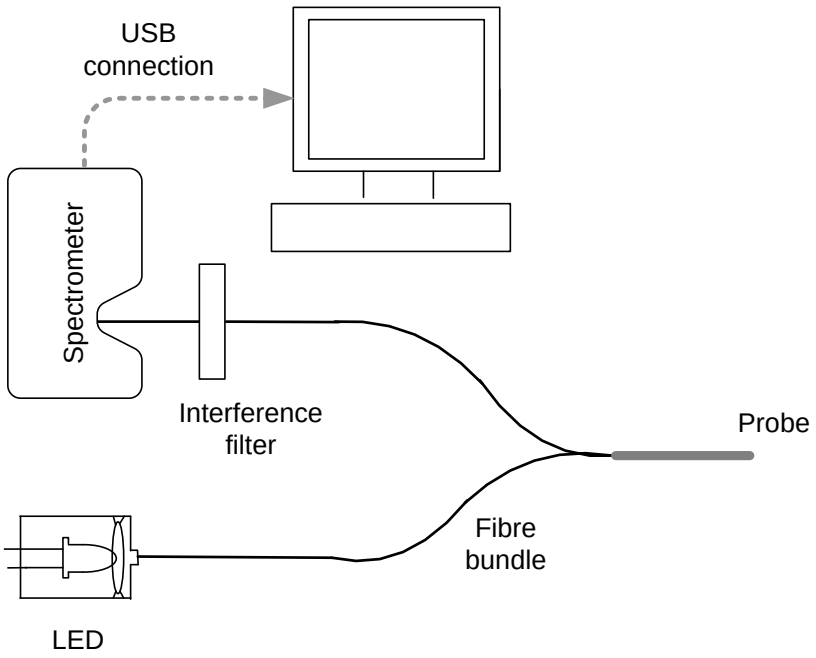

Fig. 5.3. Layout of the main components for fluorescence measurements. A 435 nm LED is used for excitation light guided along a single fibre of the fibre bundle. A spectrometer together with an interference filter to block residual excitation light is used to measure the emission radiation. The computer collects and processes the data from the spectrometer using the LabVIEW software.

The LabVIEW program used to collect and process the data from the spectrometer output is depicted in Fig. 5.4a and 5.4b. The front panel displays the actual interference-filtered emission spectrum although this in itself contains little information. One graph displays the emission intensity summed over the wavelength range 480-525 nm and plotted against time. This graph was used for the measurements and the LabVIEW program was able to store the data. The other graph for the range 515-525 nm was used for work in the previous chapter.

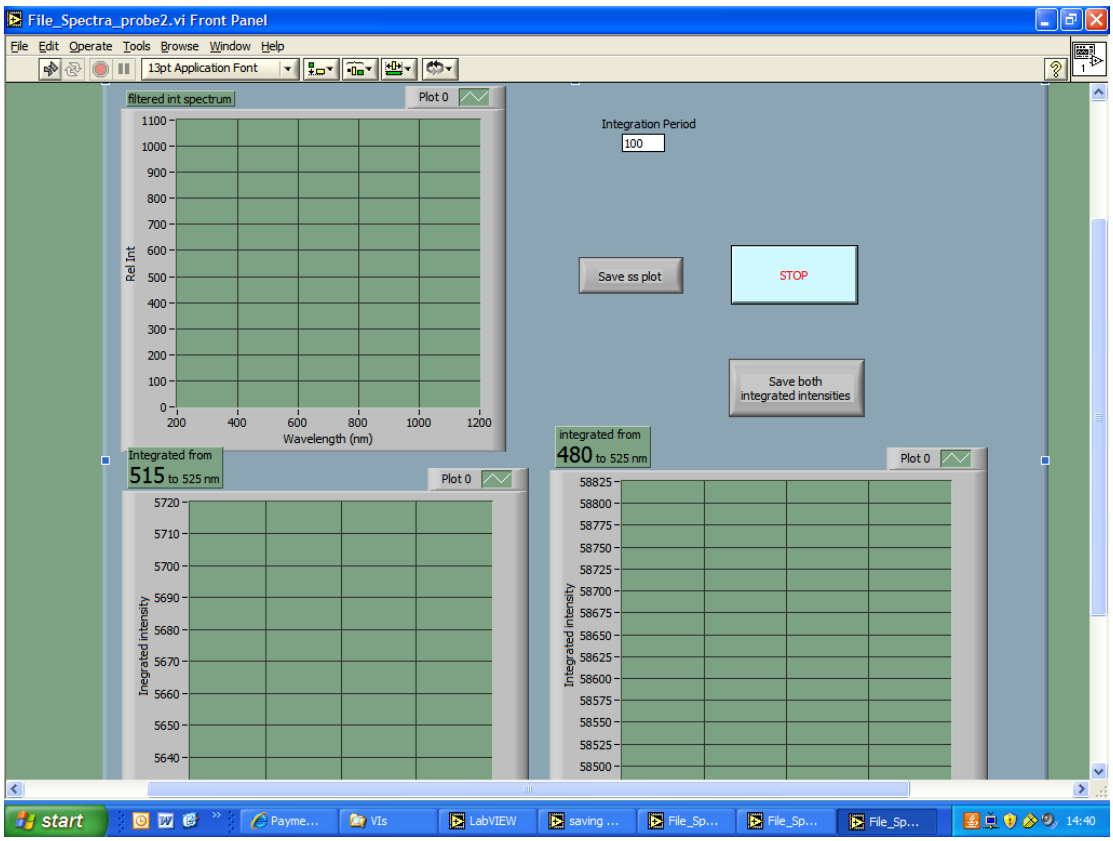

Fig. 5.4a Front panel for fluorescence measurement. The emission spectrum guided through the interference filer is displayed along with the integrated emission plotted against time for the wavelength range 480-525 nm for this work and 515-525 nm for work in the previous chapter.

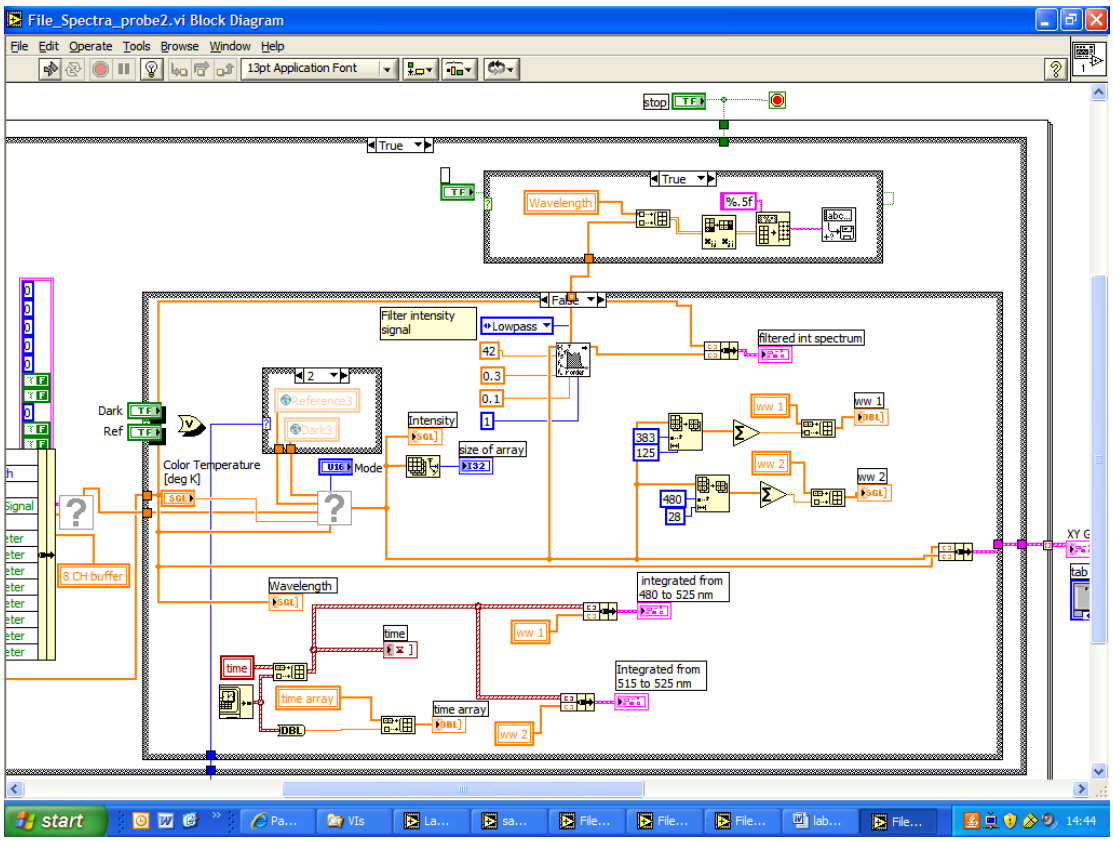

Fig. 5.4b. Back panel for fluorescence measurement. The output array from the spectrometer is split into intensity and wavelength values. A clock is added to enable the plot of emission intensity against time. The integrator block which sums up the intensity over a given wavelength range is visible on the right hand side of the VI.

The probe was specially developed for this application and is shown in greater detail in Fig. 5.5a and 5.5b. Estimations for the power budget may be done as follows. The light from the LED is launched into the single 200 mm fibre core via a system of lenses.

Pasteur pipettes, used as capillary tubes throughout this work, were cleaned thoroughly by soaking in a solution of 2 M nitric acid, this being followed by rinsing with deionized water. All reagents were of analytical grade or above; lead ions in acetonitrile were produced by dissolving known amounts of lead perchlorate.

The fluorophore solution was prepared at the desired concentration and the tip of the Pasteur pipette placed in contact with the solution. The solution rose inside the tube due to capillary action; the pipette could then be placed horizontally without the solution spilling out and the latter was allowed to evaporate completely, leaving only the fluorophore indicator behind.

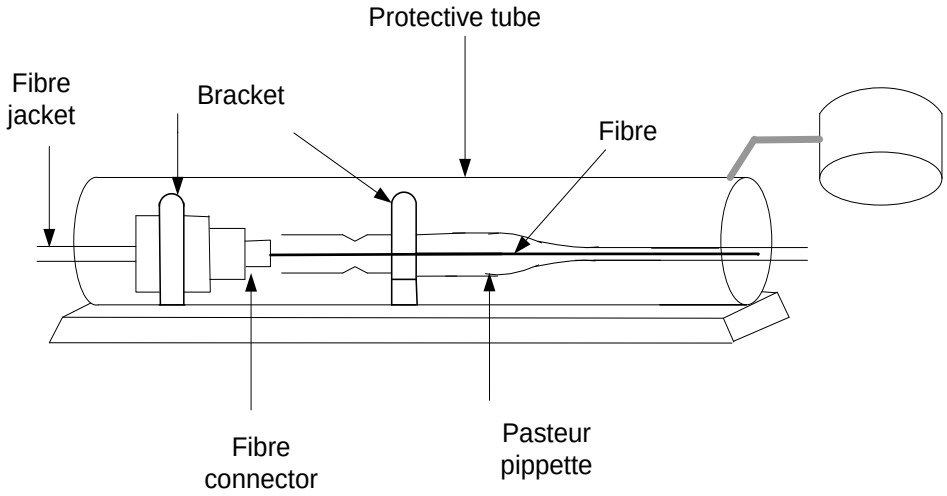

Fig. 5.5a. Diagram showing the construction of the probe approximately 20 cm in length. A cylindrical tube with the cap shown to the right is used to block external light during measurements.

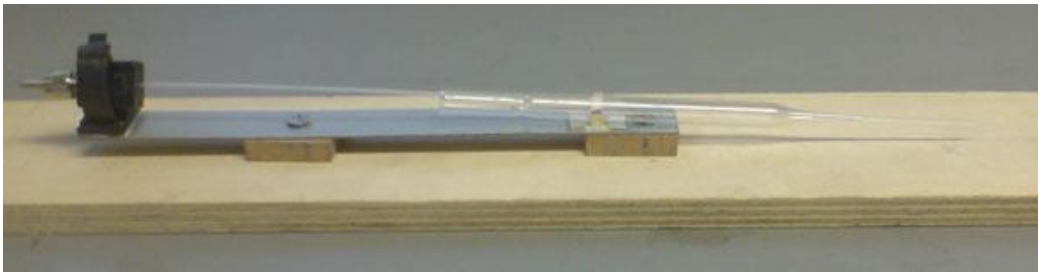

Fig.5.5b Picture of the probe used to gather experimental data. The SMA connector is o the left and will connect to the fire bundle. The glass capillary tube is on the right with the fibre probe inserted deep inside.

A number of sample probes were pre-treated as explained above. The sample liquid to be tested was introduced in the pipette using capillary action and the indicator dissolved into the sample solution. To determine the fluorescence response of the sample, a length of fibre, whose end surface has previously been polished flat, was inserted inside the tube until it reached the sample. The optical fibre was designed both to guide the excitation light and collect the fluorescence from the sample. After each use, the Pasteur pipette may be cleaned thoroughly for re-use or discarded.

5.4. Results and discussions

5.4.1. Reagent concentration

As explained previously, the indicator is not suitable for immobilisation in a sensing layer and so the indicator was deposited inside the tube such that introduction of the sample would dissolve it to a pre-defined concentration. The lead sample to be tested must have been dissolved in the same solvent used to deposit the fluorophore to ensure equation (5.1) holds and the same volume of liquid rises up the tube. In this way, the concentration of fluorophore used during the deposition process is achieved again as the same volume of solvent rises up the tube.

The lack of a membrane is advantageous as it removes many of the problems experienced with such systems, including leaching, swelling and degradation usually associated with it [14, 18].

To determine the optimum concentration of the indicator to be used, various concentrations were prepared in acetonitrile and from these the fluorophore was deposited inside the capillary tubes. These were tested using a constant lead ion concentration of 100 μM in acetonitrile, where the results obtained are displayed in Fig. 5.6. From experiment, the optimum concentration of the

indicator was found to be 50 μM; beyond this concentration, the fluorescence intensity drops as a result of quenching. In light of this positive result, all further measurements were taken using pipettes pre-treated at this reagent concentration.

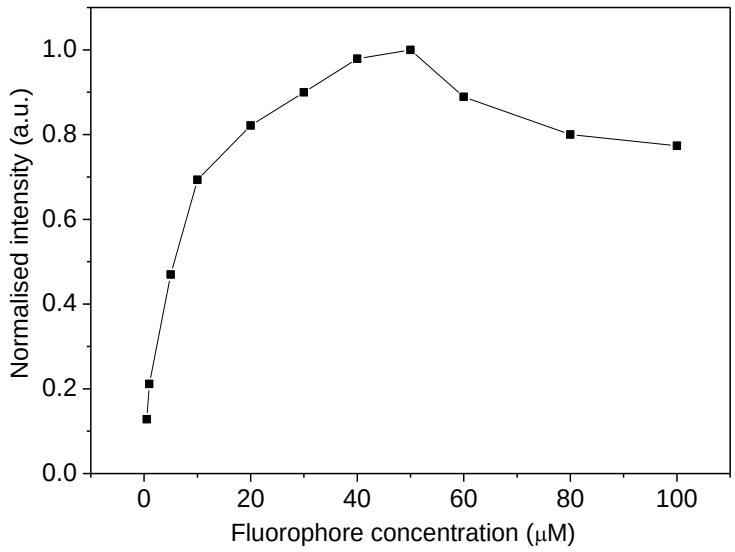

Fig. 5.6. Fluorescence intensity as a function of fluorophore concentration. The drop at high concentration is attributed to quenching effects.

5.4.2. Lead calibration

Probes created using a series of such pre-treated Pasteur pipettes were then used to measure various concentrations of lead in order to obtain a calibration curve for this type of disposable probe and Fig. 5.7 shows the results obtained, where it can be seen that the probe does not show a sensitivity to lead below a concentration of 20 μM.

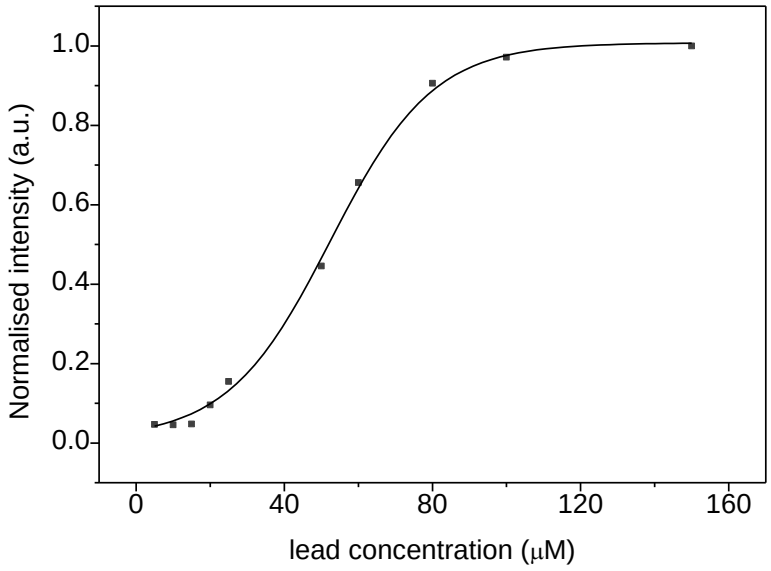

Fig. 5.7. Probe response to lead

The sensor responds to lead in the concentration range 20 μM to 150 μM with a dynamic range from 20 μM to 80 μM. The linear response may be represented by the equation $y = 0.014x - 0.188$ with $R^2 = 0.9933$ as shown in Fig. 5.8. If lead is in another solvent, the sensor response will be different due to the sensitivity of the fluorescence of molecule **1** to solvents (Chapter 4) and the sensor will have to be re-calibrated.

There are few selective fluorescent reagents for lead published in the literature for comparison; however, the dynamic range of this work is comparable to that of Deo and Godwin who achieved a dynamic range from 60 μM to 140 μM with a response starting at 60 μM. They designed a selective, ratiometric fluorescent sensor for lead ions based on the fluorescent dye dansyl conjugated to a tetrapeptide which is the lead-recognition unit [9]. Excitation was at 337 nm and emission peak shifted from 557 nm to 510 nm in the presence of lead with the reagent in solution. Subsequent tests were performed on the reagent immobilised on a copolymer resin in tissue culture plates. The primary goal of

their work was for the detection of lead in human cells which has a concentration of less than 2.5 μM. This lies well below the minimum limit of 60 μM for their sensor.

Elsewhere, Tan *et al* reported a range of 0.03-1.0 μg/ml (0.15-5 μM) for lead using a backward light scattering technique [19]. No fluorescence measurement was involved in this technique; instead, the interaction of lead with sodium tetraphenylboron in the presence of polyethylene glycol yielded large particles resulting in a strongly enhanced backward light scattering signal at 371 nm which was collected by an optical fibre.

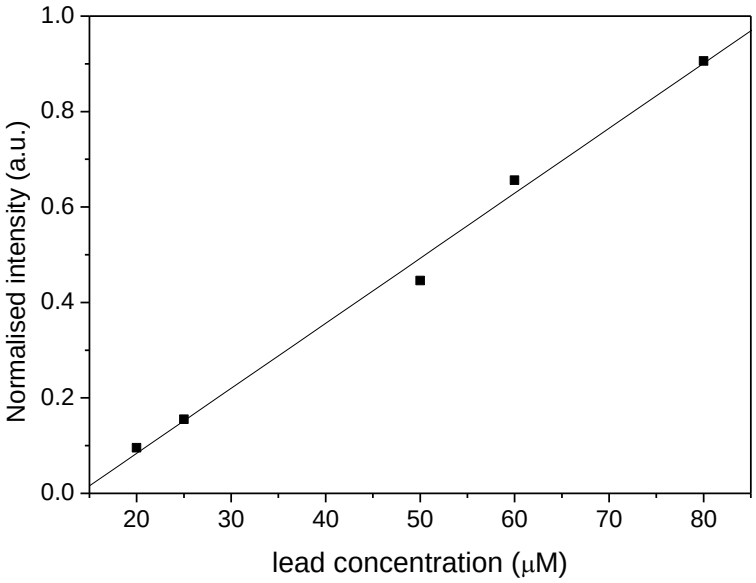

Fig. 5.8. Dynamic range of the sensor

5.4.3. Reproducibility

To investigate the impact of the use the capillary effect in the operation of the probe, as described, a series of measurements were done to determine its reproducibility and the results shown in Fig. 5.9. The data obtained show a reproducibility which was calculated to have an r.s.d. of 6.3 %. Weigl and

Wolfbeis reported a reproducibility of 5 % for a capillary sensor for carbon dioxide and blamed misalignment as a source of error [14].

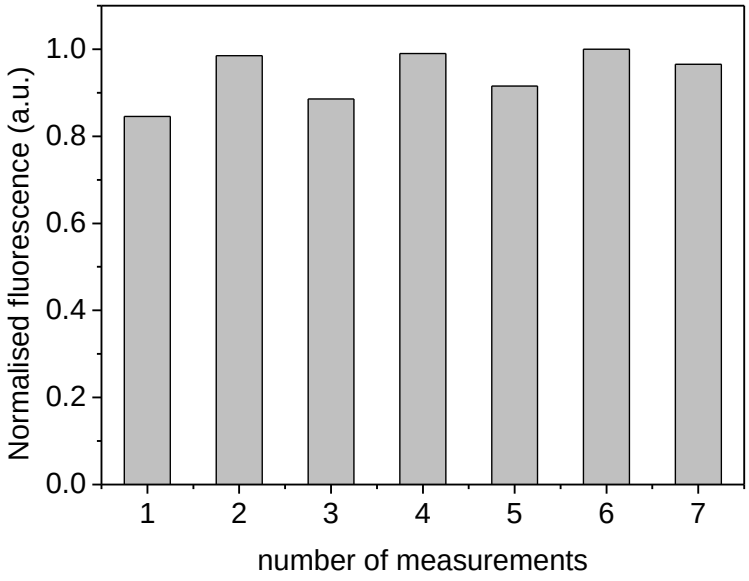

Fig. 5.9. Reproducibility of the disposable capillary probe at 60 μM lead concentration normalised at the highest value.

Here, the non-uniform deposition of the reagent during evaporation of the solvent and the optical fibre placement may affect the reproducibility of the probe performance. Positioning the capillary probe vertically while the solvent is allowed to evaporate was seen to cause most of the indicator to collect at the edge of the tube; experimental work has shown that a horizontal position leads to an improvement in the uniformity of the probes produced.

The small variation in the dimensions of Pasteur pipettes used also affects the reproducibility – the pipettes are not manufactured to exact standards as their use is generally for liquid transfer. This aspect could be improved by tighter quality control on the specification of the Pasteur pipettes. However, the dimensions of the pipette do not affect the sample volume uptake: although the

height of sample in the tube may vary from equation (5.1) due to variation in the tube diameter, the volume will be the same because the sample volume weight must balance the surface tension.

Because pre-treatment of the capillary tubes does not involve chemical modification of molecule **1,** its selectivity towards lead in the presence of foreign ions will be identical to that shown in Chapter 4.

5.4.4. Efficiency of the sensor

The efficiency of the experimental setup was measured using the spectrometer. Due to its physical shape and adaptor, it can only be connected to a fibre terminated with a fibre connector. Therefore it is not possible to connect the LED lamphouse directly to it. Instead, the light exiting from the branch of the fibre bundle connected to the LED source was measured. Then, using the same light source intensity, the probe was fixed to the fibre bundle and used in an 80 μM lead solution. The analyte optical intensity was measured using the spectrometer via the interference filter in the usual way as shown in Fig. 5.3. The ratio of the analyte optical signal to the light source measurement yielded an efficiency of 2.1% over the wavelength range 480 nm to 525 nm. It was necessary to include the filter in order to measure the analyte optical signal. However, the efficiency of the filter set-up itself was measured separately by using the broadband light source from chapter 3 with light exiting through the single fibre in the fibre bundle for consistency in the set-ups. The ratio of the light intensity before and after transmission over the wavelength range 480 nm to 525 nm was 67%. The transmittivity of the interference filter itself is around 70% according to data sheet.

5.5. Summary

A new *proof-of-principle* design for a fibre optic-based disposable fluorescent lead sensor using capillary probes has been developed and described. In this study, it has been demonstrated how chemical indicators that are not suited to immobilization due to their specific binding requirements may still be used in fibre optic sensing. This is particularly advantageous as there are many crown ether-type fluorophores designed for metal ions sensing in solution that could be used [30-32].

The capillary probe described here is easy to use and involves a simple manufacturing technique, making it inexpensive to produce and thus suitable for single tests. It also does not require a sophisticated or cumbersome light coupling configuration or equipment and may therefore be used by non-technical personnel in the field, especially given the user-friendly LabVIEW interface created for the sensor.

The probe response to lead has been shown to be in the 20-150 μM concentration range with a dynamic range of 20-80 μM and an r.s.d. of ~6 % was obtained from a series of different probes. The performance of the probe was compared with a number of sensors in published work. The limit of lead in *unleaded* fuel in the EU is 25 μM [33] and falls within range of this sensor.

The use the fluorescent reagent in evanescent wave sensing was investigated. The theory of evanescent wave was outlined and its suitability for fibre optic sensing discussed. It was shown that this approach cannot be optimised for fluorescence measurements due to compromises that have to be made between efficient excitation or efficient emission collection by the fibre.

5.6. References

1. D.S. Forsyth and W.D. Marshall, Ionic Alkylleads in Herring-Gulls from the Great-Lakes Region, Environmental Science & Technology 20 (1986) 1033-1038.
2. P. Grandjean and T. Nielsen, Organolead compounds: environmental health aspects, Residue Rev 72 (1979) 97-154.
3. J.F. Jaworski, Effects of lead in the environment--1978, National Research Council Canada, Ottawa, Canada No. 16736 (1979) 615-616.
4. Z. Mester, H. Lord, and J. Pawliszyn, Speciation of trimethyllead and triethyllead by in-tube solid phase microextraction high-performance liquid chromatography electrospray ionization mass spectrometry, J. Anal. At. Spectrom 15 (2000) 595-600.
5. G. O'Connor, L. Ebdon, and E.H. Evans, Qualitative and quantitative determination of tetraethyllead in fuel using low pressure ICP-MS, J. Anal. At. Spectrom 14 (1999) 1303–1306.
6. B.W. Pack, G.M. Hieftje, and Q. Jin, Use of an air/argon microwave plasma torch for the detection of tetraethyllead, Analytica Chimica Acta 383 (1999) 231-241.
7. S. Rapsomanikis, O.F.X. Donard, and J.H. Weber, Speciation of lead and methyllead ions in water by chromatography/atomic absorption spectrometry after ethylation with sodium tetraethylborate, Analytical Chemistry 58 (1986) 35-38.
8. C.N. Mbileni, P. Ngobeni, D.A. Katskov, and N. Panichev, Determination of lead and cadmium in organic solutions by electrothermal atomic absorption spectrometry with a transverse heated filter atomizer, J. Anal. At. Spectrom 17 (2002) 236-241.
9. S. Deo and H.A. Godwin, A selective, ratiometric fluorescent sensor for Pb 2, J. Am. Chem. Soc 122 (2000) 174-175.

10. S. Tao, S. Gong, J.C. Fanguy, and X. Hu, The application of a light guiding flexible tubular waveguide in evanescent wave absorption optical sensing, Sensors and actuators. B, Chemical 120 (2007) 724-731.
11. D. Kieslinger, S. Draxler, K. Trznadel, and M.E. Lippitsch, Lifetime-based capillary waveguide sensor instrumentation, Sensors and Actuators. B, Chemical 39 (1997) 300-304.
12. H.S. Dhadwal, P. Kemp, J. Aller, and M.M. Dantzler, Capillary waveguide nucleic acid based biosensor, Analytica Chimica Acta 501 (2004) 205-217.
13. M.E. Lippitsch, S. Draxler, D. Kieslinger, H. Lehmann, and B.H. Weigl, Capillary waveguide optrodes: An approach to optical sensing in medical diagnostics, Applied Optics 35 (1996) 3426-3431.
14. B.H. Weigl and O.S. Wolfbeis, Capillary Optical Sensors, Analytical Chemistry 66 (1994) 3323-3327.
15. D. Kieslinger, B.H. Weigl, S. Draxler, and M.E. Lippitsch, Capillary waveguide optrodes for medical applications, Optical Review 4 (1997) 85-88.
16. R.K. Rajput, A textbook of Fluid Mechanics, 3rd ed., Ram Nagar, India,2006.
17. M.A. Quesada, H.S. Dhadwal, D. Fisk, and F.W. Studier, Multi-capillary optical waveguides for DNA sequencing, Electrophoresis 19 (1998) 1415-1427.
18. I. Oehme, S. Prattes, O.S. Wolfbeis, and G.J. Mohr, The effect of polymeric supports and methods of immobilization on the performance of an optical copper (II)-sensitive membrane based on the colourimetric reagent Zincon, Talanta 47 (1998) 595-604.
19. K.J. Tan, C.Z. Huang, and Y.M. Huang, Determination of lead in environmental water by a backward light scattering technique, Talanta 70 (2006) 116-121.
20. B.D. Gupta, C.D. Singh, and A. Sharma, Fiber optic evanescent field absorption sensor: effect of launching condition and the geometry of the sensing region, Optical Engineering 33 (1994) 1864-1868.

21. G.P. Anderson, J.P. Golden, and F.S. Ligler, An evanescent wave biosensor--Part I: Fluorescent signal acquisition from step-etched fiber optic probes, IEEE Trans Biomed Eng 41 (1994) 578-584.
22. P.N. Moar, S.T. Huntington, J. Katsifolis, L.W. Cahill, A. Roberts, and K.A. Nugent, Fabrication, modeling, and direct evanescent field measurement of tapered optical fiber sensors, Journal of Applied Physics 85 (1999) 3395-3398.
23. R. Falciai, A.G. Mignani, L. Ciaccheri, and F. Cosi, Tapered multimode optical fibers for enhanced evanescent-wave absorption spectroscopy of liquids, Proceedings of SPIE 3105 (1997) 2-12.
24. W. Henry, Evanescent field devices: a comparison between tapered optical fibres and polished or D-fibres, Optical and Quantum Electronics 26 (1994) 261-272.
25. P. Poscio, Y. Emery, P. Bauerfeind, and C. Depeursinge, In vivo measurement of dye concentration using an evanescent-wave optical sensor, Medical and Biological Engineering and Computing 32 (1994) 362-366.
26. K.T.V. Grattan and B.T. Meggitt, Optical Fiber Sensor Technology, Vol. 4, Kluwer Academic Publishers. (1999).
27. D. Marcuse, Launching light into fiber cores from sources located in thecladding, Lightwave Technology, Journal of 6 (1988) 1273-1279.
28. T. Grady, T. Butler, B.D. MacCraith, D. Diamond, and M.A. McKervey, Optical Sensor for Gaseous Ammonia With Tuneable Sensitivity, The Analyst 122 (1997) 803-806.
29. B.D. MacCraith, C.M. McDonagh, G. O'Keeffe, A.K. McEvoy, T. Butler, and F.R. Sheridan, Sol-gel coatings for optical chemical sensors and biosensors, Sensors & Actuators: B. Chemical 29 (1995) 51-57.
30. R.S. Addleman, J. Bennett, S.H. Tweedy, S. Elshani, and C.M. Wai, Response of a benzoxainone derivative linked to monoaza-15-crown-5 with divalent heavy metals, Talanta 46 (1998) 573-581.

31. J. Bourson, M.N. Borrel, and B. Valeur, Ion-responsive fluorescent compounds. III: Cation complexation with coumarin 153 linked to monoaza-15-crown-5, Analytica chimica acta 257 (1992) 189-193.
32. S. Fery-Forgues, M.T. Le Bris, J.P. Guette, and B. Valeur, Ion-responsive fluorescent compounds. 1. Effect of cation binding on photophysical properties of benzoxazinone derivative linked to monoaza-15-crown-5, The Journal of Physical Chemistry 92 (1988) 6233-6237.
33. European Directive 98/70/EC, Official Journal of the European Community L350 (1998) 58-67.

Chapter 6

Conclusions

6.1. Summary

An introduction to the field of chemical sensing and monitoring has been provided. The toxicity of lead and its compounds has been covered and is an incentive in monitoring applications, especially with regards to compliance with legislations. However, from a wider perspective, other factors such as process control and financial expenditure may also act as an impetus for monitoring activities. Portable sensors for field applications are able to fill a gap in the market for smaller, simpler yet highly-customised sensing devices without competing directly with more well-established conventional instrumentation.

The advantages of FOCS were mentioned and their shortcomings viewed as challenges to be met during their development by the sensor designer. A general overview of the field of fibre optic chemical sensing was given and covered the most popular chemical sensing schemes.

Thereafter followed in Chapter 2 a breakdown of the major components involved in a fibre optic chemical sensing system. Each was critically reviewed as well as other alternatives in terms of their characteristics to justify their selection in the assembly of a general experimental set-up adopted throughout subsequent experiments. Later modifications made to the set-up involved only the choice of components especially the light source as required by each sensing scheme and the photophysical properties of the reagents involved. Two examples of such experimental lay-outs were analysed to support our argument.

The measurement techniques to be used in later experiments were presented. Instead of making a point measurement at a specific wavelength in time and subject that measurement to strong noise interference, alternatives were proposed. As a result of this, the *rate* of change of intensity was measured and correlated to the analyte concentration instead of a simple intensity level measurement. This was implemented in Chapter 3. The fluorescent indicator displayed a different behaviour whereby measuring the gradient was not suitable. Instead, the intensity across a range of wavelengths was integrated to spread out and minimise the effect of interfering noise.

Each measurement technique was closely tied to the referencing scheme used and the advantages of the software environment LabVIEW to control the sensor were fully exploited to implement them. An important feature of all sensors is the ability to make robust measurements in the presence of adverse environmental conditions and this is met by the use of referencing techniques. Many papers in the published literature, although presenting interesting work, often lack this feature.

The incorporation of a suitable referencing method was a primary goal that was sought to be addressed in the development of the dithizone probe in Chapter 3. Given the characteristics of the dithizone reagent, i.e. its broad spectrum which presented an isosbestic point, it was possible to adopt the ratiometric approach and implement it by appropriate modification of the LabVIEW program used to run the sensor. This ratiometric technique also proved resistant against indicator leaching as it is based on two quantities whose values depend equally on the amount of reagent present and thus cancel each other out exactly.

The use of these resin beads in FOCS is popular and is reflected by the number of papers published on them; however, these papers present a cursory overview of the factors affecting the probe construction and are acknowledged only when reporting the sensor reproducibility. In contrast to this, work reported

in Chapter 3 involves building the sensor probe and studying the factors affecting it such as the dimensions and quantity of resin particles and the amount of indicator adsorbed onto them. The qualitative observations made reflect the fact that it is not possible to control exactly the amount and distribution of the resin beads in the probe. The limited selectivity of dithizone towards lead ions in the reflectance sensor eventually led to the search for a more selective reagent.

The chosen reagent reported in Chapter 4 is a novel fluorophore with high affinity for lead. There are few fluorophores available for lead sensing and even fewer which can display a fluorescence enhancement in the presence of lead as it is, along with other heavy metal ions, an efficient quencher of fluorescence. In this chapter, the characteristics of the fluorescent reagent were investigated with a view to implementation in a fibre optic sensing configuration as it has absorption and emission spectra lying in the visible wavelength which makes it compatible with optical fibres with high transmittivity at these wavelengths.

The high affinity towards lead ions was explained by introducing the topic of molecular recognition and chemoreceptors. In general, the selectivity of a macrocycle is determined by the match of its cavity size with the size of the guest ion. It was explained how, by coupling a molecular recognition unit together with a fluorophore moiety, it is possible to synthesize a fluoroionophore whose fluorescence mechanism depends on both units to successfully detect lead ions. The operation of the fluorescence mechanism PET was described.

Due to the adoption of the fluorescence sensing design, certain modifications were necessary with the experimental lay-out used previously. An LED provided strong illumination at the excitation wavelength which was not possible with the broadband light source used in Chapter 3 and an interference

filter was included to reject stray excitation light from the emission radiation. The instrument dark noise was removed by subtracting it from the measured signal. This was not necessary in the dithizone experiment as the ratiometric measurement cancelled out instrument noise drift. In this experiment, the LED output was found to be stable due to the use of a dc power supply, making a reference scheme unnecessary; nevertheless, a suggestion was given as to how to incorporate a referencing method into the set-up.

A sol-gel approach for immobilisation was deemed appropriate based on the binding mechanism of the fluorophore to produce a fibre optic probe. The sol-gel probe was implemented and enhanced experimentally and the detected fluorescent signal was confirmed as arising from the reagent and was not subject to stray background light or interfering chemical species within the sol-gel matrix.

Tests showed that the fluorophore did not respond to lead in this matrix despite producing a rapid and strong fluorescence increase in an organic solvent. This signal increase demonstrates that the compound has not been corrupted while the lack of response to lead suggests that binding is not occurring, possibly as a result of covalent bonding between the reagent and the sol-gel structure.

As a result, it was decided to exploit the fluorescent reagent in solution where it is known to function effectively. In Chapter 5, an optical sensor probe was configured to use the fluorophore in solution by exploiting of the capillary effect. A literature survey was provided to give a background to the ‘capillary sensor’. The work on the capillary probe builds heavily from the information on the reagent from Chapter 4 so that this chapter is able to focus more on the design and implementation of this type of sensing technique.

The capillary probe was built, optimised and tested and a calibration curve for lead obtained and acts as a proof-of-principle for this concept. In fact, this is

the *first* reported use of a FOCS incorporating a selective fluorescent reagent for lead ions. The advantage of this technique is that it is able to make use of reagents not suitable for immobilisation and might therefore open up the field of fluoroionophores to fibre optic sensing. The lack of a membrane also avoids issues with leaching and long-term deterioration whilst the reagent is still protected within the glass tube.

The adaptation of the capillary probe to use an evanescent wave sensing technique was also studied but due to unfavourable practical issues, in particular the fragility of the unclad fibre and the short length of fibre interacting with the sample, this was not pursued. In addition, evanescent wave sensing is not suited for fluorescent measurements as compared to absorbance, although many such sensors have been developed. This is due to the fact that if the fibre is optimised to propagate a large amount of optical power in the cladding for maximum interaction with the sample, then the amount of fluorescence entering and propagating along the fibre core is minimised. It is not possible to satisfy both conditions at once.

It is important to realise that in designing FOCS, the chemical indicator or transducer plays a key role in defining the system design and capabilities. It is the transducer which will set the optical parameter to be measured. It is the transducer which will determine what sort of measurement scheme to be adopted: reflectance, fluorescence intensity or lifetime measurements. It is also the transducer which will determine the detection limit of the sensor, its selectivity and dynamic range.

All the other aspects of the system such as the instrumentation, the experimental set-up, the packaging and the reference techniques only serve to optimise the sensor performance such as detection limit, ruggedness, life-time, dynamic range via the encapsulation method and the *modus operandi* – in a flow-cell, by evanescent wave or using a probe approach.

At the moment, the overall detection system may be regarded as a light-emitting diode causing electrons to emit photons, these photons being modified in population size (light intensity, e.g. absorption) or energy (frequency of light or wavelength, e.g. fluorescence). Upon detection by a photo-diode, these photons will be used to generate electrons for quantification by a meter more often than not linked to a computer for data processing. There is a degree of inefficiency and redundancy here from the electron-photon-electron cycle that may be improved upon with the advent of photonic computers.

Nevertheless, the field of sensors is a dynamic one which will find a wide range of applications in all sorts of environments in the years to come.

6.2. Further work

It is suggested to study the immobilization of the fluorophore described here onto nano-particles and to aim to extend its sensing properties to aqueous solutions. This will open up new areas of applications for this molecule.

There are other possible approaches for the detection of lead ions that merit in-depth investigation. The microcantilever based on the swelling of a hydrogel in the presence of lead was described in Section 1.2.2. The swelling property of this particular lead-sensitive hydrogel may be exploited with optical fibres to produce a lead sensor. The hydrogel recognises lead ions due to the presence of a crown ether within its polymer network. The presence of the crown ether will therefore impart high selectivity to lead unlike most other existing indicators for lead. There are several ways to combine this crown ether-doped hydrogel with optical fibres, some of which have been reviewed in sections 1.3.9 and 1.3.10.

A multimode fibre may have its cladding replaced with the hydrogel. Swelling of the hydrogel will change its refractive index and affect the transmission of light through the fibre.

For more sensitive results, an LPG may be coated with a thin layer of the hydrogel. The swelling action will cause a change in refractive index which will be picked up by the LPG.

In both cases where refractive index measurements are involved, knowledge of the refractive index changes of the hydrogel will be required to design the sensor. Where the index value falls outside the required range, say greater than the core index, the hydrogel will have to be modified to achieve a suitable index value.

The swelling action may be used to impose strain on the fibre. This can be picked up by an LPG or an FBG covered with that hydrogel. No knowledge of the refractive index value is then required, especially if an FBG is used.

Rare-earth doped fibres exhibit fluorescence whose intensity is a function of temperature and strain. By coating the rare-earth doped fibre with the hydrogel, it will impose a strain upon the fibre which will affect its fluorescence intensity when photo-excited. This scheme has all the advantages of fluorescence measurement, namely detection upon a dark background, low-cost devices for excitation and detection of the optical signal and possible lifetime measurements.

In both FBG and fluorescent fibre, the conversion of the swelling action into strain along the fibre is not very efficient as the swelling occurs in all direction, especially in an outwards direction where it is unconstraint by the fibre but is picked up by the latter only along its length, i.e. in one direction only. The fluorescent fibre has the advantage of being developed into a fully distributed

sensor whereas the FBG scheme can at most attain a quasi-distributed network by writing several gratings along the fibre.

Fibre grating physical sensors are now a mature field. The chemistry and synthesis of hydrogels are an active and better understood field. The author believes that the combination of hydrogels and fibre gratings to result in new chemical sensors has a lot of potential in light of the following:

- The wide variety of molecular recognition units such as crown ethers that may be combined with the wide variety of hydrogels capable of being synthesized;
- The drastic change in numerous properties of hydrogels, especially their swelling ability
- The multiple sensing optical configurations with or without fibre gratings incorporating these polymer gels.

List of publications

1. H.Guillemain, M. Rajarajan, K.T.V Grattan, T. Sun, Y.-C. Lin, C.-T. Chen, “A Disposable Optical Fibre-Based Capillary Probe for Sensing Lead Ions,” IEEE Sensors, 10 (2008) 1656-1662.

2. H.Guillemain, M. Rajarajan, K.T.V Grattan, T.Sun “A self-referenced reflectance sensor for the detection of lead ions using optical fibres,” Meas., Sci and Technol., 20 (2009) 045207-045214.

3. H.Guillemain, M. Rajarajan, K.T.V Grattan, T. Sun, Y.-C. Lin, C.-T. Chen, “Feasibility studies of thin sol-gel films doped with a novel lead-selective fluorophore,” Paper submitted to the Journal of Measurement June 2009

4. H. Guillemain, “Optical fibre sensing techniques for the detection of lead ions,” Webminar presented on the Measurement & Standards Knowledge Transfer Network (KTN) website at www.mset.org.uk on the 14.02.2008.